MR IMAGING IN MENIERE'S DISEASE - Developing a local protocol

Author: Mr Raul Simon, MRes student, ID 20417859

Supervisors: Prof Dorothee Auer, Dr Ian Wiggins and Mr Anand Kasbekar

ABSTRACT

Ménière's disease (MD) is a debilitating condition typically presenting with slow-developing unilateral symptoms of hearing loss, vertigo, tinnitus and aural fullness. The disease progresses to the contralateral ear in up to 50% of cases. Currently, there is a significant delay between symptom onset and diagnosis, and therefore effective treatment. Contrast-enhanced Magnetic Resonance Imaging (MRI) for diagnosing MD is currently used in research settings to detect endolymphatic hydrops (EH), which can be present in unaffected ears and other audio-vestibular conditions but is universally recognised as a biological marker consistent with the diagnosis of MD. MRI could expedite diagnosis and guide management as it could detect EH in the unaffected, clinically 'silent', ear which would develop symptoms later, detracting from ablative treatments which control symptoms by destroying the function of the ear rendering the patient with severe bilateral hypovestibular function. MRI is currently not used for diagnosis of MD outside of research settings in the UK and there is no globally accepted scanning protocol adopted in wider clinical practice as image quality and interpretation depend on the different settings and image parameters enabled in different makes of MR scanners, different image acquisition parameters and observer expertise. MRI is not yet a part of the NICE diagnostic pathway for MD.

This motivated an exploratory study at the Sir Peter Mansfield Imaging Centre, University of Nottingham to develop an MR scanning protocol for MD patients. The overall aim was to optimise an MR image acquisition protocol for EH detection in MD which would be translatable into clinical practice. This was supported by a comprehensive scoping review synthesising the evidence behind the use of MRI in EH detection and MD diagnosis. First, MR images of 4 healthy participants for anatomical reference and experience of image interpretation were obtained; then images of 4 MD patients were obtained both with and without contrast enhancement and 4 hours post-IV contrast administration using a 3D Fluid Attenuation Inversion Recovery sequence on a 3 T MR scanner. One MD patient was also scanned with a 3D Real Inversion recovery sequence and 2 hours post-contrast for a single-case comparison. The following scanning parameters were adjusted throughout the study for optimisation of the scanning protocol on a case-by-case basis; repetition time, inversion time and slice thickness which also influenced scanning time.

All images were qualitatively and semiquantitatively analysed by a single, unblinded observer. Image quality was measured by contrast to noise ratio and EH was detected and graded as per established criteria. All MD patients had EH in the affected ears, and 3 MD patients (75%) had EH in the unaffected ear consistently throughout contrast-enhanced scans. All healthy participants showed EH on at least one of the scanning protocols likely due to the quality of images produced by a specific acquisition sequence. Non-contrast enhanced images were inconclusive.

The study was limited by a small sample size and a lack of interobserver agreement. However, the scanning protocol using a 3D Fluid Attenuation Recovery with a repetition time of 12000 ms, slice thickness of 0.7 mm and inversion time of 2500 ms was deemed optimal given the consistency of image quality and accuracy of EH detection. This constitutes an applicable scanning protocol which was developed and can be implemented into local clinical practice in Nottingham.

Table of Contents

1. INTRODUCTION

This section details the anatomical and pathophysiological background of Ménière's disease (MD), and current challenges in its diagnosis and introduces the concept of Magnetic Resonance Imaging (MRI) use in diagnosing MD. Subsequently, it highlights current gaps in the literature and explains the aims of the MRes research project on the use of MRI in the diagnosis of MD undertaken at The Sir Peter Mansfield Imaging Centre (SPMIC), University of Nottingham.

1.1.1 ANATOMICAL INTRODUCTION

This brief anatomical introduction is provided to facilitate understanding of the main concepts of MD pathology and interpreting MR images in the context of endolymphatic hydrops (EH), detailed later in the text.

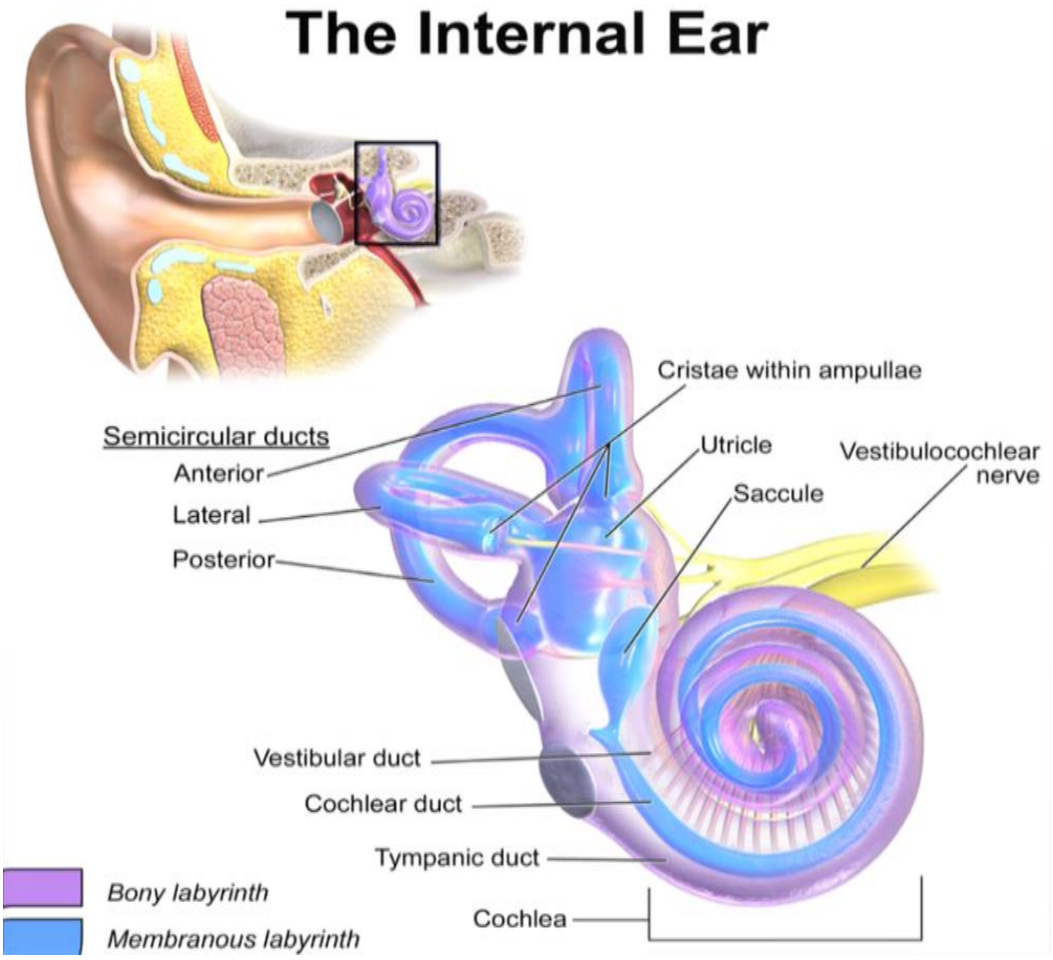

Figure 1 - Anatomy of the inner ear. Taken from Dougherty et al., 2023.

The inner ear is comprised of the bony labyrinth, which consists of the cochlea, vestibule and semicircular canals and is filled with perilymphatic fluid (perilymph) and the membranous labyrinth entirely within the bony labyrinth comprising of cochlear duct, saccule, utricle and semicircular ducts filled with endolymphatic fluid (endolymph). All of the structures of the membranous labyrinth communicate. The main structures of the inner ear are **the cochlea** (responsible for hearing) and **the vestibule with semicircular canals** (responsible for balance).

The cochlea is a narrowing tubular structure wrapped 2.5 times around the bony axis (modiolus) resulting in a snail-like shape consisting of three turns, the basal, the middle and the apical turn. On the cross-section, each cochlear turn is divided into three levels (scalae), the perilymph-filled **scala vestibuli** and **scala tympani** and the endolymph-filled **scala media (endolymphatic duct)**. The scalae are delineated by the **basilar membrane** and **the spiral laminae** inferiorly and the **Reissner's membrane** superiorly. The scala vestibuli and the scala tympani communicate at the cochlear apex through an opening called **helicotrema**. The basal turn of the cochlea attaches to the bony vestibule.

The bony vestibule contains two main endolymphatic organs, the larger, **utricle**, situated postero-supero-laterally and the smaller, **saccule**, located anteriorly, inferiorly and medially. These two structures are orthogonal to each other as they are responsible for the perception of linear motion in two perpendicular planes, horizontal and vertical. The surrounding area in the vestibule is filled with perilymph. There are three **semicircular canals**, the lateral semicircular canal (LSCC), the anterior semicircular canal (ASCC) and the posterior semicircular canal (PSCC). They protrude from the bony vestibule in orthogonal planes and make a semi-circle before returning to the vestibule. Each of the canals contains a **semicircular duct** filled with endolymph which has widenings (**ampullae**) at the anterior end of the semicircular duct containing the sensory organs, **cristae**.

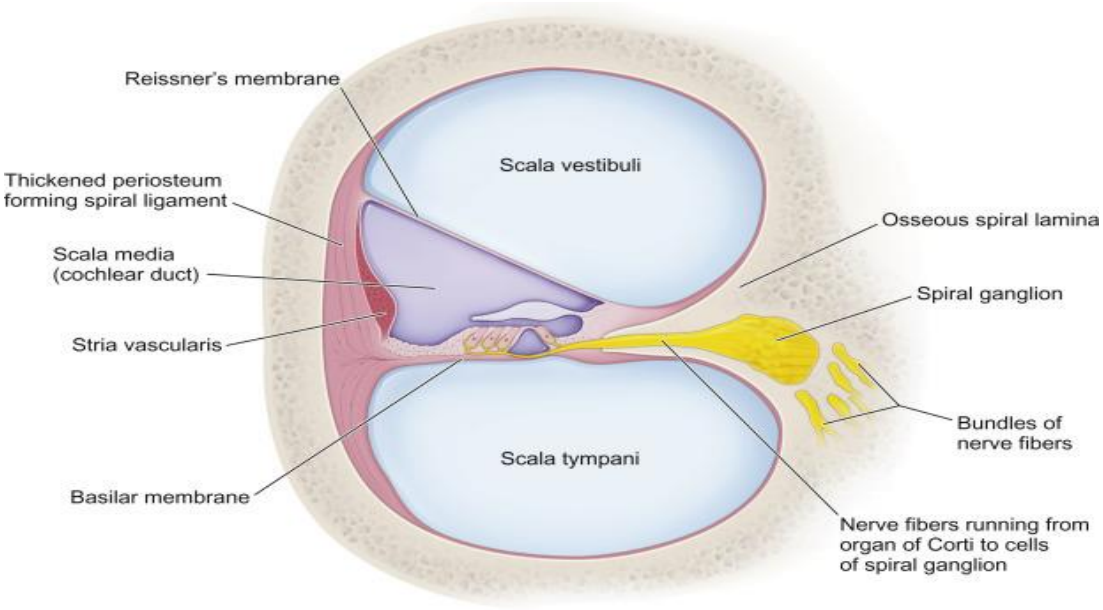

Figure 2 - A cross-section of a normal cochlear turn, dividing the space into three compartments, scala vestibuli and scala tympani filled with perilymph and scala media filled with endolymph. It is the bulging of this compartment on the side of Reissner's membrane into the scala vestibuli that is visualised as endolymphatic hydrops. This image represents a normal cochlea and is used for anatomical reference. Taken from Leonte.eu, n.d.

1.2.1. MÉNIÈRE'S DISEASE: DIAGNOSTIC CHALLENGES, CURRENT TREATMENT OPTIONS AND LINK TO ENDOLYMPHATIC HYDROPS

Ménierè's disease is a progressive, debilitating condition presenting classically with episodes of unilateral spontaneous vertigo attacks and hearing loss with accompanying ear symptoms, i.e., feeling of 'fullness' in the ear or tinnitus. The incidence has been approximated at 13.1 per 100,000 person-years and prevalence at 0.27% in most recent studies (Tyrrell et al., 2014). It carries an enormous healthcare cost, estimated at between £541.30 million and £608.70 million annually, and burden, as patients are often incapacitated and unable to return to work during the debilitating vertigo episodes (Tyrrell et al., 2016; Basura et al., 2020).

There is no definitive cure for MD, but the treatment options are aimed at either treating acute attacks (vestibular sedatives) or preventing future attacks, i.e. lifestyle changes (reducing salt intake) or medical treatment (betahistine, steroids), although the evidence for this is unclear (Sharon et al., 2015; Adrion et al., 2016). There are

also surgical (labyrinthectomy, vestibular neurectomy) and intratympanic (IT) treatments that destroy balance function in the affected ear (ablative therapy) (Sharon et al., 2015; Hoskin, 2021). In the latter case, the other 'healthy' ear partially takes over the function of balance. Since the disease can progress to the contralateral ear in up to 50% of patients, ablative therapy or surgery might be an unwanted option as it could leave the patient with a severe vestibular hypofunction if one ear is destroyed and the other gets affected by the diseases (Frejo et al., 2016). Treatment options are usually offered in a 'ladder' fashion, from least to most invasive.

CONSERVATIVE AND MEDICAL MANAGEMENT
Diet and lifestyle modifications (i.e., reduced caffeine or salt intake)
Vestibular rehabilitation
Betahistine
Steroids – intratympanic or oral *
SURGICAL MANAGEMENT
Grommet insertion (for aural fullness/pressure relief)
Ablative treatment – Intratympanic gentamicin
Endolymphatic sac surgery
Labyrinthectomy
Vestibular neurectomy

Table 1 - A representation of the 'ladder' of treatment options for MD

**Oral steroids can be used in the treatment of MD, although this is currently not endorsed in NICE guidelines – Morales et al., 2005*

Conservative and medical treatment -

Diet & Lifestyle – MD patients are often advised to reduce salt and caffeine intake and avoid alcohol whilst reducing exposure to stress. However, a recent systematic review by Webster et al., showed that the evidence that is currently available is of very low certainty and there is a lack of placebo-controlled randomised controlled trials (RCTs) providing further insight into the effects of these measures (Webster et al., 2023).

Vestibular rehabilitation – Although commonly recommended to MD patients, it is still inconclusive whether there are any positive effects in vestibular rehabilitation, as one systematic review demonstrated that the evidence available comes from low-quality studies with a high risk of bias (Van Esch et al., 2016).

Betahistine – a recent systematic review demonstrated that there is a lack of high-quality studies confirming the efficacy of betahistine and the same review found one study with a low risk of bias which showed no difference in vertigo symptoms (primary outcome) compared to placebo in MD (Van Esch et al., 2022).

Steroids - intratympanic or oral – they're cheap and effective, particularly in hearing preservation, and the effects are often compared to gentamicin (as detailed below).

Surgical treatment –

Grommet insertion – Minimally invasive, available under local anaesthesia; it can alleviate aural fullness and improve hearing, particularly when combined with other treatment modalities, i.e. intratympanic steroids (Kanegaonkar et al., 2019).

Ablative treatment - **IT gentamicin** – according to one systematic review, has a stronger effect on vertigo control than both betahistine and steroids but an inferior effect to the latter two in hearing improvement as the treatment itself is ototoxic, although a meta-analysis highlighted that there is no statistical significance in the control of vertigo symptoms between IT steroids or IT gentamicin (Ahmadzai et al., 2020; Lee et al., 2021).

Endolymphatic sac surgery (endolymphatic sac decompression, endolymphatic duct blockage) – works by alleviating increased pressure in the inner ear fluid system caused by excessive fluid accumulation (hydrops), it is targeted and effective but technically challenging and invasive with potential for severe complications, i.e. facial nerve palsy, CSF leak, brain injury, CNS infection, worsening vertigo and hearing etc. (Devantier et al., 2019; Mavrommatis et al., 2020). In the famous 'Sham' study, interestingly, outcomes between endolymphatic sac decompression and placebo surgery (simple mastoidectomy) were similar and both patient groups had their symptoms improved significantly after surgery which raises questions about the true effectiveness of endolymphatic sac decompression surgery (Thomsen et al., 1980).

Labyrinthectomy - destroys both the hearing and the balance function of the affected ear alleviating symptoms but compromises hearing outcomes and shares the same risk profile as endolymphatic sac surgery.

Vestibular neurectomy - destroys the balance function of the affected ear preserving the hearing, but is technically more challenging than the latter method of labyrinthectomy with essentially the same risk profile.

Although surgical treatments are effective, they are also highly invasive, usually require a general anaesthetic (GA), destroy the hearing and the vestibular function of the affected ear and carry an increased risk of morbidity (Mavrommatis et al., 2020).

MD is closely associated with the finding of dilatation (excessive fluid accumulation) of the membranous compartment of the inner ear (membranous labyrinth) – 'endolymphatic hydrops' (EH). Although Prosper Ménière, whom the disease was named after, first described the classical triad of symptoms in the 19th century, the first description of EH as a potential cause of MD dates back to 1938, separately described by Hallpike and Cairns and by Yamakawa (Hallpike and Cairns, 1938).

Several mechanisms underlying the development of endolymphatic hydrops have been proposed, including blockage of endolymphatic flow, increase in osmotic pressure, disturbance in calcium homeostasis and hormonal disbalance. However, these have not yet been conclusively demonstrated and the true origins of endolymphatic hydrops remain largely conjectural (Takeda et al., 2020).

In a seminal study in 2005, preceding the MRI era of detecting EH, Merchant et al tried to ascertain if EH was truly the direct cause of the symptoms of MD. If the hypothesis that EH directly causes MD is true, that would mean that every single patient with MD would have histopathological evidence of EH on temporal bone samples, and every patient with a temporal bone sample demonstrating hydrops would have to exhibit symptoms of MD during their lifetime. They examined histopathological samples of the temporal bones of patients who, during life, exhibited classic symptoms of MD (n=28). They also examined temporal bones (n=79) with EH and retrospectively established the presence of symptoms during the patient's lifetime from their respective case notes. While every patient with classic MD symptoms (episodic vertigo and sensorineural hearing loss) did have EH on their histopathological temporal bone sample, not every patient with EH had exhibited

classic symptoms of MD (9 out of 79 patients with hydrops did not exhibit classic MD symptoms in their lifetime). The authors suggested that this could mean that EH should be considered as a histological marker for Meniere's disease instead of being directly responsible for its symptoms (Merchant et al., 2005). The first part of the aforementioned hypothesis (every patient with MD would have to have EH on histopathological sample) was ultimately corroborated in a comprehensive review of histopathological evidence done by Foster et Breeze on 53 papers including 541 temporal bone samples in total where they summarised that 'an individual meeting the 1995 diagnostic criteria' (then valid) 'has a near certain probability of having endolymphatic hydrops in at least 1 ear' (Foster et Breeze, 2013). However, the second part of the hypothesis(every individual with EH would exhibit symptoms of MD) is not easily corroborated, as Gluth states in his review, 'physiology and human disease rarely interact in a manner that is so predictable for clinical signs and symptoms to be observable 100% of the time without pathophysiologic anomalies', drawing a parallel with the dehiscent superior semicircular canal that causes the Tullio phenomenon (vertigo being induced by loud noises) in some patients, whereas other patients are asymptomatic (Gluth, 2020). Recently, some anatomical variations have been proposed and considered in accounting for asymptomatic patients with endolymphatic hydrops (Monsanto et al., 2017).

Several literature reviews have synthesised the available evidence on the relationship between EH and MD and several studies that used temporal bone samples attempted to demonstrate causation between EH and MD (Belal et al., 1980; Fraysse et al., 1980; Rauch et al, 1989; Sperling et al., 1993; Merchant et al., 2005; Foster et Breeze, 2013; Gluth, 2020; Hoskin, 2020; Rizk et al., 2022). Even though the exact relationship between EH and MD has still not been fully elucidated, EH is considered the hallmark of MD (Merchant et al., 2005; Hoskin 2021; Rizk et al., 2022; Connor et al, 2023). The literature justifies the finding of EH for confirming the diagnosis of MD but also highlights the tentative nature of its absence in the context of refuting it.

It has previously only been possible to detect EH on a histopathology sample of the temporal bone post-mortem and not in a live patient. This was done by obtaining thin slices of the temporal bone and the inner ear and examining them carefully with a

microscope using hematoxylin-eosin (HE) staining (an example picture is provided below).

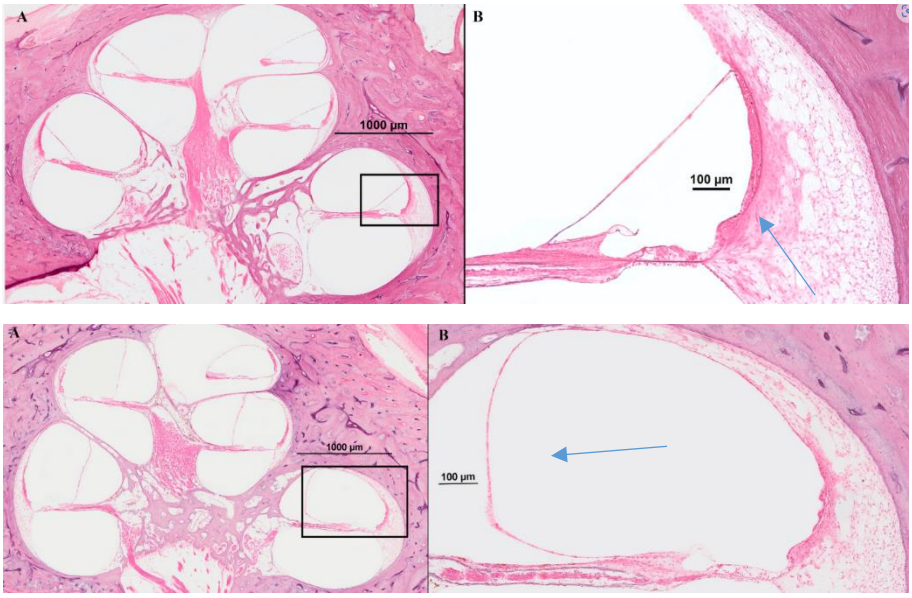

Figure 3 - A haematoxylin-eosin-stained sample of a temporal bone and cochlea without (upper image) and with (lower image) EH. The images on the right are magnified views of parts of images on the left as denoted by the black rectangle. The arrows (located in the endolymphatic space) point to Reissner's membrane with the endolymph being on the right side and the perilymph on the left side of it. Taken from Cureoglu et al., 2016.

Since this method of diagnosis is not feasible in living patients, MD continued to be a diagnostic challenge and the diagnosis often rested on the progression of clinical symptoms which can take years to fully unfold with large sample studies (n>1000) demonstrating that approximately 20% of patients have a delay greater than 5 years between initial symptoms and diagnosis (Carfrae et al., 2008; Pyykkö, 2013). Hence, clinical features were the mainstay of diagnosis.

In 2020, the American Academy of Otolaryngology-Head and Neck Surgery (AAO-HNS, also known as the American Academy) released diagnostic criteria where patients were stratified into either **'clinically probable'** or **'clinically definite'** MD (Basura et al., 2020). These criteria are endorsed by several relevant International Societies including the Barany Society and The Japanese Equilibrium Society and are widely adopted around the globe to support the diagnosis of Meniere's disease

including by the National Institute for Health Care and Excellence (NICE) in the United Kingdom (UK) (NICE, n.d.). Below is a tabular representation of the diagnostic criteria.

Table 2 - American Academy Criteria for MD, 2020.

Definite MD:

1. Two or more spontaneous attacks of vertigo, each lasting 20 minutes to 12 hours
   AND
2. Audiometrically documented low- to midfrequency sensorineural hearing loss (SNHL) in the affected ear on at least 1 occasion before, during, or after 1 of the episodes of vertigo
   AND
3. Fluctuating aural symptoms (hearing loss, tinnitus, or ear fullness) in the affected ear
   AND
4. Other causes excluded by other tests

Probable MD:

1. At least 2 episodes of vertigo or dizziness lasting 20 minutes to 24 hours
   AND
2. Fluctuating aural symptoms (hearing loss, tinnitus, or fullness) in the affected ear
   AND
3. Other causes excluded by other tests

Since MD symptoms are heterogeneous and gradual in onset, the full complement of symptoms doesn't develop simultaneously, usually takes a long time and the symptoms often overlap with a myriad of other audio-vestibular illnesses, there are still significant challenges in accurately and timely diagnosing the condition (Sharon et al., 2015). Consequently, there is a significant delay between symptom onset, referral to an Ear Nose and Throat (ENT) or Audio-vestibular specialist and diagnosis,

and therefore, effective treatment. Eventually, over several years to decades, MD can progress and cause a complete loss of balance and hearing function in the affected ear in as many as 50% of cases (Liu et al., 2015; Frejo et al., 2016). It is important to distinguish MD in early stages from other audio-vestibular conditions to optimise treatment (Sharon et al., 2015). Once the patients are under the care of an ENT surgeon, they are investigated for the potential causes of their symptoms, with the main differentials being Vestibular Migraine (VM), Vestibular Schwannoma (VS), Sudden Sensorineural Hearing Loss (SSNHL) and Vestibular Neuritis (VN).

Currently, in the UK, patients with audio-vestibular symptoms undergo investigations such as Pure Tone Audiometry (PTA; a hearing test), Vestibular Evoked Myogenic Potential (VEMP) and MRI with or without contrast enhancement as well as less readily available, but still used diagnostic methods, such as electrocochleography (Obeidat et Bell, 2019).

These investigations are usually used to rule out or diagnose other pathologies. However, they might also corroborate the diagnosis of MD. Currently, electrocochleography and VEMP are used to diagnose vestibular or cochlear dysfunction and can, to a varying degree of reliability, be used to detect EH and facilitate the diagnosis of MD (Fukuoka et al., 2012; Gurkov et al., 2016; Obeidat et Bell, 2019). Their use in the diagnosis of EH is reflected upon later in the thesis in the subheading 'Correlation of EH MRI with different neurotological tests'. An MR scan is often used to rule out different pathologies that could be accountable for audio-vestibular symptoms, most notably VS which is the most common tumour of the lateral skull base with the cited mean incidence of 2.2 per 100000 person-years (Fernández-Mendéz et al., 2023). It usually presents with unilateral hearing loss, tinnitus and vertigo or a cluster of these symptoms, often mimicking MD symptomatology. The main diagnostic criteria warranting a referral for an MR scan of the internal acoustic meatus (IAM), the origin point of the lesion, are unilateral tinnitus and an asymmetry in the patient's hearing thresholds between the two ears on the PTA. The MR scanning technique in this case would be T2-weighted cisternography, usually CISS (constructive interference in steady state) and FIESTA (fast imaging employing steady-state acquisition) depending on the vendor (CISS for

Siemens and FIESTA for GE) but this would only aid in ruling out a differential and is, hence, not specific to the diagnosis of MD (Schmalbrok,2000; Benson et al., 2020).

It wasn't until the pivotal work in 2007 by Nakashima who succeeded in the first *in vivo* demonstration of EH in a patient with MD that the doors for using MR scanning techniques to diagnose MD were opened (Nakashima et al., 2007). The main premise of the use of MRI in the diagnosis of MD is the radiological detection of its hallmark, EH. The collation of the history of the development of different MRI techniques for diagnosing MD and a description of what is seen as EH is detailed later in the subheading 'Development of different MRI acquisition protocols for EH'. Thanks to Nakashima's pivotal work, EH could now also be used as a radiological marker for MD. In a few UK centres, this premise is put to practice as MRI enhanced with intravenously (IV) administered contrast is used to detect EH, but this is mainly done in research settings using specific scanning techniques and imaging protocols which will be detailed later in the text. MRI is otherwise routinely used in the context of MD when planning for certain surgical interventions and to rule out other structural abnormalities causing the pertinent symptoms (National Institute on Deafness and Other Communication Disorders – Ménière's disease, 2024).

This forms the basis of the MRes research project with the main aim being to contribute to establishing a particular MR scanning protocol with sensitivity for EH which would then be available for wider clinical use locally and, potentially beyond.

1.3.1. THE ROLE OF MRI IN DETECTING ENDOLYMPHATIC HYDROPS AND DIAGNOSING MENIERE'S DISEASE

Nakashima's pivotal work in 2007 allowed the use of MRI for the diagnosis of MD (Nakashima et al., 2007). They imaged EH *in vivo* utilising MRI with IT administered contrast, a 3 Tesla Siemens MRI machine, and a three-dimensional fluid-attenuated inversion recovery (3D-FLAIR) imaging technique which was performed 2 hours and 24 hours post intratympanic injection of gadolinium(Gd)-based contrast. The images (Figures 4 and 5) obtained show gadolinium-based-contrast-agent (GBCA) concentrated in the perilymph with no evidence of EH. Since it took time for the contrast to be distributed within the inner ear, the scan taken 2 hours post-injection was not of sufficient diagnostic quality as opposed to the one taken 24 hours post-contrast. It was shown that contrast collects in the perilymph and can delineate between perilymph (bright, contrast-enhanced) and endolymph (dark, unenhanced). This is the basic principle of imaging and depicting endolymphatic hydrops on an MRI scan. This is visible in Figures 6 and 7, where a space that was occupied with contrast-enhanced perilymph is now occupied with non-enhanced, low-signal intensity endolymph, indicating EH (Nakashima et al., 2007). Their study indicated MRI diagnosis may play a key role in understanding Meniere's disease without obtaining temporal bone histopathologic specimens. Figure 8 provides an anatomical reference to the relevant structures as they're seen on MRI. The navy-coloured endolymphatic duct on the horizontal cross-section, normal in this picture, is usually extremely difficult to visualise on an MRI scan. However, it is enlarged in the case of EH which makes it much more visible on an MRI image distinguishing hydrops from normal cochlea. The anterior ampulla of the LSCC is an important structure when assessing for hydrops on an MRI scan as it can be mistaken for an enlarged (hydropic) utricle or saccule thus falsely representing EH.

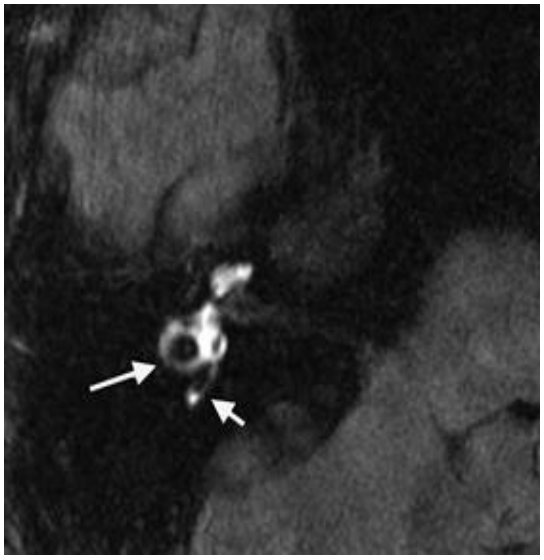

Figure 4 A

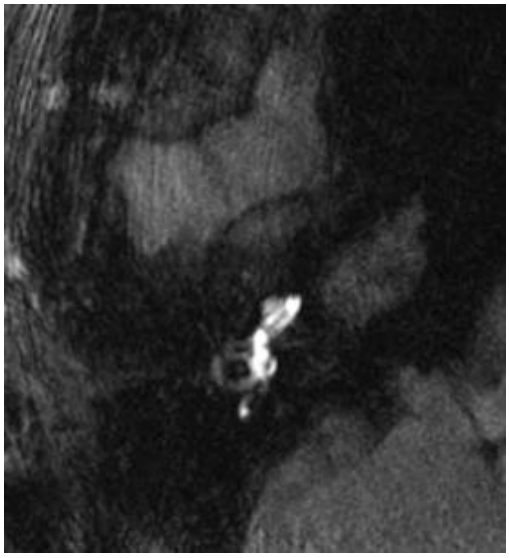

Figure 4 B

Figures 4 A and 4 B - Image of a normal ear. GBCA is concentrated in the vestibule and the cochlea in an ear with no EH. In Figure 4A, the long arrow shows the lateral semicircular canal (LSCC) and the short arrow shows the posterior semicircular canal (PSCC). In Figure 4 B, it is visible that both scala tympani and scala vestibuli are shown as enhanced, high-signal-intensity structures throughout the entire cochlea. In Figure 4 A, only the second and apical turns of the cochlea are visualised, whereas in Figure 4 B, the basal and the second turn of the cochlea are visualised and the LSCC is less enhanced than in Figure 4 A indicating that this is a more caudal slice. Taken from Nakashima et al., 2007.

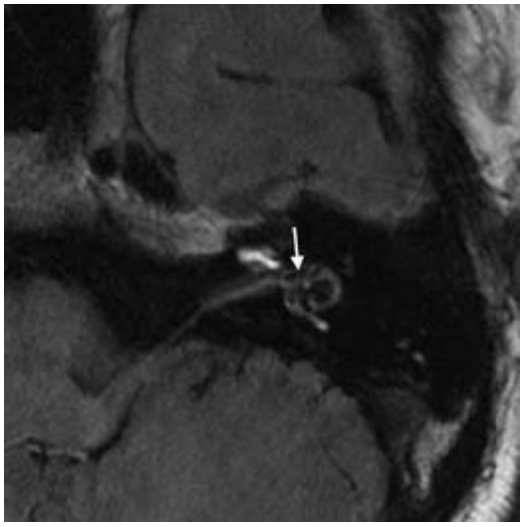

Figure 5 A

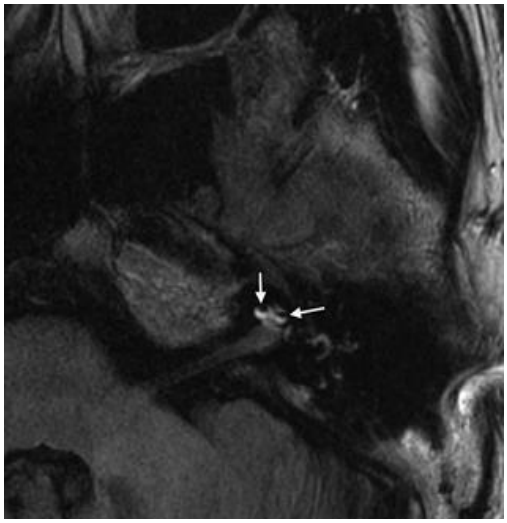

Figure 5 B

Figures 5 A and 5 B - Image of an ear with endolymphatic hydrops (EH) visible as a non-enhanced, low signal intensity space occupying most of the vestibule (arrow) and encroaching on the less prominent perilymph in Figure 5 A. Figure 5 B shows gadolinium present only in scala tympani of the cochlea, suggesting that the enlarged endolymphatic space in the cochlea (the cochlear duct or scala media) has blocked the passage of perilymph from scala tympani to scala vestibuli hence there is no contrast present in the scala vestibuli. Taken from Nakashima et al., 2007.

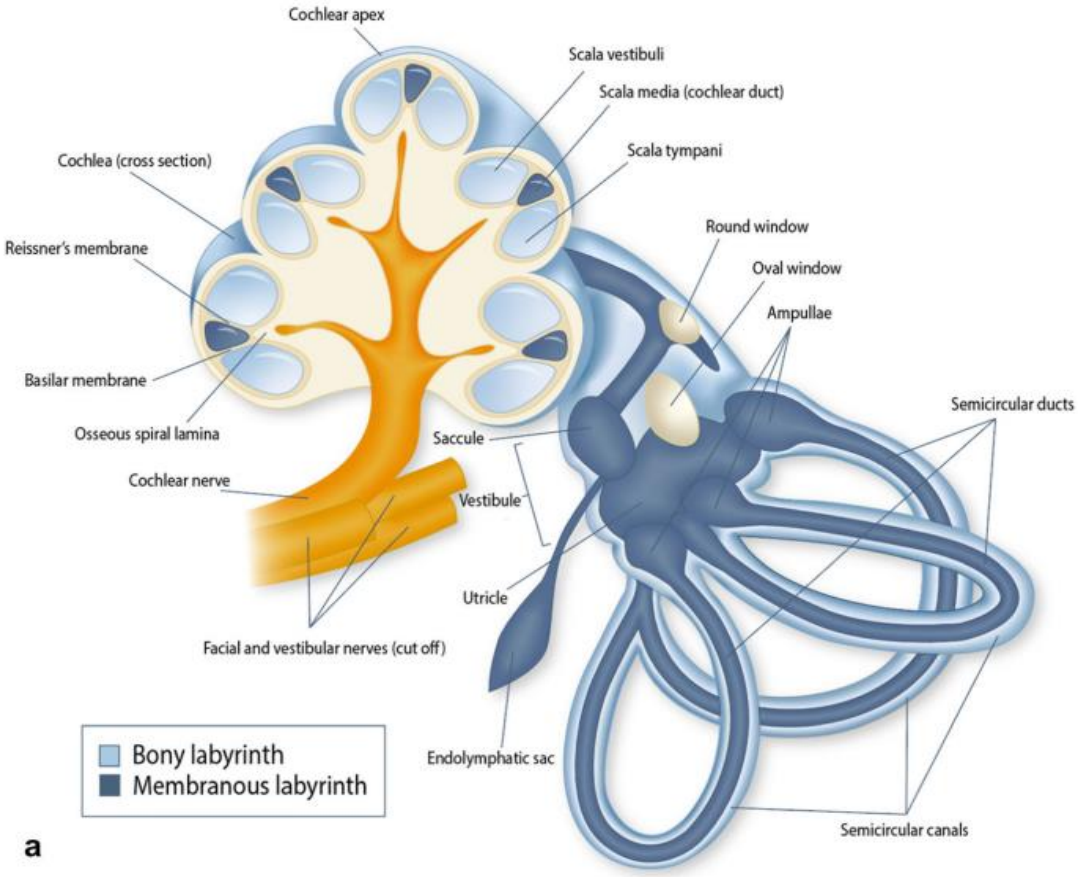

Figure 6 - A schematic representation of the inner ear looking from cranial to caudal which is the same perspective as the axial plane of the MRI slice seen on MRI when assessing for EH. The perilymphatic area (light blue) is enhanced or bright on an MRI scan and the endolymphatic area (navy) is unenhanced or dark on an MRI scan. Taken from de Pont et al., 2020.

In the last 17 years, MRI has been successfully used to diagnose EH and consequently MD. In the UK, this has not yet reached wider clinical practice, and MRI is not yet being used to diagnose Meniere's disease outside of the research environment and emerging dedicated centres. Within the research settings, MR scans have been utilised to visualise, and grade, endolymphatic hydrops which is the proposed pathological substrate of MD and is considered its hallmark. The severity (grade) of EH has been demonstrated to correlate with the severity of symptoms and

impairment of cochlear and vestibular function (Nakashima et al., 2009; Hoskin, 2020; Connor et Pai 2021; Connor et al., 2023). Nakashima et al. were the first to successfully image EH in an MD patient *in vivo* in 2007 and since then, MR scans have been used within research settings to visualise EH and diagnose MD (Nakashima et al., 2007). This was achieved using a 3 T MRI and 3D FLAIR imaging technique with images of the inner ear obtained 24 hours after the intratympanic (IT) administration of GBCA

In their landmark paper, Nakashima et al. have clearly and simply demonstrated EH in both the cochlea and the vestibule (Nakashima et al., 2007). Their team has subsequently developed criteria which could be used to not only detect but also grade EH on MRI demonstrating a correlation between the severity of hydrops and the severity of symptoms (Nakashima et al., 2009). In the latter years, these grading criteria have been expanded and refined as well as new ones proposed with varying degrees of diagnostic certainty (Barath et al, 2014; Bernaerts et al, 2019; Connor et Pai, 2020; Connor et al, 2023). Also, different imaging techniques and image acquisition protocols have been proposed and invented with the vast majority of literature converging on the delayed post-GBCA IV administration imaging using either 3D Real IR or 3D FLAIR image acquisition sequences; various MRI descriptors of EH have been identified and their performance evaluated (Conner et al, 2023). The imaging techniques used in the detection of EH have been evolving and the image analysis has been standardised to a degree; however, there remain the differences in the MR scanning machines and image acquisition protocols used, different observers of varying experiences analysing the images and patients being imaged with varying symptomatology which all increases the potential for diagnostic pitfalls. It is also important to appreciate the clinical feedback following a radiological diagnosis of EH which is not always possible due to participant dropout and lack of follow-up. Other factors, such as invasiveness and drawbacks of contrast administration and the optimal timing of delayed post-contrast imaging need to be considered. Hence, despite promising results of researchers from different countries and different units, MRI is still not widely used in clinical practice for diagnosing Meniere's disease although the body of research available today supports the use of MRI (Hoskin, 2020; Connor et al., 2023). The NICE guidelines stipulate that there is no specific diagnostic

test for MD and have not yet included MRI in their diagnostic algorithm for MD (NICE, n.d). This leaves scope for further progress in the UK where MRI might be included in the diagnosis of MD and expedite and improve the accuracy of the process enhancing the patient experience and providing timelier targeted treatment.

1.3.2. CURRENT GAPS AND RESEARCH QUESTIONS

MRI appears to be a promising tool that would greatly aid in expediting the diagnosis of MD. However, there are still gaps that need to be overcome for it to be widely used clinically and there is a lack of a gold standard for MRI protocols and image analyses. The questions that remain unclear and pose a challenge in adopting a widely applicable MRI protocol in diagnosing MD- –

1) What is the optimal image acquisition sequence (strength and type of MR scanning machine, scanning parameters etc.) that provides the best resolution images and enables the detection and grading of EH but is also not overly time-consuming?
2) What is the best route of contrast administration and the optimal scanning time post-contrast administration?
3) Is contrast essential and could it be avoided, enhancing the logistics of the scanning process and its safety profile? Can a valid comparison between non-contrast-enhanced and contrast-enhanced images be demonstrated?
4) What are the optimal assessment methods for interpreting EH on an MRI?
5) What is the diagnostic performance of MRI in MD?
6) What are the barriers to the introduction of MRI into broad clinical practice for the diagnosis of MD?

Firstly, a scoping literature review on MRI of EH in the context of MD to address the above questions was conducted by the MRes (Master of Research) student. The review aimed to provide a focused narrative of the development of the image acquisition and analysis techniques, including grading and diagnostic criteria, and subsequently synthesise the evidence behind the use of MRI in diagnosing MD then finally offer a comprehensive insight into its development and clinical application to inform decisions about the pilot study and contextualise the students work as part of the MRes degree.

Secondly, the MRes student performed an exploratory pilot study that aimed to implement MRI protocols on local scanners to detect EH and diagnose MD and to pave the way for future work on the optimisation of scanning protocols and quantitative evaluation of the diagnostic accuracy of MRI. The main rationale for the

study is to propose a scanning protocol using local MRI equipment that can be translated into wider clinical practice which could potentially help patients reach diagnosis quicker and facilitate their treatment.

1.3.3. STUDY AIMS

The aim of the study was primarily to implement, and potentially optimise, established contrast-enhanced EH imaging protocols on local MR scanners. Firstly, the MRes student imaged the inner ears of healthy participants defining pertinent anatomical structures for valid reference and assessing for potential radiological signs of EH. Subsequently, both symptomatic and asymptomatic ears of MD patients were assessed for signs of EH.

The MRes student then hypothesised that the inner ears of healthy participants would exhibit normal inner ear anatomy and would provide a valid reference. Conversely, the MRes student hypothesised that the symptomatic ear of MD patients would exhibit EH. Subsequently, the potential detection of EH in the asymptomatic ear could perhaps provide an earlier indicator of MD before symptom development.

Secondly, the MRes student aimed to evaluate whether inner ear anatomy could be appreciated and whether EH could be detected in the same groups of participants using non-contrast enhanced MRI scans, since, if possible, this would remove the logistical and safety drawbacks of contrast administration.

Lastly, the MRes student hypothesised that the contrast-enhanced images would be superior to non-contrast-enhanced images in the imaging of EH.

2. METHODOLOGY

The following text will, firstly, present and synthesise the current evidence in the use of MRI in the diagnosis of EH and MD.

Secondly, it will describe the original research pilot study conducted at the SPMIC, Nottingham, which attempted to visualise and grade EH using the local MR scanner along with protocol optimisation attempts. The overall aim of the study would be to develop and implement a scanning protocol into wider clinical practice.

This part of the thesis will provide a review of the prevalence of EH in non-MD conditions and then detail the development and review of different MRI techniques and image acquisition protocols used to visualise and grade EH to lay the grounds for the MRes students' experimental work. By doing so, it will contextualise the work in the study.

2.1. EVIDENCE SYNTHESIS: A SCOPING REVIEW ON THE USE OF MRI IN DIAGNOSING MENIERE'S DISEASE

Many studies investigated the different aspects and various possibilities of the use of MRI in diagnosing endolymphatic hydrops in the context of Meniere's disease. Nakashima et al. not only detected endolymphatic hydrops in vivo in humans but also proposed the first criteria for grading it (Nakashima et al., 2007; Nakashima et al., 2009). These studies have paved the way for an abundance of research on the topic by different researchers to ultimately be able to use MRI to diagnose MD (Connor et al., 2023; Connor et Pai, 2020; De Pont et al., 2020).

2.1.1 EH IN CONDITIONS OTHER THAN MD

Further complicating the diagnosis of MD, EH can also be present in unaffected or 'healthy' ears of MD patients (Frejo et al., 2013; Monsanto et al., 2017; Conte et al., 2018; Hoskin, 2020). This might be the case because the hydrops wasn't detected and recognised on images due to various technical reasons (i.e. interobserver (dis)agreement, sequence with poor resolution etc.) or maybe wasn't present at the time of imaging. Furthermore, EH has also been visualised in healthy individuals with no audio-vestibular symptoms and patients with conditions other than MD, such as vestibular migraine (VM) and sudden sensorineural hearing loss (SSNHL). The significance of this is still poorly understood. It is unclear whether these represent fragments of MD symptoms and whether the individuals with asymptomatic hydrops would later develop the full palette of MD symptoms or if the aforementioned conditions are concurrent with MD (Horii et al., 2011; Nakashima et al., 2012; Pyyko et al., 2013; Nakada et al., 2014; Ito et al., 2016; Pyykkö et al., 2019; Hoskin, 2020).

Since the reported incidence of MD progression into the contralateral ear has been reported as high as 50% of cases, the radiological finding of EH in an unaffected ear of an MD patient could, on one hand, potentially predict disease progression to the contralateral ear before symptoms occur (Frejo et al., 2016). The same could be valid for healthy individuals with no symptoms; detecting EH in these cases might mean these individuals will later develop MD.

On the other hand, the presence of EH in patients without the typical cluster of clinical symptoms specific to MD could aggravate the diagnostic difficulty and distinction between MD and other audio-vestibular conditions, i.e., isolated SNHL, VM etc.

Shimono et al. attempted to visualise EH in acute SSNHL using MRI and successfully detected both cochlear EH, 92% of affected ears, and vestibular EH, 88% of affected ears in a sample of 25 patients. Five patients had IT contrast and twenty had IV contrast. Different severities of EH were evaluated in all these cases with the majority being diagnosed with significant hydrops (Shimono et al, 2013). Interestingly, EH was present in the vestibule which is not directly responsible for hearing and hence is not theoretically expected to be associated with the symptom of a sensorineural hearing loss. EH was also observed, with a high prevalence, in the unaffected ears of 8

patients (40%) in the case of cochlear hydrops and 17 patients (85%) in the case of vestibular hydrops (Shimono et al., 2013). It is unclear if the symptom of sensorineural hearing loss was part of an MD presentation with an undeveloped clinical picture. The 'healthy', unaffected ears with hydrops could potentially represent the contralateral ears which have radiological features of the disease but are presymptomatic.

Horii et al. also compared the detection rate of EH between patients with MD and sudden deafness (used as controls) by using Gd-enhanced MRI. Although not explicitly stated, by sudden deafness they presumably meant SSNHL as the authors did exclude patients with low-tone sudden deafness which is more present in MD and included only high-tone sudden deafness more commonly present in SSNHL. They scanned 10 patients with unilateral MD and 8 with sudden deafness (presumably SSNHL). Due to faint enhancement, images could not be evaluated in 1 of 10 patients with MD. However, hydrops (both cochlear and vestibular) was present in the other 9 patients together with two of the eight patients with sudden deafness. The difference in detection rates between the two diseases was statistically significant indicating that EH is more pertinent to MD, but the fact remains that hydrops was indeed present in cases with sudden deafness, a condition which is distinct from MD. Despite the images being taken after partial recovery from hearing loss several months after the onset, so a degree of follow-up was present, it is not known whether the hearing loss was potentially just the first presentation of MD or not. Unfortunately, these patients weren't followed up long enough to exhibit other typical symptoms, i.e. vertigo, tinnitus etc. (Horii et al., 2011).

Gurkov et al. investigated the occurrence of EH on MRI in patients with VM. This was particularly of interest as this condition often overlaps with MD and can pose a significant diagnostic challenge due to similar patient demographics and presenting symptoms (episodic vertigo, pain or fullness in the ear or ipsilateral side of the head). Of the 19 included patients, four patients (21 %) demonstrated evidence of both cochlear and vestibular hydrops. However, it remains unclear whether these patients suffer from MD only and are misdiagnosed as VM, or suffer from both VM and MD or just VM (Gurkov et al., 2014).

Nakada et al., assessed and compared the size of endolymphatic space in seven patients diagnosed clinically as having VM and MD using IV contrast-enhanced MRI. The patients were age and sex-matched. EH was observed in the vestibule of two out of seven (28.5%) patients with VM (one patient had unilateral and the other patient had bilateral hydrops). In contrast, all patients with vestibular symptoms of MD had significant EH in the vestibule, bilaterally or unilaterally (Nakada et al., 2014). The size of the endolymphatic space was found to be different in these two cohorts of patients and that fact suggests that there could be a morphological difference between MD and VM patients. However, there remains the question of why the pathological substrate of MD is present in VM although explanations detailed earlier in the text might help shed more light on the matter.

A study by Li et al. featured 178 definite, unilateral MD patients imaged with contrast-enhanced MRI. EH was detected on the affected side in all patients, whereas it was detected on the unaffected side in 32 patients (18.0%). This could potentially indicate that this group of patients will develop MD in the unaffected ear rendering ablative (inner ear destroying) treatments undesirable. The authors also examined the relationship between the severity of hydrops and disease progression, which was classified by the authors into three stages based on hearing levels, as, although initially fluctuant, hearing intractably deteriorates with time in MD patients. The severity of EH was determined using published radiological criteria which correspond to the size (extent) of EH stratifying it into different degrees as explained later in the text. The results showed that disease progression corresponded to EH severity (Li et al., 2020). Additionally, according to this study, the progression of EH appears to be directional and cochleocentric, initiated in the cochlear apical turn and then progressing distally towards the vestibule which is consistent with the existing literature and the previous study by Li et al (Pender et al., 2014; Li et al., 2020).

In one of the largest sample studies, reported on 198 MD patients, 100% of MD patients had EH on the affected side and 8.6% on the asymptomatic side. However, the data provides an element of heterogeneity because a proportion of patients(n=54) were scanned using IT contrast and the other patients(n=144) were scanned using IV contrast administration which introduces potential differences in

hydrops detection rate as the image quality differs by contrast-administration method (Shi et al,2019).

Pyykkö demonstrated EH in 90% of 224 MD patients (largest sample size yet) on a 3 T MR scanner but also used a mixture of IT (119) and IV (105) contrast. They demonstrated a pickup rate of 65% amongst unaffected ears which is considerably higher than the previous study by Shi et al conducted on a sample of a comparable size (Pyykkö et al., 2013).

Liu et al. examined the contralateral ear of patients with unilateral MD using a 3 T MRI machine with IT-administered contrast to assess the incidence of EH in the unaffected ears. Their results were consistent with previous similar research (Gurkov et al, 2011; Fiorino et al., 2011). Of the total of 30 patients, endolymphatic hydrops was present in the contralateral ear of 7 patients (20.3%). They further correlated the presence of contralateral endolymphatic hydrops with hearing levels using pure tone audiometry testing (PTA) and found that patients who had hydrops in the unaffected contralateral ear had worse hearing levels in both the affected and the unaffected ears than the patients without hydrops in the contralateral ear. Moreover, they found that the patients with observed contralateral hydrops exhibited a significantly longer duration of the disease compared with the non-hydrops patients (6.7±6.3 vs. 2.9±3.1 years, respectively) (Liu et al., 2015). This might point to the fact that the contralateral ears exhibit radiological evidence of the disease before it presents clinically and that it takes a long time for the contralateral ear to develop symptoms, or it potentially means that endolymphatic hydrops is more of a marker of the disease rather than a causative factor as suggested by Merchant et al. However, the authors did not follow their patients up to corroborate the theory of clinical latency in the presence of radiological evidence of MD (Liu et al., 2015).

The current consensus as confirmed by several systematic and scoping reviews, is that MD is a multifactorial condition and that EH is closely associated with MD and should be considered as a histological, and more recently, a radiological biomarker for MD rather than being directly responsible for its symptoms. The available literature suggests that EH is present in almost every ear affected by MD. Still, it is, however, also present in a minority of unaffected, healthy ears and other audio-vestibular conditions. It is not yet fully understood why, but several explanations are possible,

most notably, other conditions being misdiagnosed as MD, symptoms discovered before the full clinical picture developed and radiological findings of EH in clinically silent ears predicting disease progression. If EH is causative of MD, it is insufficient to do so alone, indicating that there must be one or more additional cofactors (potentially vascular or autoimmune) that cause asymptomatic hydrops to become symptomatic MD or there are certain patient factors (i.e. anatomical variations) which render them having asymptomatic EH (Merchant et al., 2005; Foster et Breeze, 2013; Monsanto et al., 2017; Hoskin, 2020; Gluth, 2020; Rizk et al., 2022). In effect, the relationship between EH and MD has not yet been fully elucidated, but given the fact we are now able to directly observe and grade EH *in vivo* by using MRI and link it to symptoms and their progression and severity, this knowledge gap would decrease as MRI of EH *in vivo* becomes more widespread and develops further. This could aid in early detection of MD if silent ears are imaged, or ruling out MD in the absence of EH on MRI in favour of other conditions.

Even though large sample studies like the ones by Pyykkö et al. and Shi et al. greatly aid in providing consistency of evidence and increasing the depth of knowledge in both EH imaging *in vivo* in MD patients and clarifying the relationship between EH and MD, ideally, prospective longitudinal studies following patients for an extended period(i.e. decades), would be crucial to fully understand the behaviour of EH and it's connection to the clinical symptoms of MD and other audio-vestibular conditions. This could signify a knowledge gap and a potential paradigm shift in the approach to patients with audio-vestibular symptoms in clinical practice as a combination of a high-quality, early EH-detecting MRI and subsequent clinical and radiological follow-up could help increase diagnostic accuracy and treatment efficiency for MD. This area of literature is discussed further in the text with evidence from the available longitudinal studies.

Year of Publication	Author(s)	Percentage of unaffected(healthy) ears with EH	Total number of patients (N)	Method of contrast administration (IT/IV)
2005	Merchant et al.	**11.40%**	107	N/A
2013	Shimono et al.	**85%**	25	IT + IV
2013	Pyykkö et al.	**65%**	224	IT + IV
2014	Barath et al.	**22.00%**	53	IV
2015	Liu et al.	**20.30%**	60	IT
2019	Li et al.	**18%**	152	IT + IV
2019	Shi et al. *	**8.60%**	198	IT + IV
2019	Bernaerts et al.	**11.50%**	148	IV
2020	Van Stekeelenburg et al.	**4.70%**	137	IV
2022	Wnuk et al.	**11.00%**	110	IV
2022	Chen et al.	**16.70%**	36	IV
2023	Leng et al.	**10%**	70	IT

Table 3 - A tabular representation of the EH pickup rate in the unaffected ears of MD patients or healthy controls. N.B. The first study by Merchant et al. examined a large sample of temporal bone histopathology samples which is, by nature, more accurate than an MR scan and could potentially present the true prevalence of EH in unaffected or healthy ears. The list is inclusive of several studies mentioned later in the text to demonstrate a general downward trend of the EH pickup rate on MRI over the years ending in the approximate range as the prevalence in the study Merchant et al. This could potentially indicate that the quality of MR images, the robustness of grading and identification criteria and observer expertise have improved significantly over the last 15 years coming even closer to the level of confidence and accuracy in detecting EH on a histopathology sample. N.B. The study by Merchant et al did not utilise MR scans, but rather analysed histopathology samples of temporal bones, hence, no route of contrast administration was given.

**The study by Shi et al, was the only one where EH was detected in 100% of affected ears.*

2.1.2. WAYS OF CONTRAST ADMINISTRATION, TIMING OF THE SCAN POST-CONTRAST INJECTION AND DOSAGE REGIMENS

There are two main routes or methods of administering gadolinium-based contrast in inner ear imaging, intratympanic (IT) and intravenous (IV).

The intratympanic route is performed under local anaesthesia (LA) where the contrast is injected through the tympanic membrane into the middle ear cleft. It is then absorbed through the round window into the perilymphatic space of the cochlea and further distributed throughout the inner ear. This process requires some time and logistical effort and is dependent on the round window permeability.

There is also a risk of bleeding and infection, although the IT route of drug administration is generally considered safe. The patient is required to lie supine for another 30 minutes afterwards with their head turned 45 degrees to the contralateral side and they cannot speak or chew during this period not to allow for the contrast to leak from the middle ear cleft through an open Eustachian tube during these manoeuvres. The MR scan is performed 24 hours post-injection as the contrast agent achieves the optimal distribution in the inner ear structures and provides optimal contrast and resolution on the images. Although achieving high concentrations in the inner ear, IT administration of contrast did not show evidence of ototoxicity, at least when it comes to auditory function (Louza et al., 2015).

The intravenous route is less invasive, and the contrast agent takes less time to be distributed in the inner ear. The scan is usually performed 4 hours after injection because it appears that in that time contrast achieves the highest concentration in the inner ear providing the greatest signal intensity (Naganawa et al., 2012; Naganawa et al.,2014). A delayed MR scan post-intravenous injection helps to distinguish perilymph from endolymph as it cannot penetrate through the blood-labyrinth-barrier enabling the visualisation of dilatation of endolymphatic space which is shown as an enlarged dark area on the scan encroaching on the gadolinium-enhanced perilymphatic space (Nakashima et al., 2007; Basura et al., 2020).

However, GBCA administration is not without its risks which range from mild reactions such as nausea and headache to severe reactions like anaphylaxis or grave consequences such as nephrogenic systemic fibrosis with the double dose bearing more risks of these side effects. Although this hasn’t been conclusively and

consistently shown, the double dose remains off-label use (www.medicines.org.uk, n.d). More details on this are provided in the methodology section.

In recent years, intravenously injected gadolinium started to gain prevalence (Naganawa et al., 2019; Connor et Pai, 2020; Hoskin, 2020; Connor et al., 2023). This thesis and the research study along with the bulk of the literature are focussed on the intravenous method based on risk profile, acceptability and the skills required.

Contrast agents have been used in MRI because of their ability to affect either the T1 or T2 properties of tissues being imaged via MRI. The most common way to produce MR images is to exploit the relaxation properties of hydrogen nuclei (which act as tiny bar magnets in the body) to generate contrast (n.b. not the same contrast implied when the contrast agent is administered) between different tissues. These tiny magnets are aligned along the same axis using a strong magnetic field called B_0 (longitudinal) and then tipped out of that alignment with another magnetic field, B_1, which is perpendicular (transverse) to B_0. Relaxation describes the processes of the net magnetization of hydrogen nuclei returning to alignment with the B_0 magnetic field and this produces a measured signal. The return to alignment has two main components, the transverse and the longitudinal. The transverse component reduces according to T2 (shorter) and the longitudinal component increases according to T1 (longer). The T1 and T2 are relaxation times which depend on tissue properties. Hence, in basic terms, the contrast between different tissues is generated by measuring signal intensity at different points in time leading to T1 or T2-weighted images depending on whether the signal was measured earlier or later during the relaxation. Adding contrast agents allows for manipulation of relaxation times optimising contrast in MR images.

The most common contrast agent is based on gadolinium, introduced in the form of chelate, which suppresses its toxicity, but water molecules can still interact with it and influence the image signal on MRI. Gadolinium shortens both the T1 and T2 times. The T1 effect is mostly used to observe when the contrast agent leaves the bloodstream. By allowing dilute contrast to accumulate within the perilymphatic compartment, where the blood-labyrinth barrier is permeable, outlining the impermeable endolymphatic compartment where there is no contrast and hence very low signal intensity, it is possible to discern between endolymph and perilymph

on an MR scan. Due to the tight junctions aforementioned in the subheading of the overview of the inner ear anatomy, the contrast accumulates in the perilymphatic compartment. It cannot pass into the endolymphatic compartment (Niyazov et al., 2001).

Both IT and IV administration of contrast result in an accumulation of the dilute contrast agent in the perilymph, which appears bright by FLAIR imaging due to its sensitivity to T1 shortening. 3D FLAIR detects signal from the perilymph while suppressing the signal from the endolymph (Naganawa et al., 2008). The membranous labyrinth, impermeable to contrast appears as a signal void on these images, allowing for evaluation of an increase in size of the endolymphatic compartment (EH).

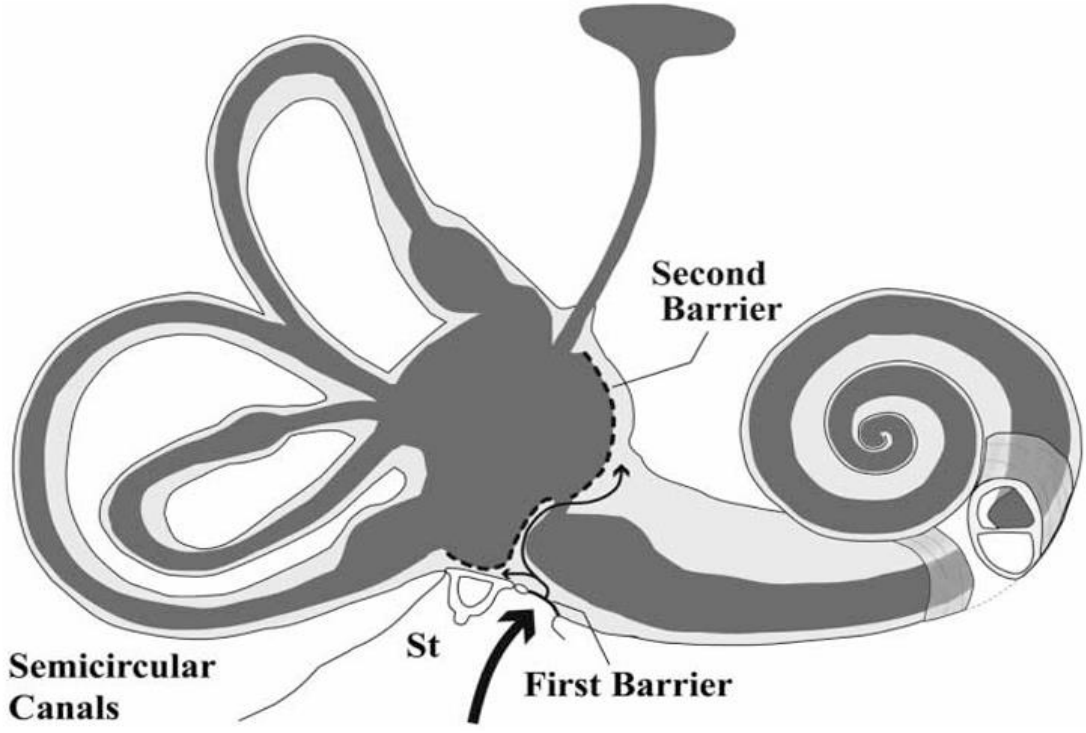

Figure 7 - As described in Nakashima's paper, the path of intratympanically injected GD-contrast, where the round window acts as the first barrier to contrast distribution. When engorged, as in cases of EH, the vestibular endolymphatic space can act as a second barrier reducing the Gd distribution in the semicircular canals and hence signal intensity. This could potentially be the reason why EH in semicircular canals is not as prominent and is not usually considered on MRI. Taken from Nakashima et al., 2009.

The first successful high-quality imaging of the inner ear in Meniere's disease patients with IV Gd-based contrast (a double-dose) was done by Naganawa et al. on a 3T MRI scanner using both 3D FLAIR and 3D Real Inversion Recovery (3D Real IR) imaging technique 4 hours after IV administration. They were able to produce images of sufficient quality and resolution to detect endolymphatic hydrops by using IV contrast (Naganawa et al., 2010). This opened the door for more widespread usage of IV contrast thus eliminating the drawbacks of the intratympanic route of contrast administration. It also allowed for the simultaneous assessment of the contralateral ear.

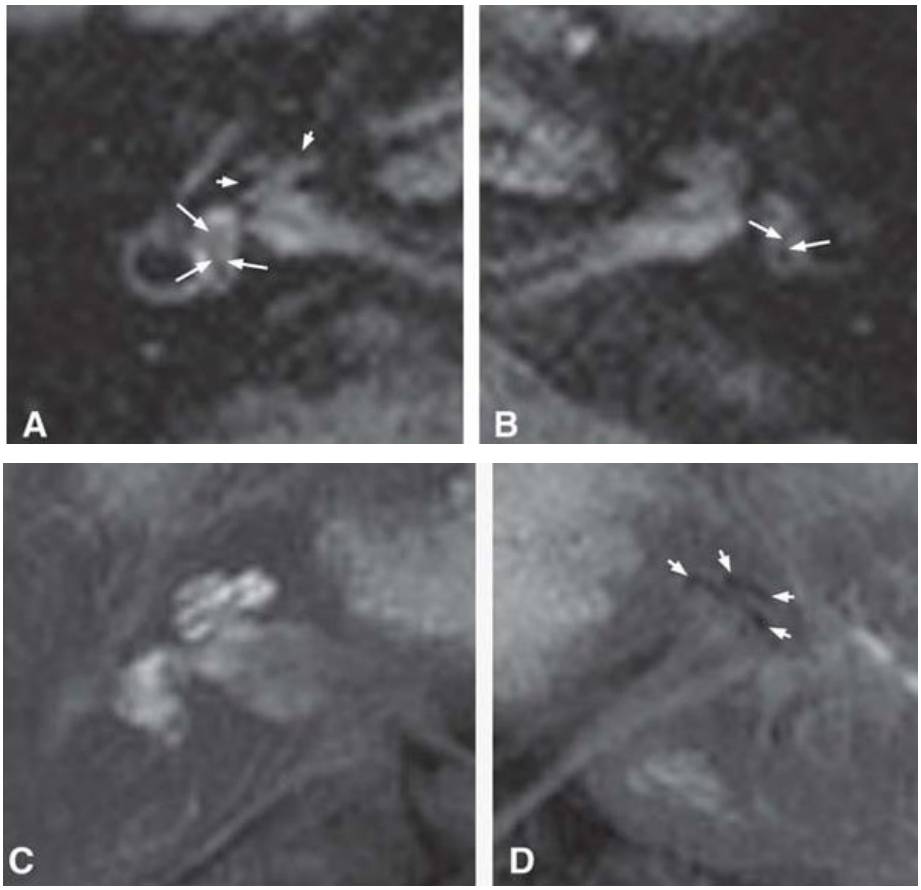

Figures 8 A, 8 B, 8 C and 8 D - An example of the first images depicting endolymphatic hydrops with IV contrast using both 3D FLAIR (8 A and 8 B, 8 A – right ear, 8 B – left ear) and 3D Real IR (8 C and 8 D, 8 C – right ear, 8 D – left ear). Short arrows on both 8 A and 8 D images point to the enlarged unenhanced (dark) area occupied by the endolymph encroaching on the bright, enhanced perilymph indicating cochlear hydrops. In 8 A and 8 B, long arrows indicate endolymphatic space in the vestibule. Taken from Naganawa et al., 2010.

As is visible from the above images, the 3D Real IR provides a much better delineation between endolymph and bone than 3D FLAIR but is very sensitive to the concentration of gadolinium in the inner ear which is lower in the IV route than the IT route as explained next.

A study by Yamazaki et al. described the differences in the cochlear perilymph enhancement between the intravenous and the intratympanic contrast administration method in 61 patients with unilateral Meniere's disease. Both methods were used with a single dose of gadolinium (1 mL/kg). Regions of interest of the cochlear perilymph and the medulla oblongata were determined on each image, and the signal-intensity ratio (SNR) between the 2 regions (the cochleomedullar, or CM ratio) and the differences in the CM ratio between the 2 methods were evaluated on a 3D FLAIR MRI. For clarification, SNR is a measure of the image signal in an area of tissue concerning the background tissue. The Contrast to Noise Ratio (CNR) in an MR image is the contrast between the average image values in a tissue of interest relative to the background and is more commonly used as it's easier to identify the tissue of interest. Both terms will be further explained in the subsequent text of the thesis. In summary, Yamazaki et al found that the perilymphatic enhancement was higher with the intratympanic rather than with the intravenous method (CM ratio 2.98 ± 1.15, vs. 1.61 ± 0.60, $p < .001$), and in patients with unilateral MD who underwent IV-contrast administration, the affected side had a higher contrast effect. Coincidentally, this was not the authors' intention, but, this supports the claim that cochlear perilymphatic enhancement is a reliable MRI descriptor of MD (Yamazaki et al., 2012; Bernaerts et al., 2019; Connor et al., 2023). However, this study didn't comment on the presence and grade of EH. They also did not evaluate the vestibule, with their argument being they 'chose the cochlea for the assessment of inner ear contrast effect because the presumed location of diffusion of intratympanically injected gadolinium from the middle ear is the round window' and hence the contrast would mostly be distributed in the cochlea (Yamazaki et al., 2012). Perhaps, their study could have contributed more to the subject of EH imaging, if they attempted to compare the performance of each method of contrast administration in detecting and grading it.

Li et al. also compared the two methods, in 73 MD patients who received IT contrast and 79 MD patients who received it IV. The detection rate of EH, signal-to-noise ratio (SNR), and contrast-to-noise ratio (CNR) of the two methods were compared, and images were obtained by the 3D real IR sequence and then reviewed by two independent radiologists. On the sample of 152 patients, they found that the SNR in the region of interest (ROI), which they set as the perilymphatic-filled scala tympani of the affected cochlea, and CNRs were almost double in the images obtained using the IT method than those that were obtained using the IV method. They also found that in patients with unilateral MD who received IV contrast, the cochlear perilymph exhibited a greater contrast effect in the affected ear. This further supports the claim that cochlear perilymphatic enhancement could potentially be a reliable MRI characteristic for MD. The brainstem was used as the reference ROI. This means that the reference region was not susceptible to change and was consistent throughout participants. Ultimately, although the images and resolution were superior with the intratympanic method, no statistical significance was found between the two methods regarding the detection rate of both cochlear and vestibular endolymphatic hydrops, $p = .058$ for cochlea and $p = .850$ for the vestibule (Li et al., 2019).

Naganawa et al. conducted a compelling study in which they simultaneously delivered contrast into one ear intravenously (IV side) and into the other ear both intravenously and intratympanically (IT + IV side) to evaluate EH in 10 patients with MD. They then compared a HYDROPS2 image (image processing technique and resultant image explained later in the text), with an image obtained by 3D-Real IR (Naganawa et al., 2013; Naganawa et al., 2014). They found that they could evaluate endolymphatic hydrops in all ears on the HYDROPS2 image but only in the IT + IV side on the 3D-real IR image. This means that the concentration of contrast delivered to the perilymph with the IV method was insufficient to adequately show the perilymphatic space on and subsequently detect endolymphatic hydrops on the MR image on 3D Real IR (Naganawa et al., 2014).

An additional method of delivering contrast into the inner was evaluated by Liu et al. who applied a slightly less invasive intratympanic gadolinium (Gd) delivery through the Eustachian tube of healthy volunteers and then performed 3D-FLAIR MRI proving

the presence of Gd in the inner ear and displaying the endolymphatic space with a visible borderline between the perilymph and the endolymph (Liu et al., 2011).

Lastly, an invasive method of delivering contrast to the inner ear has been described by Coletti et al in their paper where they described an intraoperative delivery of contrast agent to the inner ear directly through the endolymphatic sac (Coletti et al., 2010). This enabled the contrast to be injected directly into the endolymphatic space and provided excellent delineation of the endolymphatic space. However, it is highly invasive and does not rule out the possibility of diffusion or regurgitation of contrast to perilymphatic space via modiolar vasculature or other pathways. It does, however, potentially have a role as an effective treatment strategy for delivering treatment for inner ear conditions.

Most authors use a double dose of GBCA (0.2 mmol/kg, which is an off-label use!) for IV contrast administration which is now predominantly used to increase enhancement and facilitate image representation; but it is possible to obtain high-quality images with a single dose (0.1 mmol/kg) (Suzuki et al., 2011; Connor et al., 2023). The 0.1 mmol/kg dose is however recommended as per the Electronic Medicines Compendium UK, from a safety perspective, and this is what was used in this study (www.medicines.org.uk, n.d.). The dosage of IT-administered GBCA is more difficult to reckon due to the method of the administration itself and is usually expressed as a volume of a diluted (usually 8-fold) gadolinium solution with a known concentration injected in the middle ear. The solution is injected in the middle ear until contrast is seen leaking back in the external ear (Naganawa et al., 2009).

One study done by Suzuki et al. compared the signal intensities with the use of a double-dose (0.2 mmol/kg) GBCA and a single-dose (0.1mmol/kg), which theoretically renders a safer profile, and semi-quantitatively evaluated the contrast enhancement in the basal turn of the cochlea. They concluded that imaging of the endolymphatic space was possible even with a lower (single) dose of contrast agent (Suzuki et al., 2011).

This effectively means that regardless of the method or dose of contrast administration used in the imaging of the inner ear, endolymphatic space and hence, EH, would be displayed albeit with a varying degree of contrast and quality which would affect the interpretation of images. The intravenous route (with both single

and double doses) has now become the most prevalent method in research practice, most likely due to its convenience, availability and reproducibility of results, and the bulk of the literature is reported on IV contrast-enhanced images.

The optimal timing of acquiring the MR scan after IV administration of a Gd-based contrast agent is still not specifically determined as this would require a large cohort of patients across many centres and researchers, but the current consensus states that the images enhanced with a single or a double dose of contrast should be obtained at 4 hours post contrast injection.

Sano et al. were among the first to try and define the optimal point in time for image acquisition post-contrast injection in MD patients after Nakashima's landmark paper. They compared images obtained 10 minutes and 4 hours post-contrast injection. They found that contrast enhancement was superior when the scan was performed 4 hours post-injection of contrast rather than 10 minutes (Sano et al., 2012). Two studies examined the signal intensity in different parts of the brain and cranium of healthy participants, including the cochlear perilymphatic space and labyrinthine perilymphatic space. The first study examined signal intensity at 10 minutes, 4 hours and 24 hours post-IV administration, and found the highest signal intensity in the cochlea at 4 hours, and the other study looked at the signal intensity in the labyrinthine perilymph (along with other spaces in the brain), at 0.5, 1.5, 3, 4.5 and 6 hours post IV contrast administration affirming that the maximum enhancement in the perilymphatic space was achieved at 4.5 hours post-contrast (Naganawa et al., 2020; Naganawa et al. 2014). Another study by the same author suggested that the optimal timing for endolymphatic hydrops contrast-enhanced imaging is between 3.5 to 4.5 hours post-contrast administration. They measured and compared signal intensity ratios (SIR) between perilymph and pons and also graded the EH of 10 MD patients divided into two groups. One group (Group A) had scans 3.5 hours and 4 hours post-contrast administration and the other group (Group B) had scans 4 hours and 4.5 hours post-contrast administration. Although the authors also scanned participants 10 minutes after IV contrast administration, these scans were not included in the results. The EH grading agreed between two observers in both groups and there was no statistical significance. Although the SIR showed a tendency to be higher in later scans (4 hours post-contrast in Group A and 4.5 hours post-contrast in

Group B), this also did not reach statistical significance. The authors implied this observed trend might indicate the optimal timing of the scan to be 4 hours or 4.5 hours post-contrast administration. However, statistical significance eluded them and limited their results (Naganawa et al., 2012). Yet another study by Naganawa et al. assessed the percentage of endolymphatic space 1.5, 3, 4.5, and 6 hours after single contrast administration using subtraction techniques and found that the endolymphatic space appeared larger on images taken 1.5 hours after contrast administration than 4.5 or 6 hours for both cochlea and the vestibule (Naganawa et al., 2014). That could potentially mean that early on the concentration of contrast in the perilymph is not high enough to register a signal, hence the unenhanced area is easily overestimated.

Although the literature suggests a nuanced view with inconsistent evidence, imaging 4 hours after IV contrast administration is the most commonly used post-contrast timing for MR imaging of EH.

2.1.3 DEVELOPMENT OF DIFFERENT MRI ACQUISITION PROTOCOLS FOR EH

The most commonly used MRI techniques for EH imaging today are 3D FLAIR and 3D Real IR with the most common field strength of the MR scanner being 3 Tesla (T) in the vast majority of published literature (Kontorinis et Han, 2022; Connor et al., 2023). They are usually supplemented with a scan for anatomical reference, but they can also be used in subtraction techniques done to enhance the appearance of hydrops or scanning time as explained later in the text (Naganawa et al., 2013, Naganawa et al., 2015). These two imaging techniques have proved to be reproducible in imaging EH across many different centres, scanners, observers and participants (Kontorinis et Han, 2022; Connor et al., 2023).

They are both inversion recovery sequences which means that one of the key parameters for optimal signal intensity is the inversion time (TI), hence this parameter needs to be precisely set.

A recent study by Eliezer et al demonstrated that the assessment of the endolymph to perilymph surface area ratio (semiquantitative criteria in the detection and grading of endolymphatic hydrops explained later) is highly dependent on the TI parameter and adjustment of this parameter can lead to great differences in the grade and location of EH on MR images using the 3D FLAIR technique (Eliezer et al., 2017). Although this parameter can be changed within the confines of a particular scanner machine, not every manufacturer offers the same options for TI intervals as different vendors have different limits to the TI parameter. Relative uniformity is still achieved as in the majority of reported literature, the TI value is set between 2000ms and 2500ms for the inversion recovery sequences used to image EH (Eliezer et al., 2017).

As explained earlier in the text, the main feature that helps us detect EH on MR imaging is the delineation between endolymph and perilymph. Most adjustments in the image acquisition sequences have been focussed on improving this characteristic on an MR image as well as shortening the scanning time. Although the physics of MRI are outside the scope of this thesis, a basic description of the principles of scanning and image acquisition parameters and their role in the development of EH image acquisition protocols are defined and explained below.

As explained earlier, MRI operates on the principle that the net magnetisation of all the protons (hydrogen nuclei) in the water molecules (more generally, MRI can do

this for any spin-½ nucleus) in the body are aligned by putting the patient into a homogenous magnetic field (B_0) along a single axis. These aligned protons are then tipped away from this axis of alignment into a new axis perpendicular to the B_0 magnetic field. This is called excitation and is achieved by a radiofrequent pulse of another, temporary, magnetic field called the B_1 field. Alternatively, in inversion techniques, the net magnetisation is completely tipped to point in the opposite direction to the B_0 field. The new net magnetisation can now be measured as a signal. Repetition time (TR) is the time taken between excitations of the same region. Echo time (TE) is the time taken between the excitation and the measuring of the signal. Inversion time (TI) is the time during which the longitudinal magnetization recovers towards its initial value, after the inversion pulse. The rate at which this recovery occurs is determined by the tissue's T1 relaxation time. The flip angle is the angle that the magnetization vector is tipped to by a radiofrequency pulse, relative to the main magnetic field. Smaller flip angles favour T2 weighting whereas larger flip angles favour T1 weighting.

Firstly, lengthening the inversion time (TI) was employed because a longer inversion time suppresses the signal from endolymph. As Naganawa et al. demonstrated in their work, the adjustment of TI can produce both perilymph-enhancing (long TI) and endolymph-enhancing (short TI) images which they employed to better describe the perilymph-endolymph-bone delineation. They also used this property to develop their subtraction-enhanced HYDROPS imaging protocol which is described later in the text (Naganawa et al 2008; Naganawa et al., 2013). Currently, in the literature on hydrops imaging, the TI values range from 2000ms to 2500ms (Nakashima et al., 2009; Naganawa et al., 2009., Liu et al., 2012; Barath et al., 2015; Bernaerts et al., 2019).

Secondly, an increase in the TR better suppresses the signal from CSF and improves the signal intensity ratio (SIR) and signal-to-noise ratio (SNR). This has been corroborated in a sequence development study by Zou et al where the image quality and SIR were consistently higher in the images acquired with a longer TR (12000-16000ms). Also, the longer TR images showed higher sensitivity across different concentrations of gadolinium contrast and also provided better delineation between

perilymph and endolymph (Kato et al., 2019; Zou et al., 2022). Increasing TR, however, comes at the slight expense of increasing scanning time.

Thirdly, TE can be increased to produce a heavy T2-weighted image which, theoretically, should be more sensitive to low concentrations of Gd. This has been explored in several developmental studies with contrast-enhanced images, but also in non-contrast-enhanced imaging studies as will be detailed later in the text (Naganawa et al., 2008; Homann et al., 2015; Simon et al., 2017).

Lastly, reduced (usually variable) flip angle techniques with turbo spin echo (TSE) sequences were employed to shorten scanning times and comparable CNRs were provided by the introduction of head coils with higher numbers of channels (Nakashima et al., 2007; Naganawa et al., 2008; Naganawa et al., 2014). These sequences have vendor-specific names (SPACE -Siemens, CUBE-GE, VISTA-Philips). The number of head coil channels in MR machines used for EH imaging has increased from 8 to 32 and 48 since Nakashima's landmark paper as the machines became more technologically advanced providing superior imaging capability. Currently, the majority of studies reporting on EH imaging utilise a 32-channel head coil (Nakashima et al., 2007; Barath et al., 2015; Fukutomi et al., 2022).

Additionally, different generic MRI acceleration techniques have been employed in various studies over the years to reduce scanning time while maintaining image quality and resolution, but the description of these falls outside of the scope of this thesis.

Nakashima and his research group first introduced 3D FLAIR as a technique of choice in EH imaging before experimenting with different variations and tried to compare 3D FLAIR CONV (conventional turbo spin echo) and 3D FLAIR VFL (variable flip angle) with longer echo trains hence shorter scanning time (Nakashima et al., 2007; Naganawa et al., 2009). This feature enabled its previous use in inner ear disorders hence why they tried to use it for EH imaging. CNR was defined by the difference in the signal of the basal turn of the cochlea and cerebellum divided by the standard deviation (SD) of the air signal. They compared CNR in 3D FLAIR CONV and 3D FLAIR VFL. 3D FLAIR CONV had higher CNR and correlated better with clinical diagnosis. The size of endolymphatic space in the vestibule was the same for both techniques in all cases, but it was not the same in the cochlea in 3 cases, possibly due to lower in-plane

resolution in FLAIR VFL. Images were evaluated independently by two radiologists, but no inter-observer agreement was reported. Additionally, there was no mention of controls, as all participants were MD patients, but even their contralateral ears (potentially normal) were not mentioned in the analysis. They concluded that 3D FLAIR VFL as it stood, is of insufficient quality to compare with images obtained via 3D FLAIR CONV which performed better in the imaging of endolymphatic hydrops (Naganawa et al., 2009).

The main drawback of 3D FLAIR was poor delineation between endolymph and surrounding bone which prevented more precise quantification of endolymphatic space (Nakashima et al., 2007; Naganawa et al., 2008). In 2008, Naganawa et al. introduced 3D Real IR in inner ear imaging to address this problem. In their study they compared 3D FLAIR and 3D Real IR images; the latter were obtained by setting the TI between the null point of Gd-containing perilymph fluid and the Gd-free endolymph fluid, the signal from the perilymph could be reduced and from the endolymph maximised so the border between bone and endolymphatic space could be visualised. As the suppression of fluid without Gd could be achieved with a TI of 2,500 ms on 3D-FLAIR images, a **TI of 1,700 ms**, which is near the midpoint between 1,000 ms (which nulls the signal of Gd-containing perilymph) and 2,500 ms, was selected to assign positive longitudinal magnetisation to perilymphatic fluid, negative longitudinal magnetisation to endolymphatic fluid and zero magnetisation to compact bone and air' resulting in an image which depicts endolymph as black, perilymph as white and bone as grey on 3D Real IR. This reduction in TI has effectively facilitated bone-endolymph-perilymph delineation and optimal image quality for EH detection and grading (Naganawa et al., 2008). In 2009, the same research group imaged the inner ears of patients with inner ear disease by using both the 3D FLAIR and 3D Real IR enhanced with intratympanic Gd-contrast of different dilutions and compared the results. They used both 8-fold diluted and 16-fold diluted Gd-based contrast. Patients included in the study (n=73), were afflicted with an array of conditions, i.e. idiopathic SSNHL, MD, delayed EH, fluctuating hearing loss without vertigo, or acute hearing deterioration with large vestibular aqueduct syndrome. The authors also used the contemporary American Academy guidelines for diagnosing MD. Despite clinical heterogeneity, the authors were able to ascertain that the 3D

real IR MRI was generally better than 3D FLAIR MRI for visualizing the endolymphatic space after intratympanic Gd injection because the 3D-real IR MRI could discriminate the perilymphatic and endolymphatic space from the surrounding temporal bone. The authors compared perilymphatic enhancement on images obtained with both 16-fold and 8-fold gadolinium dilutions and concluded the enhancement was fainter with the 16-fold diluted contrast. However, when Gd concentration was lower in the perilymph (16-fold vs 8-fold dilution), it was more difficult to visualize the Gd in 3D-real IR than in 3D-FLAIR MRI. The Gd concentration in the perilymph after intratympanic administration of the 8-fold Gd dilution was estimated to be 0.1 mmol/L, which is 5000 times the concentration of the original Gd fluid. Thus, the Gd concentration was 625 times less in the perilymph than in the intratympanic Gd fluid. Both the 3D-real IR and 3D FLAIR allowed the observation of various degrees of EH in the basal and upper turns of the cochlea and, in the vestibular apparatus, both techniques demonstrated significant EH using MRI in patients with 'probable' MD after Gd injection. The overall conclusion drawn was that although 3D Real IR provides better delineation between perilymph, endolymph and surrounding bone, and is potentially superior to 3D FLAIR in detecting and grading EH, it is quite sensitive to low Gd concentration (Naganawa et al., 2008; Nakashima et al., 2009). However, both studies were limited by a lack of reporting on quantitative analysis (SIR, SNR, CNR) and inter- or intra-observer agreement.

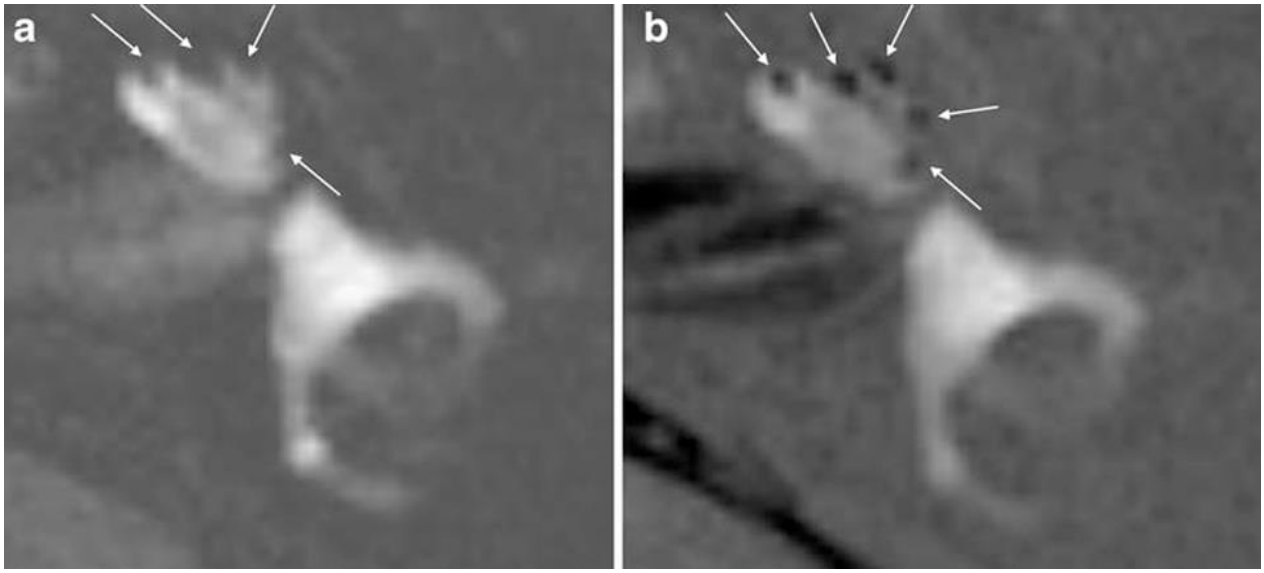

Figures 9 A and 9 B - A 33-year-old man with delayed endolymphatic hydrops. All images were obtained 24 h after the intratympanic injection of Gd DTPA. 9 a: 3D-FLAIR (TI 2,500) shows enlarged endolymphatic space in the cochlea (arrows), but not in the vestibule. The boundary between endolymphatic space and surrounding bone is unclear. 9 b: A 3D-real IR sequence (TI 1,700) visualises severely enlarged endolymphatic space in all cochlear turns (arrows) as negative signal intensity values, while the surrounding bone area has near zero signal intensity. This image makes possible the delineation of the scala media (negative signal intensity; black on this image) from perilymph space (scala tympani and scala vestibuli with positive high signal intensity; white on this image) and surrounding bone (near zero signal; grey on this image) on a single image. Taken from Naganawa et al., 2009.

A more recent study by Suárez Vega et al. built on this and expounded by describing and comparing both the 3D FLAIR and 3D Real IR imaging techniques in MRI detection of EH by reporting on the concordance between observers (using Cohen's *kappa* K statistic) of both hydrops detection and hydrops severity using both techniques. On a sample of 41 MD patients (20 definite and 21 probable), using single-dose IV contrast they demonstrated that both techniques detected EH in 100% of clinically 'definite' MD patients, but the EH detection rate was higher with 3D Real IR in the clinically 'probable' group which showed consistent lower severity of hydrops. They did not, however, report on the prevalence of EH in asymptomatic ears. The overall agreement (*kappa* value) between both sequences was 0.821 ($p<0.01$) with a higher

agreement in the vestibule than in the cochlea (0.658 vs 0.393) which is consistent with the literature (Bernaerts et al., 2019). The 3D Real IR technique also demonstrated higher sensitivity in the detection of EH in the cochlea (Suárez Vega et al, 2020). These results suggest that EH in the cochlea is more challenging to identify and grade, but that 3D Real IR appears to be a more promising technique in EH detection and grading of cochlear hydrops. This was corroborated in another study (Bernaerts et al., 2019). EH can be present in both the cochlea and the vestibule or just one of them, cochlea and vestibule are both subparts of the inner ear as per anatomical recount in the introduction.

Previously, only IT contrast was used in EH imaging, because the concentration of Gd in the perilymph with a single dose IV contrast-enhanced image was too low to be detected with a 3D FLAIR technique (Tagaya et al., 2010). As detailed in the subheading regarding contrast, the IT administration has a lot of drawbacks compared to IV, hence there was clear motivation to find a way to successfully image EH using IV contrast-enhanced MRI. In 2010, the heavy T2-weighted 3-dimensional fluid attenuated recovery (hT2w 3D FLAIR) MR imaging technique was introduced to facilitate EH imaging following IV contrast administration (Naganawa et al, 2010). The authors used the fact that even after IT contrast administration, both endolymph without Gd and perilymph with high Gd concentration are shown as high signal areas on heavily T2-weighted Magnetic Resonance Cisternography (MRC), hence the T2 value of fluid with very low Gd concentration is, at least theoretically, long enough to be detected by a heavily T2-weighted sequence. This concept was used to visualise the perilymph which has a much lower concentration of Gd after IV administration. Their sequence was optimised on phantoms (filled objects calibrated as per varying concentrations of Gd in saline) and then tested on 18 human subjects suspicious of having EH (grade not taken into account). All but one participant, who received a single dose due to advanced age (0.1 mmol/kg), received a double dose of IV Gd-based contrast agent. The authors optimised the CNRs on the phantom study for each different Gd concentration calibrating values of TR (repetition time), TE (echo time) and flip angle values before settling for TR of 9000 ms, TE 540 ms and flip angle of 120°.

Their image analysis consisted of circular ROIs drawn in the basal turn of the cochlea and posterior ampullar endolymph (both 1 mm) for signal intensity ($SI_{perilymph}$ and $SI_{endolymph}$) as these are most anatomically replicated structures containing perilymph and endolymph, respectively. Noise was defined as the standard deviation of the artefact-free air area (SD_{noise}) near the ipsilateral external ear (ROI 5 mm). Contrast to noise ratio (CNR) was defined as $SI_{perilymph}$ - $SI_{endolymph}$ divided by SD_{noise}.

They compared the hT2w 3D FLAIR sequence to the 3D FLAIR CONV sequence in human subjects and results showed that the mean CNR between perilymph and endolymph was greater with hT2w 3D FLAIR than with 3D FLAIR CONV (59.2 vs 23.1, p<0.01). The interobserver agreement between two readers interpreting images, expressed as kappa values for both cochlear and vestibular endolymphatic recognition, was also greater with hT2w 3D FLAIR than RD FLAIR CONV (0.833 vs 0.34 for cochlea, and 0.903 vs 0.823 for vestibule). Interestingly, in the images of a patient who received a single dose of GBCA, EH could only be visualised on the hT2w 3D FLAIR sequence. This effectively demonstrated that the hT2w 3D FLAIR was more sensitive to the faint enhancement of low-concentration gadolinium. Additionally, the scanning time of hT2w 3D FLAIR was shorter compared to 3D FLAIR CONV, 10.7 min vs 15 min (Naganawa et al., 2010). Their results have been corroborated and expounded in a further study where anatomically appropriate visualisation of enlarged endolymphatic space as a negative signal, perilymphatic space containing diffused Gd as a high signal, and surrounding bone as zero signal in all patients were provided using the same hT2W 3D FLAIR sequence with all participants (n=3) receiving only single dose of IV GBCA (Naganawa et al., 2010).

Their work showed promising results in terms of quicker, safer and logistically easier (single dose and IV administration of contrast) endolymphatic hydrops imaging.

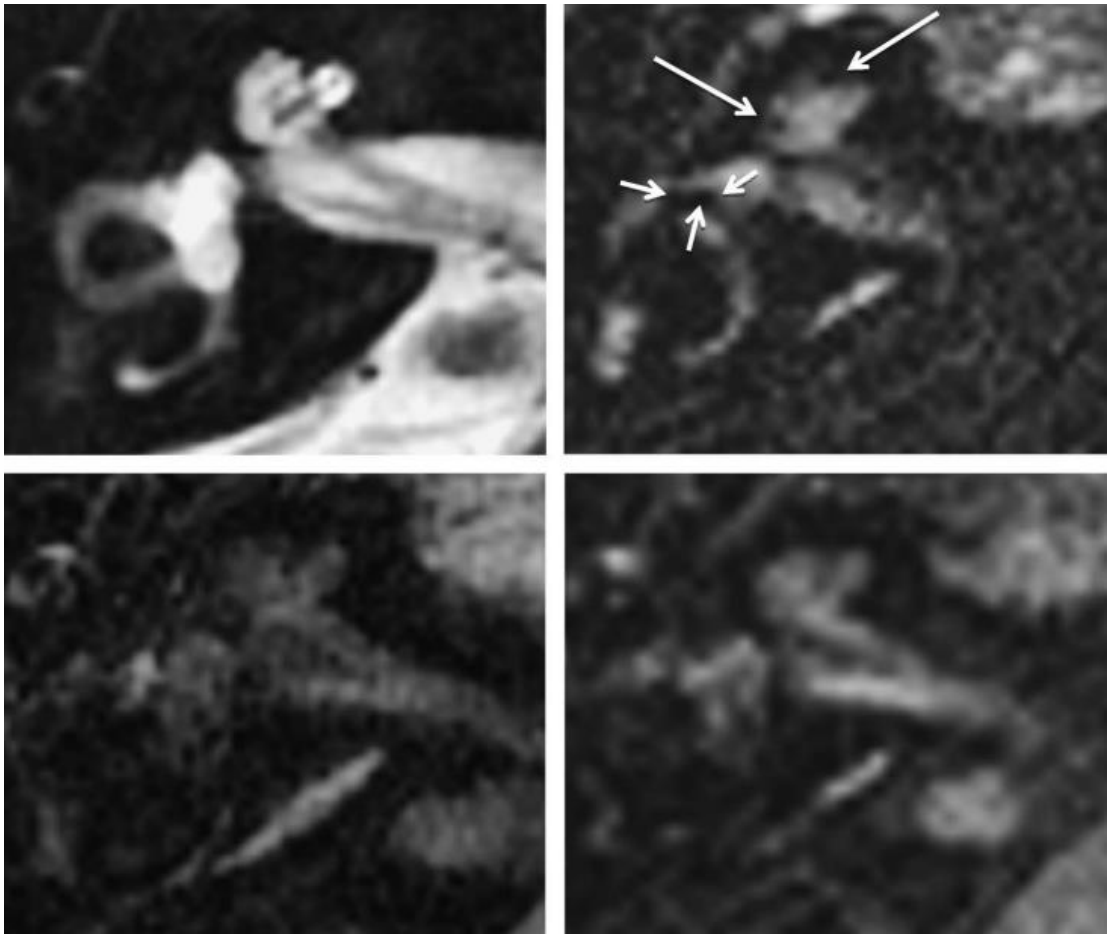

Figure 10 - Comparison of different techniques from the above study. In the upper left corner is an example of MR cisternography of the inner ear showing the entire fluid-filled space. In the upper right corner is the hT2w 3D FLAIR image displaying significant EH in the cochlea (long arrows) and non-dilating endolymphatic space in the vestibule represented with the ampoule of LSCC. In the bottom left corner, an image obtained using a 3-dimensional FLAIR conventional turbo spin echo sequence (3D FLAIR CONV) is visible, but the perilymphatic enhancement is so faint that it is impossible to distinguish the endolymphatic space. In the bottom right corner, an image obtained with 3D FLAIR using variable flip angle turbo spin-echo sequence (3D FLAIR VFL) shows stronger perilymphatic enhancement than 3D FLAIR CONV, but it is still impossible to accurately assess the endolymphatic space. Taken from Naganawa et al., 2010.

Naganawa et al. then compared the detection rates of endolymphatic hydrops between 2D Real IR and 3D Real IR as 2D Real IR is more easily implemented on

various manufacturers' scanners and there is a varying degree of software and hardware flexibility in replicating protocols between scanners of different manufacturers. They established that both techniques were likely sufficient to detect and adequately grade endolymphatic hydrops, although 2D images were noisier, with the added benefit of the 2D Real IR scan time being one-third of the 3D Real IR (6 minutes vs. 15 minutes). All patients (n=9) were also scanned using the 3D FLAIR technique. CNR was defined as the difference between perilymphatic and endolymphatic signal intensity divided by the standard deviation of the ROI in the ipsilateral cerebellar peduncle (noise). Both endolymphatic and perilymphatic ROIs were placed in the vestibule, ROI=2 mm for endolymph and ROI=1 mm for perilymph, and the ROI for the ipsilateral cerebellar peduncle was 3 mm. The authors suggested that if only the centre of the labyrinth was scanned with 3 or 4 slices the scanning time could be as short as 2 minutes. However, almost all of the participants (8 out of 9) had significant hydrops, which means it was easier to detect and a 2D Real IR might not have detected a lower degree of hydrops. Furthermore, in one patient the cochlea only showed faint enhancement insufficient to detect hydrops on 2D and 3D Real IR images, but hydrops were detected on 3D FLAIR. Similarly, in one patient where mild hydrops was detected in 2D and 3D Real IR images, it was not detected in 3D FLAIR. The mean CNR between perilymph and endolymph values were higher in 3D Real IR than in 2D Real IR, which in turn demonstrated higher values than 3D FLAIR (17.0 vs 11.2 vs 6.7) although statistical significance was not mentioned. The three radiologists evaluating images completely agreed in their grading of all the assessed cochleas and vestibules. These results suggest that 2D or 3D Real IR and 3D FLAIR images might still potentially complement each other (Naganawa et al., 2011).

The same authors further experimented with different image processing techniques by building on their previous work where they demonstrated that the filling defect in the endolymphatic space observed with 3D-FLAIR after IT injected contrast material is not due in part to a volume artefact of bone or air, by shortening the inversion time of the 3D-FLAIR to suppress the signal of the perilymph. Consequently, the signal from the endolymph increased while the signal from surrounding bone and air remained low providing a positive endolymphatic image (PEI) (Naganawa et al., 2008; Naganawa et al., 2013). The authors employed MR Cisternography (MRC), hT2W 3D

FLAIR with an inversion time of 2250 ms (positive perilymph image, PPI), and hT2W-3D-IR with an inversion time of 2050 ms (positive endolymph image, PEI) 4 hours after intravenous administration of single-dose gadolinium-based contrast. They manually drew the outer border of the inner ear fluid space on MR cisternography and fused this region of interest to an IV contrast-enhanced 3D Real-IR MR sequence-like image. They subtracted the PEI from the PPI and were able to produce an image of endolymphatic hydrops (HYDROPS -HYbriD of the Reversed image Of the Positive endolymph signal and a native image of the positive perilymph Signal) with superior quality allowing for more accurate measurement of the size of endolymphatic space (figure 11). The same authors used this technique to image EH in MD patients using a 1.5 T MRI scanner (Naganawa et al. 2013). HYDROPS2 imaging was subsequently proposed to shorten the scan time while retaining a similar contrast as HYDROPS. HYDROPS2 images are generated by the subtraction of MR cisternography from the positive perilymphatic image (figure 12). To further increase the CNR another image was created by multiplying MRC onto the HYDROPS image. This resulted in almost a 200-fold increase in CNR between perilymph and endolymph. The resultant image was called HYDROPS-Mi2(hydrops multiplied by T2) (figure 13). By using specific image-processing techniques, in their sample size (n=24) they demonstrated that these techniques might enable superior, and potentially quicker, semi-quantification of endolymphatic size with little observer dependency (Naganawa et al., 2010; Naganawa et al., 2013).

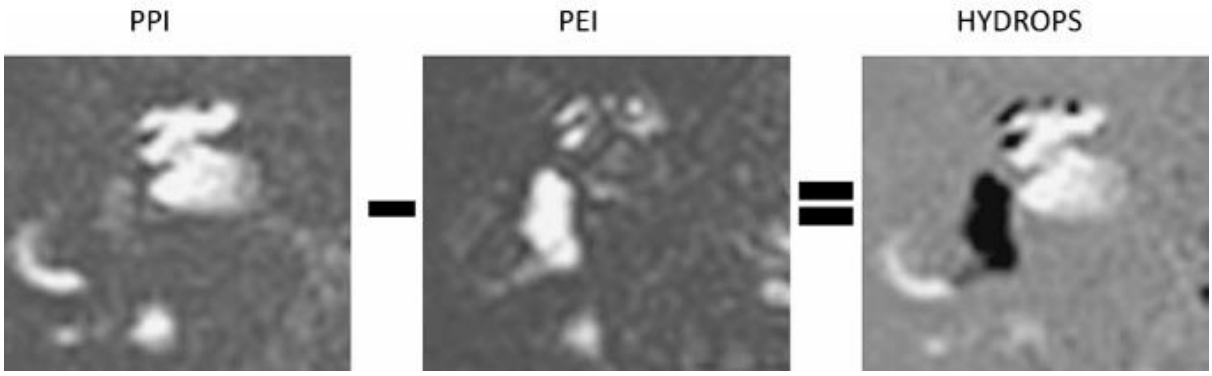

Figure 11 - A conceptual diagram of the HYDROPS image created in the above paper by subtracting PEI (positive endolymphatic image) from PPI (positive perilymphatic image). Taken from Naganawa et al., 2013.

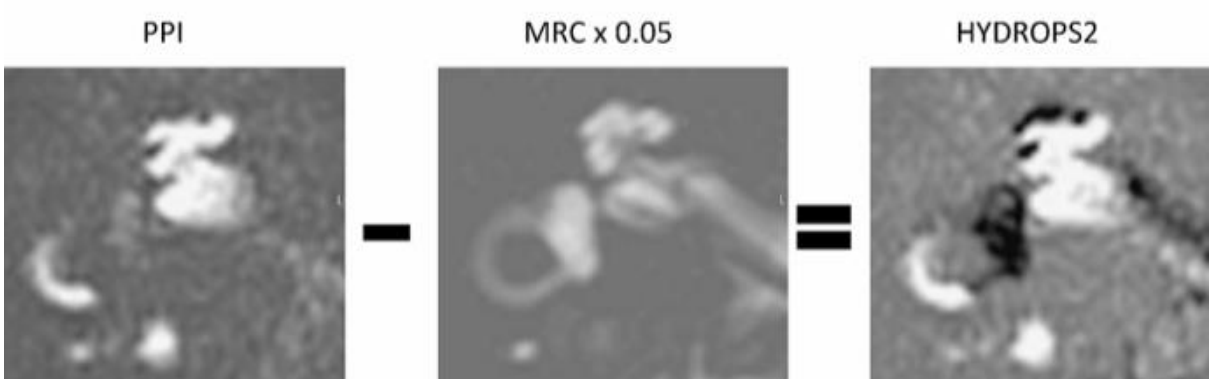

Figure 12 - A conceptual diagram of the HYDROPS2 image created in the above paper by subtracting the MRC (magnetic resonance cisternography) from the positive perilymphatic image. Taken from Naganawa et al., 2013.

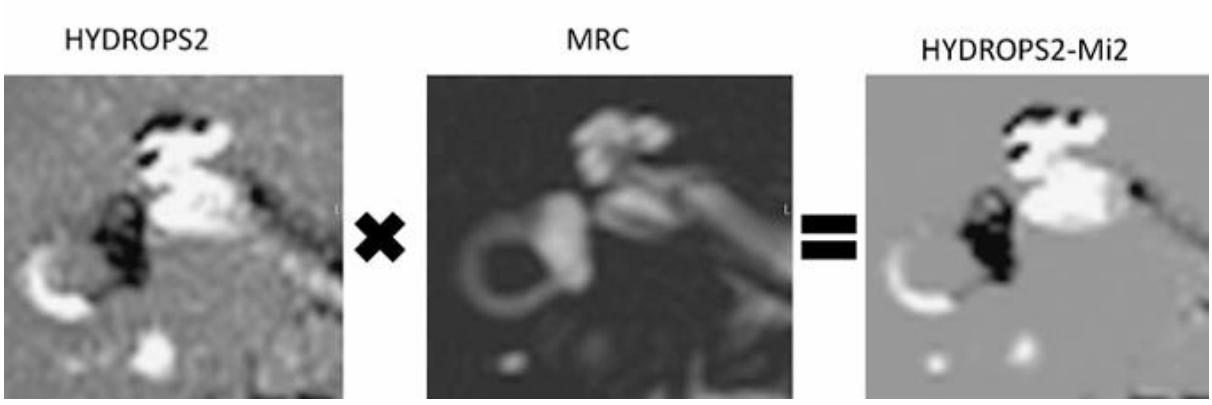

Figure 13 - A conceptual diagram of the HYDROPS-Mi2 image created in the above paper by multiplying the MRC (magnetic resonance cisternography) onto the HYDROPS image. Notice the black, unenhanced endolymph starkly demarcated form the white, enhanced perilymph whilst the background remains uniform in signal intensity providing optimal CNR. Taken from Naganawa et al., 2013.

Two years later, Naganawa et al. proposed an even faster scanning protocol than HYDROPS-Mi2 which cut down the image acquisition time from 31 minutes to 10 minutes. With the obvious benefit of making the scan more practical and easier to fit into a busy clinical setting. This was achieved by generating an image consisting of a positive perilymphatic image (PPI – explained earlier in the text) with a reduced number of excitations (7 minutes) and an MR cisternography image (3 minutes) which brought the total image acquisition time to 10 minutes.

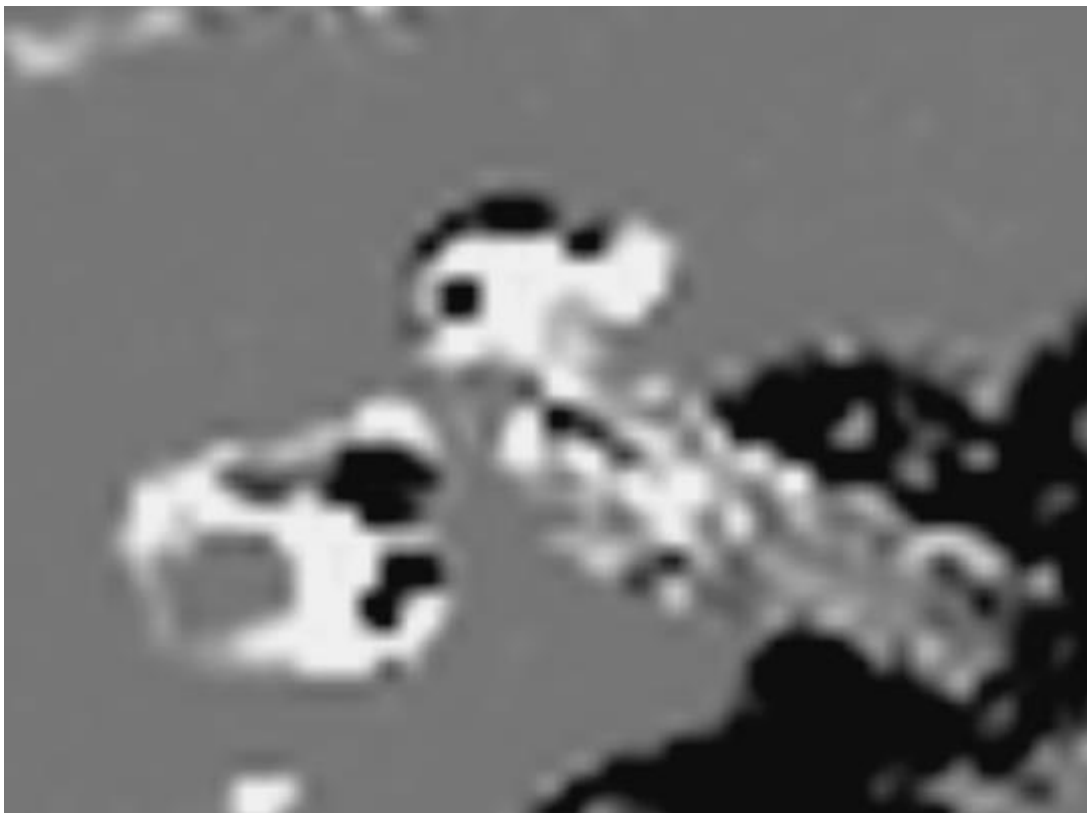

Figure 14 - An example of a 10-minute image derived from the HYDROPS Mi2 protocol. Even with a shorter image acquisition time and even though the size of the endolymphatic space is smaller, the image quality is good enough to appreciate cochlear EH and endolymphatic space in the vestibule. Taken from Naganawa et al., 2015.

Naganawa et al. further expounded on this idea and built on their previous work with hT2w 3D FLAIR and HYDROPS by experimenting with an even shorter image acquisition protocol and volumetric assessment after IV contrast. They performed MR

imaging of 40 ears in 20 patients with clinically suspected EH and calculated ratios of endolymphatic space to total lymphatic space. They found a strong linear correlation between the longer image acquisition protocol (18 minutes) and a shorter image acquisition protocol (HYDROPS2-Mi2), which took only 8 minutes, indicating that images of good quality could be generated with a reduced scanning time (Naganawa et al., 2013, Naganawa et al.,2015; Naganawa et al., 2015).

Moreover, the same research group has explored an innovative technique of further reducing the scanning time by evaluating the feasibility of a simple estimation for the endolymphatic volume ratio (endolymph volume/total lymph volume = $\%EL_{volume}$) from an area ratio obtained from only one slice ($\%EL_{1slice}$) or three slices ($\%EL_{3slices}$). They compared these estimations to actual measurements obtained by using IV contrast-enhanced previously reported HYDROPS2-Mi2 image acquisition protocol. This does not constitute an image acquisition protocol adjustment *per se* but is rather an innovative way of shortening scanning time. A strong linear correlation was observed between the $\%EL_{volume}$ and the $\%EL_{3slices}$ or the $\%EL_{1slice}$ in both the cochlea and the vestibule. High intra-class correlation coefficients (0.991-0.997) between the endolymph volume ratios by two observers were observed in both the cochlea and the vestibule for values of the $\%EL_{volume}$, the $\%EL_{3slices}$ and the $\%EL_{1slice}$ which would indicate good reliability (Naganawa et al., 2016). This study was included in the review because it demonstrated an innovative way of accelerating not the image acquisition, but analysis and interpretation which improves feasibility in assessing for EH on MRI. Whilst initially only detected by MR scanners with 3 Tesla (3 T) strengths which are usually not available in routine clinical use, a recent study has shown that it is possible to image the inner ear and detect EH using a 1.5 T scanner after IV contrast administration. The 1.5 T MR scanner is the work-horse MR scanner in most hospitals and accounts for 71.3% share of the global market of MRI machines; hence its use in the detection and grading of EH could greatly help in developing a widely applicable scanning protocol (Global Market Inc., n.d). The study was performed on 5 ‘clinically definite’ and 4 ‘clinically probable’ MD patients using a four-hour delayed double-dose IV gadolinium-enhanced MRI 3D FLAIR sequence. EH was detected in all but one participant with ‘probable’ MD, but the quality of the pictures was reduced by motion artefacts in that particular case (Kenis et al., 2022). However, Grieve et al. were the

first to image EH with the use of a 1.5 T MRI scanner years earlier, albeit following IT contrast administration. They used phase-sensitive inversion recovery (PS-IR) MRI following intratympanic injection of Gd-contrast and the data were imaged by real inversion recovery (Real IR) which permitted delineation between bone, unenhanced endolymph and enhanced perilymph. Their scanning time was, however, quite long (45 minutes), but they did not report that a single image had been rendered unsuitable for analysis due to motion artefacts (Grieve et al, 2012).

Furthermore, Naganawa et al. also imaged EH in MD patients with a 1.5 T magnetic field strength MR scanner with the subtraction technique of providing the HYDROPS image, explained earlier in the, but with lower contrast and quality (Naganawa et al., 2013; Naganawa et al., 2013). Nonetheless, they were still able to recognise and grade EH in all 20 participants (Naganawa et al., 2013). Gurkov et al. conducted a study on 30 patients in 2021 in which they showed that the vestibular endolymphatic space was delineated and differentiated from the perilymphatic space in all 30 patients using a 1.5 T MRI scanner. They did, however, use the more invasive IT route of contrast administration. EH was not detected in the cochlea of 7 patients and in the vestibule of 8 patients (Gurkov et al., 2021). The majority of 1.5 T studies used the intratympanic route of contrast administration, potentially, in anticipation of lower SNR in lower-strength MR scanners and higher concentrations of gadolinium in the inner ear following IT administration. Additionally, the scanning time was markedly longer in earlier studies (Naganawa et al., 2013; Grieve et al., 2012). Only one study demonstrated EH detection with 1.5 T MRI using IV contrast and offering a comparable scanning time of 14 minutes (Kenis et al., 2022). Given that 3 T MR scanners are rarely available in routine clinical practice outside research settings, the successful imaging of EH on a 1.5 T MR scanner potentially enables the more widespread use of MRI to detect EH and diagnose MD in routine clinical practice.

2.1.4. DIFFERENT GRADING CRITERIA FOR ENDOLYMPHATIC HYDROPS–

Although initially the grading criteria were proposed as a means of standardisation of evaluation of EH, subsequent research has confirmed that radiological grading of hydrops correlates well with audio-vestibular symptoms and when combined with other imaging characteristics, can potentially help distinguish between MD and other audio-vestibular conditions (Nakashima et al., 2009; Gurkov et al., 2011; Barath et al., 2014; Sepahdari et al., 2015; Homann et al., 2015; Wang et al., 2020; Van Steekelenburg et al, 2020; Connor et al., 2023).

Several grading criteria have been suggested and used for the evaluation of EH. They all have their advantages and disadvantages.

The first semiquantitative criteria proposed by Nakashima et al. in their pivotal study and later expanded and refined in a subsequent publication, are straightforward and easily applicable, they have been corroborated by temporal bone histopathology samples and show a good correlation with the volumetric quantification of EH (Nakashima et al., 2007; Nakashima et al., 2009; Naganawa et al., 2010, Connor et Pai, 2021). The presence of EH is characterised as enlarged negative-signal spaces in the labyrinth using 3D FLAIR or 3D Real IR after GBCA administration. The main principle of Nakahima's grading criteria is that the vestibule and cochlea are evaluated separately and the unenhanced endolymphatic area in each of these components is evaluated concerning the enhanced perilymphatic area in the corresponding component (Nakashima et al., 2008; Naganawa et al., 2010; Naganawa et al., 2014).

The Nakashima grading criteria are represented in the table below (Table 4).

GRADE OF HYDROPS	*Vestibule (area ratio *)*	*Cochlea*
None	<33.3%	No displacement of Reissner's membrane.
Mild (Grade 1)	>33.3%, ≤50%	Displacement of Reissner's membrane. Area of cochlear duct ≤ area of the scala vestibuli.
Significant (Grade 2)	>50%	The area of the cochlear duct exceeds the area of the scala vestibuli.

Table 4 - Nakashima grading criteria for endolymphatic hydrops. Taken from Nakashima et al., 2009.

** Ratio of the area of the endolymphatic space to that of the total fluid space (sum of the endolymphatic and perilymphatic spaces) in the vestibule measured on tracings of images.*

The **vestibular component** is recorded at the inferior aspect of the lateral semicircular canal (the most inferior slice which captures at least 240 degrees of the LSCC) and graded as a percentage of the area of endolymph relative to the total fluid area (**grade 1**: 33-50%; **grade 2**: >50%). The **cochlear component** is graded as a measurement of displacement of the Reissner's membrane (**grade 1**- cochlear duct < scala vestibuli; **grade 2**- cochlear duct > scala vestibuli) (Nakashima et al. 2007). Two years later, in 2009, they expanded their criteria to a three-stage grading system in the vestibule and the cochlea: **none**, **mild**, and **significant**. In the vestibule, the grading was determined by the ratio of the area of endolymphatic space to the vestibular fluid space (sum of the endolymphatic and perilymphatic spaces). Patients with no hydrops have a ratio of one-third or less, those with mild hydrops have between one-third and a half, and those with significant hydrops have a ratio of more than 50%. In the cochlea, patients classified as having no hydrops show no displacement of Reissner's membrane; those with mild hydrops show displacement of Reissner's

membrane, but the area of the endolymphatic space does not exceed the area of the scala vestibuli, and in those with significant hydrops, the area of the endolymphatic space exceeds the area of the scala vestibuli (Nakashima et al., 2009). However, the vestibular section is influenced by minor changes in section selection due to the orientation of the utricle in the axial plane, and the cochlear component is affected by artefacts from inter-scalar septa (Sepahdari et al., 2015; Fang et al., 2012).

Barath et al. suggested slightly different semiquantitative grading criteria in 2014, where the **vestibular component** is recorded at the widest part of the vestibule and hydrops is diagnosed if >50% area of total fluid area is occupied by unenhanced endolymph (**grade 1** – perilymphatic space still visible; **grade 2** – vestibule entirely replaced by unenhanced endolymph). The **cochlear component** is assessed as the dilatation of the cochlear duct (**grade 1** – spares part of scala vestibuli; **grade 2**-replaces scala vestibuli) (Barath et al., 2014). These are quite similar to the Nakashima criteria for cochlear hydrops, but it is sometimes quite difficult to assign a specific grade to cochlear hydrops if the image quality is not optimal as it might not be visible on such small structures how much of the scala vestibuli is replaced with the engorged, unenhanced endolymphatic scala media (scala vestibuli completely replaced, area of scala media greater than the area of scala vestibuli etc.).

The Barath criteria are represented below in Table 5.

GRADE OF HYDROPS	*Vestibule (area ratio *)*	*Cochlea*
None	<50%	No endolymphatic (cochlear duct) dilation and no obliteration of scala vestibuli.
Mild (Grade 1)	>50%	Irregular dilation of the cochlear duct and partial obliteration of the scala vestibuli.
Significant (Grade 2)	Complete effacement of the perilymphatic vestibular area.	Total obliteration of the scala vestibuli.

Table 5 (on the previous page) – Barath EH grading criteria

** Ratio of the area of the endolymphatic space to that of the total fluid space (sum of the endolymphatic and perilymphatic spaces) in the vestibule measured on tracings of images. Adapted from Barath et al, 2014.*

The Barath criteria are further represented in Figures 15 A, 15 B and 15 C with schematic drawings alongside actual MR images of different stages of hydrops. Taken from Barath et al, 2014.

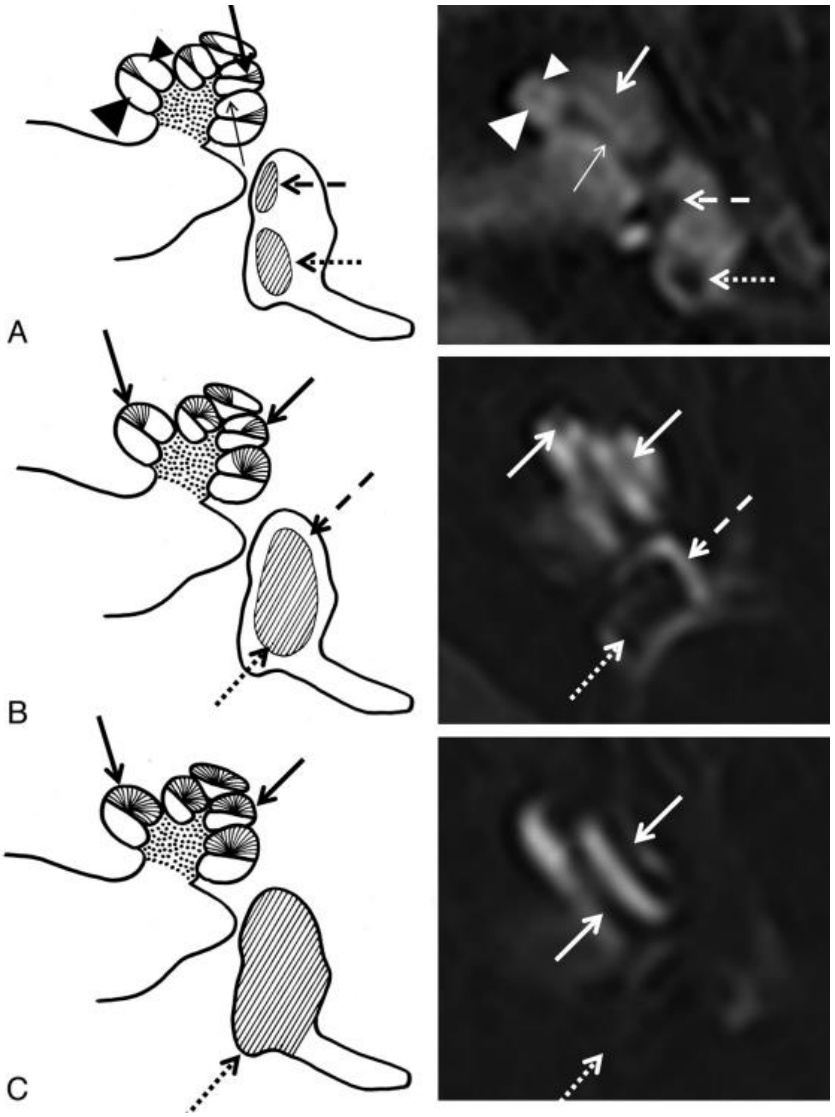

Figures 15 A, 15 B and 15 C (on the previous page) - Schematic representation of Barath criteria alongside MR images of different stages of both cochlear and vestibular hydrops. ***15 A****, Normal labyrinth: interscalar septum (thin arrow), scala tympani (large arrowhead), osseous spiral lamina/cochlear duct (thick arrow), scala vestibuli (small arrowhead), saccule (dashed arrow), and utricle (dotted arrow).* ***15 B****, Cochlear hydrops grade I with irregular dilation and partial obstruction of the scala vestibuli (arrows). In vestibular hydrops grade I, dilation of the endolymphatic space (dotted arrow) encompasses >50% of the vestibulum. A circular perilymphatic space (dashed arrow) remains visible.* ***15 C****, Cochlear hydrops grade II with total obliteration of the scala vestibuli (arrows). In vestibular hydrops grade II, dilation of the endolymphatic space leads to complete effacement of the perilymphatic space (dotted arrow). Taken from Barath et al., 2014.*

These criteria were modified again by Bernaerts et al. in 2019, as the reliability of current EH criteria on MRI was investigated. In addition, the diagnostic utility of MR imaging descriptors in MD was introduced and evaluated. This was emulated in another landmark study by Steekelenburg et al., where grading criteria for hydrops were combined with imaging signs (Perilymphatic Enhancement, PE) to produce hybrid grading criteria used to improve the diagnostic accuracy of MRI in MD (Van Steekelenburg et al., 2020). This is further discussed later in this paragraph.

In their study of 148 MD patients, Bernaerts et al. noticed that some patients with Meniere's disease demonstrated subtle abnormalities in the vestibule (essentially, the saccule being larger than the utricle but the two vestibular structures are not yet confluent with each other) which are not classified as hydrops as per Barath criteria. They demonstrated that by classifying this abnormality (saccule larger than utricle but not yet fused with it) as a fourth, lower-grade vestibular EH, the radiological findings corresponded better to the clinical criteria. The Bernaerts modification of the Barath criteria is depicted in Figures 16 A-D where MR images are displayed alongside histopathological samples and schematic drawings for better illustration. The illustration of different grades of cochlear hydrops from the same study is also included for clarity in Figures 17 A-C. In this study, Bernaerts et al. also introduced perilymphatic enhancement (PE) as an MR image characteristic (descriptor) for

diagnosing MD. The rationale behind this is that in the case of engorged endolymphatic space (hydrops), the surrounding perilymph will be compressed into the corners of the perilymphatic space resulting in accumulation and higher concentrations of gadolinium and consequently higher signal intensity or better enhancement on the scan. This was proved to be more pertinent for the cochlear perilymphatic enhancement. As per their results, combining cochlear PE and vestibular hydrops gave a sensitivity and specificity for diagnosing MD on MRI of 79.5% and 93.6% and by adding the fourth stage of hydrops, the sensitivity further increased to 84.6% without losing specificity (Bernaerts et al., 2019). Their results were corroborated by independent research done in 2020 on 38 participants and the increased sensitivity of Bernaert's modification was reaffirmed in another study including 110 patients which also demonstrated interobserver reliability in utilising these grading methods but, more importantly, they were corroborated in a recent meta-analysis of the diagnostic performance of MRI descriptors in Meniere's disease (Wnuk et al., 2022, Connor et al., 2023). The advantages of these criteria are the fact that these grading criteria are simple, easy and quick with high interobserver reliability and show a good correlation with the volumetric quantification of endolymphatic hydrops and clinical diagnostic criteria (Bernaerts et al., 2019, Connor et al., 2021). However, they're dependent on slice selection and angle of reformat, and for cochlea, where the depiction of endolymphatic space might be compromised by mimicry from interscalar septa and spiral laminae, the grade of EH may vary (Sepahdari et al., 2015; Fang et al., 2012; Connor et Pai, 2021).

Below is an image representation of the Bernaerts modification of the Barath criteria (figures 16 A-D, on the next page) and an illustration of different grades of cochlear hydrops from the same study (figures 17 A-C).

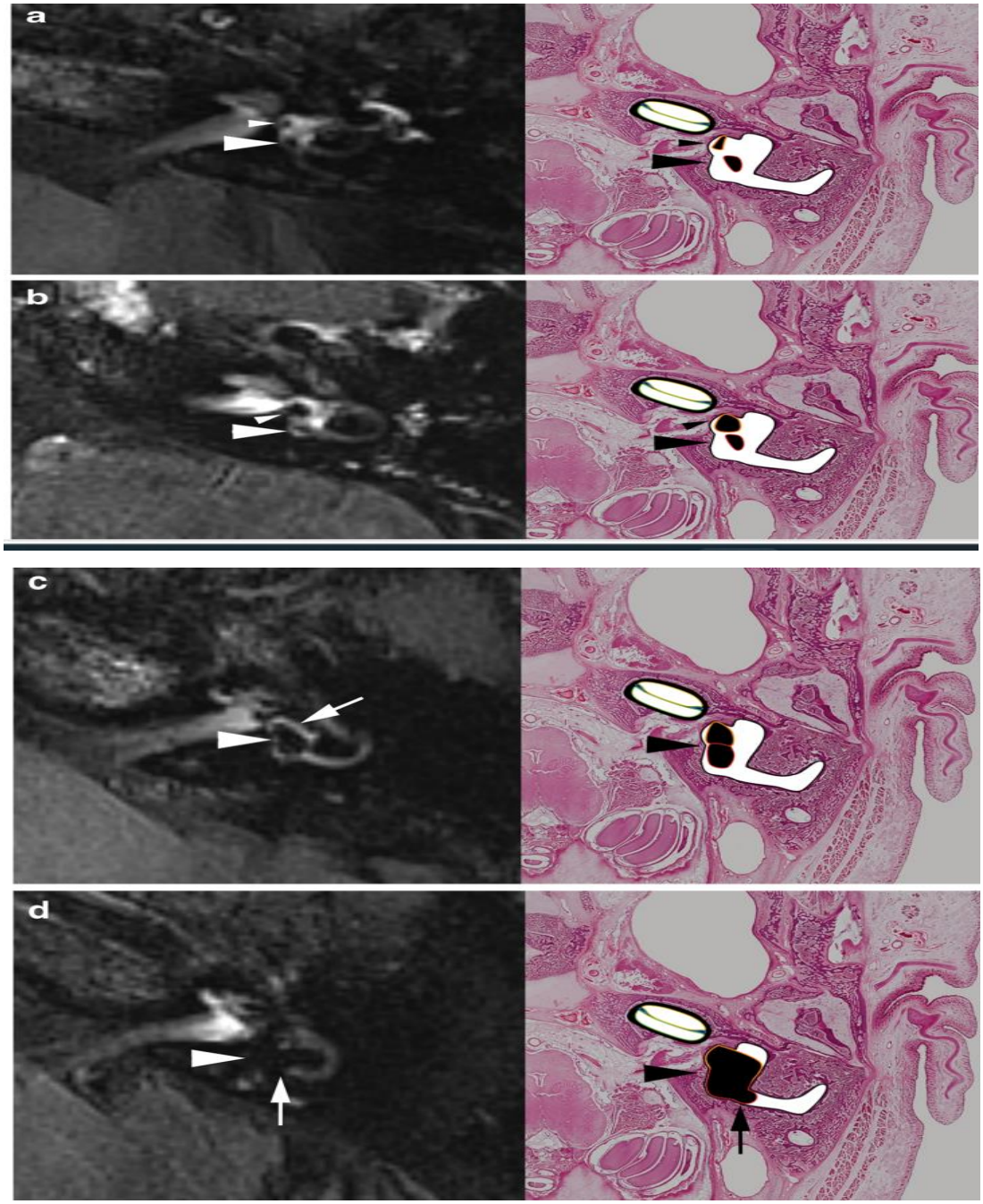

*Figures 16 A, 16 B, 16 C and 16 D - Image representation of Bernaerts modification of Barath grading criteria of vestibular hydrops on MRI correlated to histopathology samples. The small arrowhead points to the saccule and the large arrowhead points to the utricle on all images. Figure **16 A** depicts a normal vestibule, and figure **16 B** depicts an enlarged saccule compared to the utricle, but the two are not yet confluent. The arrow points to the thin peripheral rim of PE in the vestibule in **16 C** and to the utricular protrusion to the non-ampullated part of the LSCC in Image **16 D**. Taken from Bernaerts et al., 2019.*

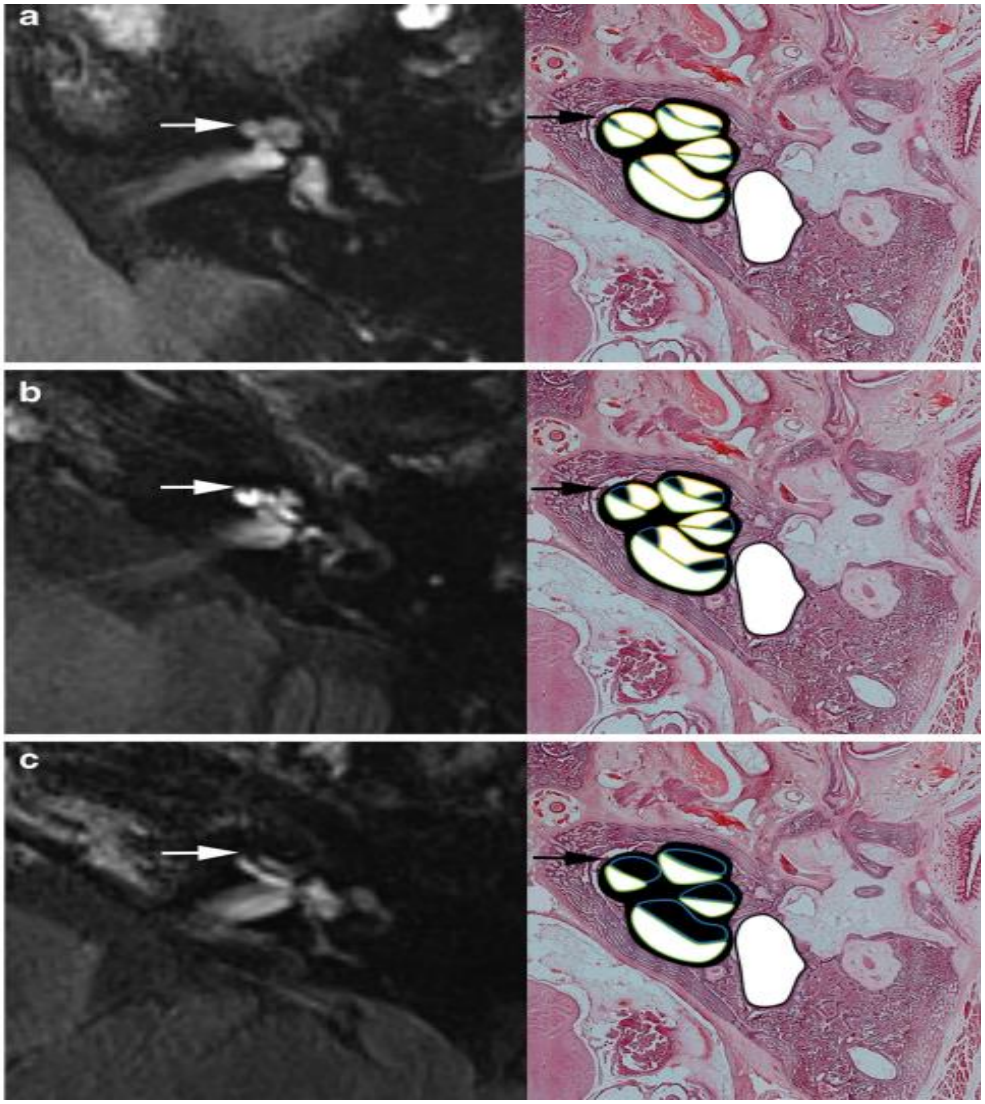

Figures 17 A, 17 B and 17 C - Cropped axial delayed gadolinium-enhanced 3D FLAIR images at the midmodiolar area of the cochlea and correlating axial cryosections with HE staining and colour overlay. ***17 A*** *Normal cochlea: In the normal cochlea, one can recognize the interscalar septum (arrow), the scala tympani, and the scala vestibuli. The scala media is normally minimally visible.* ***17 B*** *Cochlear hydrops grade I: The scala media becomes indirectly visible as a nodular black cut-out of the scala vestibuli (arrow).* ***17 C*** *Cochlear hydrops grade II: The scala vestibuli (arrow) is fully obliterated due to the distended cochlear duct. Taken from Bernaerts et al., 2019.*

In 2017, Attye et al. compared the ratio of the saccule to utricle area (SURI) to semiquantitative grading criteria developed by Nakashima and hailed SURI as the most specific criteria for diagnosing MD on MRI. Based on Nakashima criteria, all healthy subjects displayed at least one EH location, giving 100% specificity when compared with the MD group, with lower interobserver reliability than SURI, in addition (0.67 vs 1). They reported a specificity of 100% obtained on 60 participants, 30 healthy individuals and 30 MD patients with high interobserver agreement; however, the sensitivity was very poor and stood at 50% (Attye et al., 2017). While SURI>1 is indeed very specific, it has a purely dichotomised outcome and does not allow actual grading. Furthermore, the structures can sometimes be fused, and it might not be possible to assess for SURI (Connor et Pai., 2021).

Lastly, hybrid systems assessed mainly by combining the grading systems of endolymphatic hydrops with SURI and cochlear perilymphatic enhancement are currently very promising as they are specific and maximise diagnostic accuracy for MD, while the addition of cochlear perilymphatic enhancement also helps to distinguish from other vertigo-associated inner ear pathology (Van Steekelenburg., 2002; Connor et Pai., 2020; Connor et al., 2023).

Building on the work of Bernaerts et al., Van Steekelenburg et al. further demonstrated that the combination of cochlear PE with EH (they used Barath criteria) on MR imaging increases the positive predictive value for MD. Their study showed an original approach where they scanned both patients with MD and with undiagnosed and unclassified audio-vestibular symptoms clustered under the acronym Vertigo Associated Inner Ear Pathology (VAIEP) and attempted to elucidate the main distinctions between them (contralateral unaffected ears served as controls) on an MR scan. They found that a combination of EHops and PE potentially has diagnostic value in distinguishing between MD and VAIEP (Van Steekelenburg et al., 2020).

Although promising, these hybrid criteria are yet to be established and widely adopted (Bernaerts et al., 2019; Van Steekelenburg et al., 2020; Connor et Pai., 2020).

Table 6 - A comparison of different grading criteria for EH on MRI. Adapted from Connor et Pai, 2020 (pages 63 and 64).

	Details	Advantages	Disadvantages
Semiquantitative area grades (endolymph to perilymph)	**Nakashima** **Vestibular**: Recorded at the inferior aspect of LSCC as %area of endolymph relative to total fluid area. **Grade1**: >33, ≤ 50%; **Grade2: >**50% **Cochlear**: Displacement of Reissner's membrane at the mid-modiolar-level slice. **Grade1**: cochlear duct < scala vestibuli area **Grade 2**: cochlear duct > scala vestibuli area **Barath** **Vestibular**: Recorded at the widest part of the vestibule >50% area of endolymph relative to the total fluid area. **Grade 1:** perilymphatic space still visible **Grade 2:** vestibule entirely replaced	Simple and quick. Good correlation with volumetric quantification of EH.	The endolymphatic area is dependent on TI, section thickness and angle of reformat. A mismatch between the grading systems due to different levels and criteria. Vestibule: the area is markedly influenced by minor changes in section selection due to the orientation of the utricle in the axial plane. Cochlea: non-enhancing endolymph may be mimicked by artefact from interscalar septa and the grade may vary along the length of the cochlea (EH usually involves middle and apical turns first). Maximum grade is recorded.

	Cochlear: Dilated cochlear duct. **Grade 1**: spares part of scala vestibuli **Grade 2**: replaces scala vestibuli		
The ratio of the saccule to utricle area (SURI)	Assessed on double oblique reformat along the longest axial and coronal vestibular dimensions on two reference sections.	SURI is very specific. Utricle and saccule areas vary concomitantly when the parameters of the 3D-FLAIR sequence are modified.	Structures may be fused when hydropic; unable to assess SURI Only 50%sensitive. Dichotomised outcome and does not provide a "grading".
Endolymphatic extension to vestibular orifices	Extension of endolymphatic structures to the posterior limb of SCC or the oval window.	Specific.	Limited descriptions and evaluation. It only applies to vestibular structures.
Hybrid systems	Mainly combining grading systems with SURI and cochlear perilymphatic enhancement.	Maximises diagnostic accuracy.	Not yet established and widely used.

Although there are no gold standard MRI criteria for EH as such, in a recent metanalysis, Nakashima criteria demonstrated high pooled sensitivity (73%) and specificity (84%), however, SURI and Perilymphatic enhancement (PLE) were shown to have the strongest association with MD of all MRI descriptors with the highest diagnostic odds ratios (Connor et al., 2023).

As opposed to the endolymphatic hydrops grading criteria which, although widely used, are semiquantitative, only a few studies have attempted to measure the volume

of the inner ear compartments thus providing the fully quantitative and objective assessment of the inner ear and subsequently presence and grade of endolymphatic hydrops also by calculating the ratio between endolymphatic space and total inner ear fluid area (Gurkov et al., 2015; Teixido et al., 2015; Inui et al., 2016). This is usually done with the aid of computer-assisted complex computations and analysis (Gurkov et al., 2015). Given the technical challenges of accurate inner ear volume measurements, semiquantitative grading criteria are still widely used and are the most common way of assessing hydrops on MR imaging, due to the ease of their application and high interobserver agreement, but also good correlation with the volumetric assessment (Homann et al., 2015; Bernaerts et al., 2019; Connor et al., 2023).

2.1.5 CORRELATION OF EH MRI WITH DIFFERENT NEURO-OTOLOGICAL TESTS

Since the *in vivo* imaging breakthrough in 2007, especially in the early years, many authors have attempted to compare and correlate MRI findings of EH with various other functional neurootological tests, such as PTA, VEMP, caloric testing, glycerol test and electrocochleography.

However, as the body of evidence behind reliable MR imaging of EH grew, the MRI slowly became anchored as the sole diagnostic method which didn't necessitate corroboration from other methods so recent studies on MRI in MD rarely feature any other tests for EH except, perhaps hearing tests, which are often available on file from patients' historical notes and do not require to be conducted parallel to the MR scanning.

The mechanism and interpretation of the aforementioned neurotological tests fall outside of the scope of this literature review and thesis.

However, a brief description of how these tests work, followed by a review of how they compare to MRI in detecting EH, particularly in correlation with clinical symptoms, could provide further validation for the use of MRI in MD.

PTA measures the hearing thresholds in both ears, displayed in decibels (dB), thus accurately assessing patients' hearing.

Electrocochleography measures those compound electrical signals produced by the cochlea (action potential/summating potential complex) and auditory nerve in response to an auditory stimulus. The results are reported as SP/AP ratio. A very conservative criterion for abnormality is a ratio of 0.5 or greater is considered abnormal. It is in effect an "ECG" of the cochlea. It can give useful information about the function of the cochlear hair cells and in particular the pressure of endolymph fluid in the surrounding membrane compartment. Fukuoka et al compared the diagnostic utility of contrast-enhanced MRI (3 T strength, 3D FLAIR and 3D Real IR) for hydrops with two other investigation modalities, glycerol test and electrocochleography test. MRI after bilateral intratympanic injection of GBCA proved to be more useful for the diagnosis of EH with 95% sensitivity compared with the glycerol test (55%) and electrocochleography (65%). Only one patient with MD did not have evidence of EH on MRI, but this patient had a tympanic membrane perforation on the affected side hence the intratympanic distribution and

concentration of contrast, and consequently, detectability on the scan might have been compromised (Fukuoka et al., 2012).

VEMP is a relatively new vestibular function test performed by stimulating one ear with repetitive pulse or click sound stimulation and then measuring surface electromyogenic responses over selected muscles averaging the reaction of the muscle electrical activity associated with each sound click or pulse. The two most often used muscles are the sternocleidomastoid, which is used to derive the cervical VEMP, and the inferior oblique extraocular muscle used to derive the ocular VEMP. A positive VEMP response indicates normal vestibular function. An absent VEMP indicates an abnormal vestibular function. Zhang et al. conducted a meta-analysis in 2015 on the diagnostic value of VEMP in EH and concluded that it is not sufficient to diagnose EH alone, with the cited pooled sensitivity of 45%, specificity of 95% and the pooled positive likelihood ratio being 18.01 and the pooled negative likelihood ratio of 0.54 (Zhang et al., 2015).

The glycerol test is a simple test that uses the diuretic qualities of glycerol to diagnose endolymphatic hydrops. Glycerol is administered orally to patients to reduce fluid abnormalities in the inner ear, or 'dehydrate' the hydrops. Theoretically, the reduction of hydrops temporarily improves hearing, the results of which are measured by a hearing test. The reduction of hydrops by dehydration has been corroborated by MRI to an extent but the overall dynamics of glycerol effects on endolymphatic hydrops remain unpredictable (Wang et al., 2020).

Some studies combined more than one neurotological test with MRI in the assessment of EH, or in some cases, all of them.

Gurkov et al. conducted a prospective study on 41 patients diagnosed as having 'clinically definite' MD as per AAO-HNS criteria. They aimed to investigate the correlation between the degree of severity of EH detected on a 3 T MRI and audiovestibular function in MD patients. The imaging technique in this study was a 3D Real IR sequence. They concluded that with clinically and electrocochleographically confirmed definite MD, the degree of hydrops severity as seen on MRI correlates with the duration of symptoms and the impairment of hearing function (PTA) and vestibular function (VEMP) and this correlation reaches statistical significance ($p < 0.05$). The respective correlation coefficients were $r = 0.85$ for

hearing loss, r = - 0.47(negative correlation) for vestibular function and r = 0.34 for disease duration. In this paper, Nakashima grading criteria were used (Gurkov et al., 2012). In a different paper published the same year, the same authors described another morphological feature of EH, the herniation of parts of the vestibular membranous labyrinth into the horizontal semicircular canal and correlated this morphological feature with the caloric testing of the horizontal semicircular canal. Their results showed that patients who demonstrated this radiological feature had a significantly impaired caloric function (abnormal result in a vestibular test) when compared with patients without this feature suggesting a positive correlation between MRI and caloric testing in the diagnosis of EH (Gurkov et al., 2012).

Similarly, in a more recent study on 70 unilateral definite MD patients, this correlation between hearing levels with the severity of hydrops (r = 0.27 for both cochlear and vestibular hydrops) was corroborated in the affected side. Whereas, in the case of the duration of symptoms, the correlation was confirmed only for vestibular hydrops (r = 0.26). Poor agreement was observed between audio-vestibular findings and radiological EH, both cochlear and vestibular (kappa values < 0.04) but the detection rate of EH was higher in MRI than in neurotological tests. The prevalence of EH in the contralateral, unaffected side was 10% for both cochlear and vestibular hydrops which were both graded as mild in all cases (Leng et al., 2023).

The negative correlation between vestibular function and severity of EH and the positive correlation between hearing loss and EH severity was further reported in a study by Guo et al. Identically, the correlation between the duration of the disease and vestibular hydrops was also confirmed. In this study, there was no significant correlation between vestibular EH and cochlear EH indicating that the degree of EH in vestibule and cochlea is not synchronized. Unfortunately, the authors did not report on the prevalence of EH in the unaffected ears (Guo et al., 2019). This further underpinned the diagnostic utility of MRI in MD by indicating higher sensitivity than other neurotological tests, but further studies with higher sample sizes and stronger diagnostic accuracy tests are required to further corroborate.

Gu et al. corroborated the diagnostic utility of MRI in MD using bilateral IT contrast administration and subsequent MRI and comparing hydrops detection rates to caloric testing and VEMP. Their results showed that MRI had a higher sensitivity for EH

detection than the two aforementioned tests (100% vs 50% and 25%, respectively, with statistical significance (p< o.o5) (Gu et al., 2015).

Wu et al. attempted to correlate both the clinical symptoms and the duration of MD with the degree of EH on MR imaging thus trying to reinforce the theory that EH is indeed the pathological cause for the symptoms in MD. The contrast was administered intratympanically in both ears and a 3 T MR machine was used to obtain images with the 3D FLAIR and 3D Real IR techniques. The results showed that the duration of MD and low-tone and middle-tone hearing thresholds were proportional to the extent of EH in both the vestibule and the cochlea as determined by the diagnostic and grading criteria developed by Nakashima et al, similar to aforementioned studies (Nakashima et al., 2009; Gurkov et al., 2012; Gu et al., 2015, Wu et al., 2016; Guo et al., 2019; Leng et al., 2022). However, no significant correlation was demonstrated between EH and other aspects of symptoms such as high-tone hearing loss, tinnitus, and aural fullness. Additionally, 16.7% of patients who were diagnosed with unilateral MD exhibited bilateral EH in the unaffected, 'healthy' ears on MR images (Wu et al., 2016). Although these findings might suggest that EH is not a direct culprit for the full palette of MD symptoms, as some of the symptoms didn't correlate well with the degree of hydrops and hydrops was found in healthy ears, a lengthy period of follow-up would be required to ascertain if patients who had EH in the clinically unaffected ears would go on to develop symptoms in that ear. If EH potentially fluctuates in size, it might be that the patients with symptoms which didn't correlate well with the degree of hydrops had hydrops in the symptomatic ear before being imaged and just reduced in size at the time of MRI.

These studies present a further potential window into the diagnostic opportunities of MRI in MD as it could potentially replace the battery of other tests being used to detect EH and diagnose MD (VEMP, electrocochleography etc.)

Zhang et al. also explored whether the features of MD correlate with the grade of EH. On the sample size of 24 patients with unilateral MD, they demonstrated a statistically significant correlation between the hearing loss and the grades of both the cochlear and vestibular hydrops ($P < .05$), but no significant correlation between the duration of vertigo and vertigo attacks, tinnitus, caloric testing and endolymphatic hydrops was determined ($P > .05$) (Zhang et al., 2021). Still, it builds on an earlier study by Attye et

al. done on 20 MD patients, 20 sudden sensorineural hearing loss (SSNHL) patients, vertigo patients and healthy subjects, which showed that in MD patients, there is a degree of significant correlation between EH and hearing loss ($p < 0.001$). In this study, it was reported that 40 dB was the threshold above which there was a significant association with saccular hydrops, with a sensitivity of 100 % and specificity of 44% (Attye et al., 2018). In a study mentioned earlier, Shi et al. investigated the correlation between endolymphatic hydrops grades and clinical characteristics of MD patients. Similar to the previous two studies, low-frequency hearing loss was significantly correlated with the extent of both vestibular and cochlear hydrops, whereas the vertigo attack frequency showed no significant correlation with EH grades. Importantly, the duration of symptoms correlated significantly with the presence of bilateral EH supporting the notion that within its course, the disease progresses to the contralateral ear (Shi et al., 2019).

Similarly, Xie et al. investigated if the different grades of EH can be used to differentiate between clinically 'definite' and clinically 'probable' MD. Their study was performed on 51 patients and revealed a statistically significant higher degree of EH in the clinically 'definite' group ($P < 0.05$) (Xie et al., 2021).

To the author's knowledge, only two studies so far have attempted to assess EH during an acute vertigo attack. The key premise would be that if EH causes symptoms of MD, then it should be present while these symptoms are occurring.

Also, if directly responsible for symptoms, the severity of hydrops could be potentially linked to either the likelihood or severity of symptoms.

The first study by Nakada et al. describes a case report of a 78-year-old male patient who was imaged using a single-dose IV contrast and 3D Real IR technique while coincidentally having a vertigo attack. His vestibular function was also assessed at the time and then 50 days later. His hearing was also tested on the day and showed the same levels as one year before the attack. The MRI demonstrated significant (as per Nakashima criteria) bilateral EH (vestibular and cochlear) and the vestibular function was impaired on the left side. The vestibular function recovered in the subsequent testing 50 days later. Unfortunately, the MRI was not repeated (Nakada et al., 2021). Although merely a case report, this paper could suggest a closely related link between EH and symptoms of vertigo, but is however limited by the sample size and also the

fact that there were no other MR images before or after the attack to compare if EH had already been there before or had changed following the attack.

The second study by Chen et al. provided a larger sample and investigated the characteristics of EH during a vertigo attack in 36 MD patients with five of them having bilaterally affected ears totalling 41 affected ears using 3D Real IR and a double dose (0.2 mL/Kg) of IV administered contrast. As images of two ears were affected heavily by motion artefacts resulting in them not being included in the analysis there were 39 affected ears included in the final analysis. Although all affected ears exhibited a degree of hydrops (cochlear or vestibular, as per Nakashima criteria), the positive rate of vestibular EH was 37 out of 39 ears in total (94.9%), with the majority being significant EH as per Nakashima criteria (66.7%). Cochlear EH was rarer and occurred in 29 ears among 39 affected ears (74.4%). Only 1 unaffected ear exhibited EH (Chen et al., 2022).

These papers infer that vestibular EH and its severity might be responsible or closely associated with the acute vertigo attacks in MD but further research is needed to confirm this and clarify the exact mechanism.

The vast majority of the studies mentioned above used 3D FLAIR or 3D Real IR MRI sequence and gadolinium contrast on a 3 T MR scanner except for a few authors who used a 1.5 T scanner and demonstrated poorer results (Grieve et al.2012; Naganawa et al.,2013; Gurkov et al., 2013 and Kenis et al., 2022). The 3 T MRI is now considered a standard procedure for obtaining images of endolymphatic hydrops *in vivo* in humans (Hoskin, 2020, Connor et Pai, 2021; Conner et al., 2023).

2.1.6 TEMPORAL CHANGES IN EH IN MD (SPONTANEOUS vs POST-TREATMENT)

Several authors attempted to utilise and correlate the degree of EH as a means of predicting or assessing the effect of different therapeutic methods with varying results and in doing so, offered a direct comparison of EH severity at different time points in the same patients providing insight into development of EH. However, only 2 studies reported purely observation serial change in EH in MD patients without intervention and this is an important gap in the current literature as it presents one of the missing links in the study of EH *in vivo*.

For instance, Miyagawa et al. reported a case of a 53-year-old male patient with 'atypical' MD who exhibited a decrease in the size of the EH one year after osmotic treatment with isosorbide. The patient also experienced clinical improvement (Miyagawa et al., 2009). Alternatively, Fukushima et al. conducted a prospective study on 11 patients and 3 healthy control subjects to assess EH (the total EH volume was calculated semi-quantitatively on HYDROPS-Mi2) before and after medical treatment (betahistine, isosorbide) and observed no correlation (Fukushima et al., 2017). The median follow-up was 18 months. Interestingly, they found that EH developed independently of the improving vestibular symptoms in this study. The range of post-treatment to pre-treatment EH volume was 1.01-3.22, meaning that the volume of post-treatment EH was always greater than the volume of pretreatment EH, despite the improvement in symptoms (hearing improved and fewer vertigo attacks occurred) indicating that EH itself is potentially not the sole culprit for MD as it increases despite treatment and symptomatic relief. Other factors may play a role, as posited in the introduction to the thesis. In healthy controls, the EH volume, or better stated, the volume of endolymphatic space since they did not have EH, was stable. There was no statistical significance between the first and second MR scans. Healthy controls did not receive any treatment. The correlation between hearing levels and the severity (volume) of EH was reaffirmed in this study, as well. The suggested inference from this study is that EH likely progresses and does not fluctuate with time in patients with Meniere's disease (Fukushima et al., 2017). However, some of the acknowledged limitations of this study are a small sample size, relatively short follow-up and potentially too infrequent scanning. This might not have been sufficient to capture the changes in the size of EH. This study, however, corroborated the results

of a pilot study performed by Gurkov et al. on six patients that concluded that a standard dose of betahistine does not affect EH. However, the authors of that study did acknowledge that other factors might be the cause, such as a low dose of betahistine, insufficient follow-up length or the insufficient resolution of the MRI technique (Gurkov et al., 2012). A similar study was conducted in 2012 by Fiorino et al., which had a two-pronged aim, firstly, to examine the effect of IT Gentamicin administration on the size and degree of EH, and secondly, to assess the local pharmacokinetics of IT injected Gentamicin positing that the enlarged endolymphatic space will inhibit distribution of intratympanic gentamicin and hinder therapeutic response. They found that 4 patients did not show any MRI modification, 3 showed a worsening of EH in one site, and 1 patient showed a worsening in two sites. No subjects presented a reduction in the degree of EH. No statistically significant correlation between the severity of EH and the therapeutic effects of IT gentamicin has been observed. The hypothesis of a reduced effect of medication administered intratympanically in the presence of severe EH, owing to the obstacled diffusion along the perilymphatic compartments, has not been confirmed in this study (Fiorino et al., 2012). The same authors examined the effect of furosemide on EH in 12 patients 1 hour after administration, but there was also no change to the extent of the EH. (Fiorino et al., 2016). On the other hand, another study by Gurkov et al. has longitudinally followed up on one patient with clinically definite MD 2 years after the start of betahistine treatment (Gurkov et al., 2014). Although the patient's symptoms have greatly improved, EH significantly increased in size; this principle was reaffirmed in a recent prospective observational study on 192 patients which demonstrated no correlation between the severity of EH and clinical symptoms (Jerin et al, 2018).

Perhaps, this is potentially related to the modality of treatment, as the results of more radical options of treatment tend to correlate better with symptoms.

Liu et al. were the first to demonstrate the effect of endolymphatic sac decompression on the size of EH. They followed up 5 MD patients both 3 months and 2 years after decompression and a baseline scan before surgery using an IT contrast-enhanced 3 T MR scanner and 3D FLAIR imaging technique. All the patients involved demonstrated symptomatic improvement and all 5 patients exhibited a reduction of EH, both cochlear and vestibular (Liu et al., 2014). Uno et al. also examined the

changes in EH detected by gadolinium contrast-enhanced MRI (2D FLAIR) before (both IT and IV contrast used separately) and 6 months after (only IV contrast) endolymphatic sac surgery in 7 patients with unilateral MD. The method of hydrops assessment used was Nakashima's semiquantitative grading criteria although in the case of cochlear assessment, they adjusted it to accommodate their image quality (2D FLAIR used) and hydrops was qualitatively judged positive when the low-intensity signal areas corresponding to the cochlear duct were clearly noticed. They observed that after endolymphatic sac surgery, the severity of hydrops was reduced or became negative in 57.1% of cases and symptoms went into remission (both vertigo and hearing loss) in all cases (100%), outmatching the radiological improvement. In two cases, both vestibular and cochlear hydrops became negative, and both patients exhibited hearing improvement and reduction of vertigo episodes. In the third case, cochlear hydrops became negative and the vestibular hydrops was reduced but was still present and interestingly, although vertigo episodes were reduced, the hearing worsened. In the fourth case which exhibited change in EH, both cochlear and vestibular hydrops were still present post-treatment, but the overall area of endolymphatic space (or the severity of hydrops) reduced and this patient experienced no improvement in hearing but did exhibit reduction in vertigo episodes (Uno et al., 2013). In contrast to the previous study by Liu et al., this study suggests that EH is likely not causally linked to MD symptoms as not all patients who experienced symptomatic relief exhibited reduction or elimination of EH. The last two cases could potentially indicate that vestibular hydrops has a direct impact on vestibular symptoms but not hearing. It is possible that the fact hearing wasn't improved despite the reduction in cochlear hydrops is because hearing generally deteriorates in the long term in MD but the role of EH in hearing impairment is not fully understood. However, the inferences from this study are limited by a small sample size, suboptimal imaging technique and an adjusted hydrops assessment method which could have potentially led to spurious results.

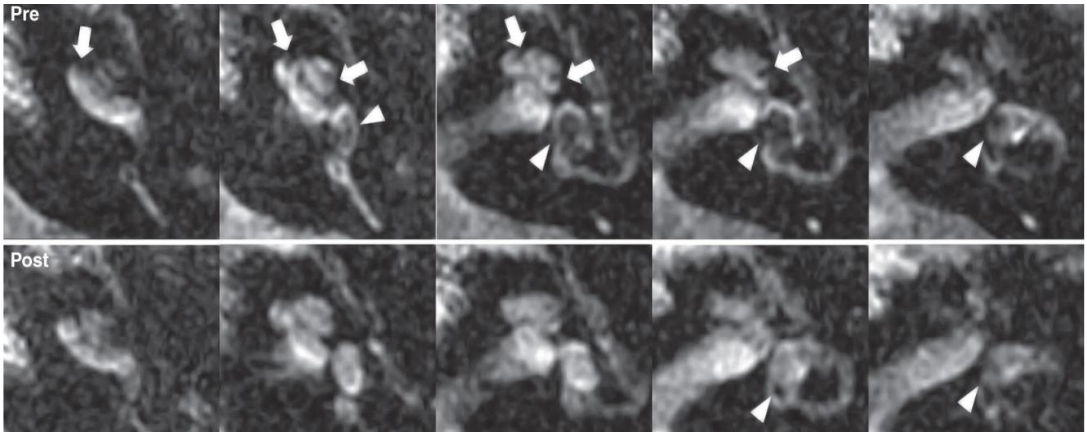

Figure 18 - A comparison of serial (from caudal to rostral left to right) axial MR images of a patient pre and post-treatment (endolymphatic sac surgery), demonstrating reduction in endolymphatic hydrops. Taken from Uno et al., 2013.

Suga et al. conducted a study where they scanned twenty ears of 12 patients with MD, who were treated conservatively, by using a 3 T MR scanner and examined if the improvements in clinical symptoms correlated with the degree of EH. 3D-FLAIR was performed 2 or 3 times 24 hours after intra-tympanic gadolinium injection or 4 hours after intravenous gadolinium injection. In the three ears in which the symptoms improved, EH was reduced in two ears, but it was also reduced in only one of 17 ears in which the symptoms did not improve. Despite this, Fisher's exact test revealed that EH reduction occurred more frequently in ears with alleviation of the symptoms ($p < 0.05$) (Suga et al., 2015). This study still does not provide evidence on the causation of MD symptoms by EH.

The results from the aforementioned studies and several others (12 in total) reporting on temporal changes of EH either through pure observation or the result of treatment were synthesised and summarised in a recent systematic literature review by Mavrommatis et al. They reported that overall, despite the alleviation of symptoms in a high proportion of patients (95.9%), either by treatment or spontaneously, 72.1% of patients still demonstrated the same or worsening EH on MR imaging. In the group receiving surgical treatment, for example, despite symptomatic improvement in 100% of patients, only 16.2% demonstrated a reduction in endolymphatic hydrops. For patients receiving medical treatment the proportion of patients with a reduction in EH was even lower at 13.6% despite 91.7% achieving symptomatic relief. This

review reaffirmed that hearing generally tends to remain poor or deteriorate over time in Meniere's disease. Interestingly, they observed that in the cohort of patients with deteriorating hearing over time, the degree of EH tended to remain poor or worsened (Mavrommatis et al., 2023). These results further dispute the hypothesis that EH is a direct cause of MD symptoms as there is a large incongruence between symptomatic relief and the grade and severity of EH. They also suggest that the grade and severity of EH on MRI are less useful for monitoring disease progression and assessing treatment response. However, MRI may still have greater clinical use in the diagnosis of EH, and subsequently MD. Consequently, the link between EH and MD symptomatology still needs to be fully elucidated. The key limitations of this systematic review are the heterogeneity in methods of assessment of hydrops across the included studies (ranging from qualitative description through semiquantitative grading criteria to volumetric assessment), small sample size, the large degree of variability between the timing of pre-and post-treatment scans (1 hour to 2 years, with a median of 8 months) and the unknown timing of MRI scans in relation to MD symptoms, leaving it unclear what are the exact effects of EH on active symptoms such as vertigo attack and what are the characteristics of EH during active symptoms, although two studies detailing this have been visited earlier in the text.

Although this might suggest the fluctuant nature of EH, further longitudinal, larger sample-sized, prospective and standardized, uniform studies including MD patients scanned at different points in time and the EH characteristics correlated to symptoms are required to fully elucidate the link between EH and MD.

Author	Year	Type of Study	Country	No. of MD pts	Mean Age	Sex	Intervention
Fiorino et al.	2011	Prospective	Italy	32	56.0	21M/11F	N/A (passive observation)
Fiorino et al.	2012	Prospective	Italy	8	60.0	5M/3F	IT single dose 0.3 ml gentamycin (40 mg/ml) diluted with 0.3 ml 8.4% sodium bicarbonate
Fiorino et al.	2016	Prospective	Italy	12	48.2	5M/7F	20 mg IV frusemide for 1 hour
Fukushima et al.	2017	Prospective	Japan	11	66.5	5M/6F	Diuretics and/or betahistine for at least 6 months (most commonly betahistine mesylate 36 mg daily dose and isosorbide 42-63 mg daily dose)
Gurkov et al.	2013	Prospective	Germany	6	53.0	N/A	Betahistine (48 mg daily) for 3-7 months, mean 5 months
Higashi-Shingai et al.	2019	Prospective	Japan	21	60.0	8M/12F	ELSS & osmotic diuretics, ameliorants of inner ear circulation, cyanocobalamin, and 'Chinese' medicine for at least 6 months
Ito et al.	02/2019	Prospective	Japan	21	61.0	4M/17F	Intra-endolymphatic sac injection 20 mg prednisolone and a bundle of absorbable gelatin film soaked with high concentration (3.3. mg/ml) dexamethasone
Ito et al.	07/2019	Prospective	Japan	20	61.5	4M/16F	Intra-endolymphatic sac injection 20 mg prednisolone and a bundle of absorbable gelatin film soaked with high concentration (3.3. mg/ml) dexamethasone
Sepahdari et al.	2016	Retrospective	USA	7	61.0	4M/3F	Acetazolamide 250 mg daily dose (duration unspecified)
Suga et al.	2015	Retrospective	Japan	12	50.8	9M/3F	N/A (passive observation)
Uno et al.	2013	Prospective	Japan	7	52.5	1M/6F	ELSS
Zhang et al.	2016	Prospective	China	13	45.0	6M/7F	ELSS +/- lateral semicircular canal plugging

† *not available*

Medical Intervention
Surgical Intervention
Neither/Observation
Both Medical/Surgical

Table 7 - Tabular presentation of the studies included in the systematic review by Mavrommatis et al on longitudinal MRI studies of EH examined either as a result of medical or surgical management or as a purely observational study. As seen, only two studies, by Fiorino et al and Suga et al monitored EH through pure observation without any interventions. Taken from Mavrommatis et al., 2023.

2.1.6 MR IMAGING OF EH WITHOUT CONTRAST

The drawbacks highlighted with the use of gadolinium-based contrasts raise questions about whether MRI without gadolinium contrast (non-contrast-enhanced MRI) can be employed to detect EH. The data on this topic is sparse with only a few papers that investigated the possibility of non-contrast-enhanced MR imaging of the inner ear and EH.

In 2017, Keller et al. conducted a retrospective case-control study to determine whether Meniere's disease (MD) produces endolymphatic cavity size changes that are detectable using unenhanced high-resolution T2-weighted MRI. Their endeavour was predicated on the premise that perilymphatic spaces have higher T2 signals than endolymphatic spaces so faint delineation is possible. Eighty-five case-control pairs were enrolled, and the cross-sectional area, length, and width of the vestibule and utricle were measured in both ears, along with the width of the basal turn of the cochlea and its endolymphatic space. The expected result would be that MD ears would show statistically significant larger endolymphatic spaces than controls. However, only two measurements reached statistical significance (in this study expressed as $p < 0.05$), the mean utricle areas and utricle to total vestibular area ratio. Mean utricle areas for affected, contralateral, and control ears were 0.038±0.12 cm^2, 0.037±0.11 cm^2, 0.033±0.009 cm^2 (p-value = 0.000102) and utricle to total area ratio 0.32±0.07 cm^2, 0.32±0.082 cm^2, 0.29±0.07 cm^2 (p-value = 0.0000192). However, on post hoc pairwise comparisons, there was no statistical significance between affected ears and contralateral ears in MD patients, but there was a statistically significant difference between the ears of healthy controls and the affected ears (p = 0.00006) of MD patients, as well as between the ears of healthy controls and the non-affected ears (p = 0.002) of MD patients. Cochlear measurements showed unexpected results where the endolymph volume was smaller in MD-affected ears. The mean basal turn of cochlea endolymph width (mm) was 0.38 ± 0.09 mm in the affected ear, 0.40 ± 0.12 mm in the contralateral and 0.40 ± 0.11 mm in healthy controls. However, these results didn't achieve statistical significance. Keller et al. derived the conclusion that the enlarged endolymphatic cavity (space) can be detected using non-contrast-enhanced T2-weighted MRI (Keller et al., 2017). This study provides weak evidence that endolymphatic space is increased in the ears of MD patients (both affected and

unaffected) suggesting EH with the novelty that this has been inferred on a non-contrast-enhanced scan, however, the main limitations are the lack of interobserver agreement report and lack of statistical significance.

Simon et al. compared the inner ear volumetrics of 36 MD patients to 36 healthy controls who underwent a 3-Tesla 3D-T2 non-contrast-enhanced MRI using a CISS (constructive interference in steady-state) sequence (0.4 mm thick slices). CISS sequence uses a strong T2-weighted 3D gradient echo technique which produces high-resolution isotropic images. Image contrast in CISS is determined by the T2/T1 ratio of the tissue. Tissues with both long T2 and short T1 relaxation times have high signal intensity on CISS images. Due to the high T2/T1 ratio, water and fat have high signals in this sequence. The CISS sequence provides excellent contrast between cerebrospinal fluid (CSF) and other structures in the brain. For these reasons, the CISS sequence is very useful for evaluating structures surrounded by CSF (e.g. cranial nerves). In their study, Simon et al. measured saccular height and width in a coronal plane, and MD patients' symptomatic ears were compared to asymptomatic and control ears. They found that saccular measurements were significantly different between symptomatic MD ears compared to healthy ears (1.59 vs 1.32 mm, $p < 0.001$ for height; 1.13 vs 0.90 mm, $p < 0.001$ for width). Symptomatic and asymptomatic ears' measurements were not significantly different ($p = 0.307$ and $p = 0.109$) (Simon et al., 2017).

A study by Venkatasamy et al. had a larger sample, 64 MD patients and 64 healthy controls and also included cadaveric samples for comparison. Participants underwent 3 T MRI using a T2-weighted steady-state free precession (SSFP) sequence without contrast material injection. Saccule was assessed on a coronal slice through the anterior and external ampullas. The following three saccular abnormalities were found in 84% of MD patients: the saccule was either elongated (height > 1.6 mm) in 86%, of increased width in 44%, or there was no saccule detected in 8% of patients. The normal saccule from the healthy controls did not show any dilatation or abnormality with a normal maximum height of 1.6 mm (1.4 ± 0.1 mm) and showed a good correlation with reference histological specimens (Venkatasamy et al., 2017). This corroborates the suggestion that the saccule is the most sensitive structure in

the vestibule and also indicates that EH is potentially detectable on non-contrast-enhanced scans (Attye et al., 2017; Connor et al., 2023).

Although it has been suggested possible to detect and grade EH on an MRI scan without contrast, there are only a few reports in the literature with great heterogeneity across imaging techniques and EH assessment methods and the variability in published results. Although these studies demonstrate the possibility of inner ear assessment on MRI without contrast administration, there is still a large gap between non-contrast-enhanced MR imaging and EH detection. However, this constitutes an area for further research, particularly as the efficacy of EH detection with contrast-enhanced and non-contrast-enhanced MRI hasn't been compared in a single study yet at the time of writing (this was part of the rationale for the MRes study); hence, further studies with widely applicable scanning protocols, standardised assessment methods and potentially direct comparison of contrast-enhanced and non-contrast-enhanced MR images are required to create a critical mass of data to infer the detection and grading of EH on non-contrast-enhanced MRI.

2.1.7. CONCLUSIONS DRAWN FROM THE SCOPING REVIEW

The literature overview outlined in the above text demonstrates that there is a definitive role of MRI in diagnosing EH in the context of MD. This can be achieved with reasonable scanning times and safe scanning profiles whilst obtaining high-quality images that are easily and widely interpretable. Also, MRI can potentially be used in assessing treatment response, in disease-modifying trials and for prospective monitoring of MD patients. Furthermore, the literature review has shown that MRI has good diagnostic accuracy for EH especially when compared to other diagnostic tests. This might reduce the need for a battery of tests and improve the cost-effectiveness of healthcare delivery in the context of Meniere's disease.

The most promising methods of MR imaging of EH from the available literature appear to be 3D Real IR and 3D FLAIR techniques enhanced with IV administered (single or double dose, 0.1-0.2 mmol/kg) gadolinium-based contrast and images obtained 4 hours post contrast injection. The 3D Real IR technique appears to be superior to 3D FLAIR, but the 3D FLAIR can still be used confidently to detect and grade EH; and 3D Real IR is more sensitive to the concentration of the contrast agent,

hence, optimally performed with double dose contrast. The most commonly used field strength of the MR machines used for this purpose is 3 Tesla, but EH imaging has been performed on the 1.5 T MR scanners with varying degrees of success.

However, even within the confines of these methods, there is still significant variety in results obtained between different image acquisition sequences, different observers interpreting the images and MR machines from different manufacturers which opens doors to further research of MRI in MD.

To achieve further progress, the author believes the emphasis should be placed on collaboration between researchers and centres, sharing raw data and employing new techniques and technology within the MR sequences in the hope of producing a widely applicable scanning protocol that can be safely and confidently used in everyday routine clinical practice. The resultant scanning protocols and subsequent image results should be used alongside the published clinical criteria for timely and accurate diagnosis of MD.

2.2. PILOT STUDY TO DEVELOP AN OPTIMISED LOCAL MRI SCANNING PROTOCOL FOR MD

Despite the above points, MRI is still not routinely used in the UK for diagnosis of MD in clinical practice and is only scarcely used in research settings. This was one of the main starting points and motivation factors for the study, where the MRI equipment at the SPMIC was harnessed to confidently detect and grade EH and further refine the scanning protocol with the overall aim of translating this effort into a widely applicable MR scanning protocol that could be used in daily clinical practice.

2.2.1. PILOT STUDY METHODS

Both healthy participants(n=4) and MD patients (n=4) underwent MR scans of their inner ears using a 3 T GE Medical Healthcare Premier, 48-channel head coil MR scanner (software version MR29.2) at the SPMIC in Queens Medical Centre (QMC) in Nottingham between January and July 2023. All participants had both non-contrast and contrast-enhanced MR scans. For the contrast-enhanced scans, the participants were injected IV with a single dose (0.1 mmol/kg) of gadolinium-based contrast agent (brand name Gadovist).

This was the first scanning of this nature at this facility and the study performed was an exploratory feasibility study.

Firstly, the MRes student aimed to locally establish high-quality MRI of inner ear structures using both dedicated contrast-enhanced MRI and non-contrast-enhanced MRI in healthy participants (n=4; phase 1).

Secondly, the MRes student tried to determine the feasibility of detecting and grading EH in patients with MD (n=4; phase 2) by MR imaging with and without contrast enhancement optimising the image acquisition protocol.

As mentioned previously (page 80), this study provides a unique methodology point in comparing both non-contrast-enhanced and contrast-enhanced images of the inner ear in the same individual.

The overall aim was to optimise an MR scanning protocol for EH and MD that can be translated into wider clinical practice locally and potentially, beyond.

Before recruitment, two meetings between the MRes student and the PPI (Patient and Public Initiative) group were held to include patients in the design of the study and several subsequent changes were made. The details are available in the Study Protocol (Appendix 1).

RECRUITMENT

The healthy participants (n=4) were recruited via information leaflets and departmental emails sent to the pool of junior doctors in the organisation and also by word of mouth. The MD patients (n=4) were identified (as either clinically probable or clinically definite) from the local Trust patient database and invitation letters were sent out to prospective eligible participants and their GPs. Subsequently, the

recruitment pool of the Nottingham Biomedical Research Centre Hearing Theme's participant database and the database of Meniere's Society were also used following successful amendments with the Ethics Committee.

The healthy participants had no history of audiovestibular symptoms or ear surgery.

The patients with MD were divided into two groups, clinically 'definite' MD and clinically 'probable' MD. This was the result of the difficulty in recruitment as initially only patients with clinically 'definite' MD were meant to be recruited because it was expected that they would be more likely to exhibit EH, as the literature suggests. However, the inclusion criteria were subsequently broadened to include patients with clinically 'probable' MD.

ELIGIBILITY CRITERIA -

Phase 1 - a group of 4 healthy, English-speaking participants, of all sexes, aged between 20 and 60 years, without audio-vestibular symptoms and any history of major ear surgery, who can give informed consent and with no contraindications to MRI or gadolinium.

There were 3 female and 1 male participant in phase 1.

Phase 2 - a group of 4 patients, English-speaking, of all sexes, aged between 20 and 60, who have been diagnosed as having either 'clinically probable' or 'clinically definite' MD as per AAOHNS 2020 criteria, who can give informed consent, with no contraindications to MRI or gadolinium.

There were 2 female and 2 male participants in phase 2.

INCLUSION CRITERIA

Phase 1 - a group of 4 healthy participants

- Participants of all sexes
- aged between 20 and 60 years
- Without any audio-vestibular symptoms
- Without any history of major ear surgery
- Who speak English

• Who can give informed consent

Phase 2 - a group of 4 patients

• Participants of all sexes aged between 20 and 60

• who have been diagnosed as having ‘clinically probable’ or 'clinically definite' Meniere's disease as per AAOHNS 2020 criteria

• Who speak English

• Who can give informed consent

EXCLUSION CRITERIA

Phase 1 participants –

• Individuals with any history of kidney disease

• Pregnant or breast-feeding individuals

• Diabetic patients and patients on metformin

• Patients in the perioperative liver transplantation period

• Patients with renal transplant, patients on haemodialysis

• Elderly and neonates and infants

• Patients with poorly controlled asthma

• Patients with multiple allergies or documented severe allergies requiring therapy

• Patients with cardiac disease

• Patients with a cochlear implant, deep brain stimulator, any metallic foreign bodies such as aneurysm clips and any query/potential metallic foreign bodies. Note that there are some pacemaker/defibrillators & wires that are compatible with MRI

• Individuals who are allergic to gadolinium contrast individuals who have taken part in a research study in the last 3 months involving invasive procedures or an inconvenience allowance.

Phase 2 participants (in addition to the above criteria for Phase 1 participants) –

• Patients with undiagnosed audio-vestibular illness

• Patients with prior ENT surgery

IMAGE ACQUISITION PROTOCOL PARAMETERS AND THEIR OPTIMISATION

The healthy participants (phase 1) were scanned first to establish confidence in the accurate identification of relevant structures providing an anatomical reference, and then, to optimise the scanning protocols. For the first purpose, initially in phase 1 images were obtained with identical image acquisition sequences. These were the first images obtained and the variation in image acquisition protocols was unwanted at this early stage. Once confidence in viewing pertinent structures was achieved, different image acquisition sequences with different parameters were slowly introduced.

Although the MRes student attempted to maintain consistency, due to the exploratory nature of the project, confined to a small sample size, several scanning parameters had to change at once introducing a significant degree of heterogeneity in the data obtained and limiting the conclusions drawn (table below).

The parameters adjusted were slice thickness (0.7 mm vs 0.8 mm), TR (6300 ms vs. 12000 ms) and, of course, contrast-enhancement vs non-contrast-enhancement. The premise for introducing the thinner slice thickness was that it would provide greater spatial resolution and a more detailed scan, particularly for non-contrast-enhanced scans. None of the studies on non-contrast-enhanced imaging of EH, however, elaborated or even mentioned the parameter of in-plane spatial resolution. Thicker slices theoretically have a greater signal-to-noise ratio due to the larger volume from which a greater signal can be measured, this could theoretically result in the greater CNR, a superior measure of image quality compared to SNR, which is used to indicate whether a structure can be visualised in relation to its surroundings. That is why CNR was chosen to be measured in this study, whereas SNR wasn't measured at all. The longer TR would theoretically provide greater CNR and hence better delineation between endolymph and perilymph which would help detect and grade EH more reliably (Kato et al., 2019; Zou et al., 2022). Contrast-enhanced imaging is currently the mainstay for EH on MRI. Hence, the contrast-enhanced thinner slices and longer TR images were expected to be of higher quality and reliability for EH. This concurs with the literature review detailed above on the optimal TR for EH imaging.

The changes in these scanning parameters affected scanning time as the scans with a slice thickness of 0.7 mm took 13 minutes 40 seconds and the scans with a slice

thickness of 0.8 mm took 8 minutes 2 seconds. These parameters were adjusted and calibrated throughout the study, within the confines of the built-in limitations of the MR scanner machine. This was done to provide higher-quality images that would be more accurate and reliable in detecting hydrops whilst maintaining scanning time to an acceptable level.

Additionally, due to scanner limitations, when the TR was changed, the TI was changed automatically by the scanner to provide optimal image contrast with a comparable scanning time. Consequently, each image obtained with a TR of 6300 ms included a TI of 1760 ms and each image obtained with a TR of 12000 ms included a TI of 2500 ms.

The images with different slice thicknesses and TR values were introduced later in Phase 1. The new images were evaluated and compared to the original sequences to reinforce the confidence in image interpretation. A professor of Medical Physics at QMC with decades of experience in MRI scanning protocol optimisation and an experienced lead radiographer at SPMIC assisted greatly with this process. Subsequently, MD patients were scanned with different optimised image acquisition protocols for case-by-case comparison. This means that all MD patients had been scanned by more than one scanning protocol and these were then compared between each other in the same participant and the same scanning protocol across different participants.

All participants had non-contrast-enhanced MR scans followed by a contrast-enhanced scan 4 hours post-IV contrast injection with exclusion criteria (above) tailored to safeguard patients from potential adverse reactions induced by contrast. Hence, each participant's ears were scanned with both contrast-enhanced MRI and non-contrast-enhanced MRI. One participant was also scanned 2 hours post-IV contrast in addition to the scan obtained 4 hours post-IV contrast. The same participant was also scanned using the 3D Real IR technique providing a two-pronged single case comparison. All participants were scanned using the TSE (Turbo Spin Echo sequence, called CUBE on a GE scanner) isotropic imaging scanning technique for anatomical reference and with the subsequent 3D FLAIR MRI technique for hydrops detection (CUBE scanning parameters in table 11).

All scans were originally planned to be done on the 3 T GE Premier scanner, however, this did not support the 3D Real IR sequence, hence Ethics were amended to enable the use of a different scanner in the unit and a single case comparison. The scanner used was Philips Healthcare Elition 3T, 32 channel head coil, scanner software version 5.7, MR scanner. The TR was 10000 ms in this particular MRI due to scanner limitations. MRI acceleration techniques were not used in the scanning protocols. All participants had padding fit snuggly in the head coil to reduce motion artefacts.

A tabular representation of different scanning parameters used in different participants is available on the next page (table 8).

	Contrast/ Non-contrast	TR (ms)	Slice thickness (mm)
1st healthy participant	Non-contrast	6300	0.8
	Contrast	6300	0.8
2nd healthy participant	Non-contrast	6300	0.8
	Contrast	6300	0.8
3rd healthy participant	Non-contrast	6300	0.8
	Contrast	6300	0.8
	Contrast	6300	0.7
4th healthy participant	Non-contrast	12000	0.7
	Non-contrast	6300	0.8
	Contrast	12000	0.7
	Contrast	6300	0.8
1st MD patient (clinically definite)	Non-contrast	6300	0.7
	Non-contrast	12000	0.7
	Contrast	12000	0.7
	Contrast	6300	0.8
2nd MD patient (clinically definite)	Non-contrast	12000	0.7
	Non-contrast	6300	0.8
	Contrast	12000	0.7
	Contrast	6300	0.8
3rd MD patient (clinically probable)	Non-contrast	12000	0.7
	Non-contrast	6300	0.8
	Contrast	12000	0.7
	Contrast	6300	0.8
4th MD patient (clinically probable)	Non-contrast	12000	0.7
	Non-contrast	6300	0.8
	Contrast – 2 hours post	12000	0.7
	Contrast – 2 hours post	6300	0.8
	Contrast	12000	0.7
	Contrast	6300	0.8
	Contrast (3D Real IR)	10000	0.8

Table 8 (on the previous page) - Different scanning parameters were used for different participants resulting in a total of 30 scans. N.B., the fourth MD patient was scanned with the 3D REAL IR technique which incurred MRI machine limitations for TR and the same patient was scanned 2 hours post-contrast to compare with the normative 4 hours post-contrast scans. Where it signifies just contrast, it implies contrast-enhanced image taken 4 hours post contrast administration. Although not represented in this table, each TR of 6300 ms was accompanied by a TI of 1760 ms and each TR of 12000 ms was accompanied by a TI of 2500 ms as per pre-set scanner settings.

A simplified tabular representation of the different scanning protocol parameters for different scans can be found in the tables below.

Scanning sequence – T2 FLAIR sag_p2_0.7 mm_FS_TR_12000 - Parameters:
TE 121.0
Number of Echoes 1
TR 12000.0
TI 2542
Echo Train Length 220
Receiver Bandwidth 62.50

Table 9 – scanning parameters for FLAIR with TR of 12000 ms

Scanning sequence - T2 FLAIR_sag_p2_0.8 mm_FS TR_6300 – Parameters:
TE 121.0
Number of Echoes 1
TR 6300.0
TI 1767
Echo Train Length 220
Receiver Bandwidth 62.5

Table 10 – Scanning parameters for FLAIR with TR of 6300 ms

Scanning sequence - 3D Ax T2 Cube 0.3 ISO – Parameters:
TE 155.0
Number of Echoes 1
TR 2661.0
Echo Train Length 130
Receiver Bandwidth 50.00

Table 11 – Scanning parameters for CUBE (anatomical reference) scan

IMAGE REVIEW AND ANALYSIS

All images were reviewed and semiquantitatively and qualitatively analysed by a single unblinded observer, the MRes student, on the GE Advanced Workstation (ADW) for diagnostic imaging in the SPMIC at QMC, for accurate image analysis, measurements and calculations. Considerable help in image analysis and scanning protocol optimisation was obtained from a Professor of Medical Physics who served as a collaborator on the project. Participants were anonymised and allocated a unique study number which was used for identification and the images were directly transferred from the scanner machine to the AD Workstation in accordance with Ethics protocol. The team of radiographers obtaining the scans at the SPMIC aided in this process.

CNR was chosen as a measure of image quality as opposed to the SNR because the readout was a comparison between two different structures or areas (endolymph vs perilymph). CNR was the most commonly used measure in the reported literature as detailed in the literature review above, hence SNR wasn't measured in this study.

To provide more detailed information about the image quality analysis, several different samples of CNRs were calculated using comparisons of mean signal intensity values across all voxels in pertinent Regions of Interest (ROIs) and standard deviations between different ROIs as explained below.

ROI – Region of interest, a sample within a dataset defined for a particular purpose; here defined by boundaries of an elliptical geometrical shape in which mean signal

intensity and SD were calculated and specifically placed in pertinent anatomical structures, as detailed below.

CNR -

$$\frac{|Perilymph\ in\ cochlea - Endolymph\ in\ vestibule|}{SD\ of\ reference\ ROI}$$

Calculated as the absolute value of the difference between the perilymph mean signal intensity in the cochlea (basal turn) and the endolymph mean signal intensity in the vestibule (utricle or posterior ampullar endolymph) divided by the standard deviation (SD) of the mean signal intensity of the reference ROI, cerebellar peduncle in this study as referenced in the literature (Naganawa et al., 2010).

CNR 1

$$\frac{|Perilymph\ in\ cochlea - Endolymph\ in\ cochlea|}{SD\ of\ reference\ ROI}$$

or

$$\frac{|Perilymph\ in\ vestibule - Endolymph\ in\ vestibule|}{SD\ of\ reference\ ROI}$$

Calculated as an absolute value of the difference between the mean signal intensity of perilymph (cochlea or vestibule, respectively) and the mean signal intensity of endolymph (cochlea or vestibule, respectively) divided by the standard deviation of mean signal intensity of the reference ROI (cerebellar peduncle).

CNR 2a

$$\frac{|Reference\ ROI - Perilymph\ in\ cochlea|}{SD\ of\ reference\ ROI}$$

or

$$\frac{|Reference\ ROI - Perilymph\ in\ vestibule|}{SD\ of\ reference\ ROI}$$

Calculated as an absolute value of the difference between the mean signal intensity of the cerebellum (reference ROI) and the mean signal intensity of perilymph (cochlea or vestibule, respectively) divided by the standard deviation of mean signal intensity of the reference ROI (cerebellar peduncle).

CNR 2b

$$\frac{|Reference\ ROI - Endolymph\ in\ cochlea|}{SD\ of\ reference\ ROI}$$

or

$$\frac{|Reference\ ROI - Endolymph\ in\ vestibule|}{SD\ of\ reference\ ROI}$$

Calculated as an absolute value of the difference between the mean signal intensity of the cerebellum (reference ROI) and the mean signal intensity of endolymph (cochlea or vestibule, respectively) divided by the standard deviation of mean signal intensity of the reference ROI (cerebellar peduncle).

Hence, 7 different CNRs were sampled from different regions of interest and background; CNR (which included signal intensity measurements from both the vestibule and the cochlea), and CNR1, CNR2a and CNR2b for both the cochlea and the vestibule separately. Each ear was separately assessed using all of the above measures.

The main, theoretical, rationale for the development of different CNRs was that if the CNR 1, CNR2a and CNR 2b were exhibiting values consistent with the 'original' CNR, most broadly used in the literature, then that would imply higher image quality and greater reliability in image interpretation but could also inform on the future ways of image analysis.

Elliptical ROIs for PERILYMPH were drawn in the medial mid-modiolar basal turn of the cochlea for the cochlear component and the visible outline of the perilymph space around the utricle and the saccule for the vestibular component. Elliptical ROIs for ENDOLYMPH were drawn in the posterior ampullar endolymph or, if visible, in the utricle for the vestibular component and the scala media in the lateral part of the basal turn of the cochlea. These areas were chosen as they are the most anatomically replicable areas of the inner ear (Naganawa et al., 2013).

For the reference ROI, the ipsilateral cerebellar peduncle was chosen.

Images were analysed in a stepwise manner where first, the main anatomical structures would be identified on carefully reformatted images producing axial slices on the anatomical reference scan (CUBE). This anatomical reference would then be

used to inform on and cross-reference the location of relevant anatomical structures (basal cochlear turn, cochlear duct, saccule and vestibule), particularly their peripheral margin on 3D FLAIR and 3D REAL IR scans.

Following window level and width adjustments, appropriate slices for endolymphatic hydrops detection would then be chosen based on both the Nakashima and Barath criteria.

Both criteria suggest a mid-modiolar level for cochlear grading and for vestibular grading, the most inferior slice which captures a minimum of 240 degrees of the LSCC for the Nakashima criteria, and the slice where the vestibule is widest for the Barath criteria. On the slices at this level, the surface area of the vestibule (total fluid area) and vestibular endolymph were measured by hand-drawn regions of interest (ROIs). Vestibular hydrops was deemed to be present if the ratio between the two surfaces (endolymph vs. total fluid area) was greater than 33% (Nakashima) or 50% (Barath) (Nakashima et al., 2009; Barath et al., 2014). When assessing the endolymphatic surface area, the ampulla of the LSCC was not included as per the pertinent literature (Naganawa et al., 2015). For cochlear hydrops, the encroachment of the scala media (unenhanced dark endolymph) on the scala vestibuli was assessed in basal and if distinguishable, the apical cochlear turns. If there was any encroachment of the dark unenhanced endolymph on the enhanced perilymph in the scala vestibuli, this was described as grade 1 hydrops. If the entire scala vestibuli was replaced by the unenhanced endolymph, then this would be graded as grade 2 endolymphatic hydrops as per established criteria. The above process was performed on contrast-enhanced images first, then subsequently on non-contrast-enhanced images.

Elliptical ROIs would then be drawn in appropriate regions to calculate CNR as described earlier in the text.

A summary of image analysis instructions is given on the next page (table 12).

Cross-reference and link to T2-weighted high-resolution images. Multiplanar reformatting. Adjust window width and level.	Cross-referencing the EH sequence to the T2-weighted sequence is helpful for defining the outer margin of the perilymphatic space and enabling appropriate reformatting. Standardised axial reformatting is performed to obtain axial images. This may be performed through the mid-modiolar section of the cochlea and the maximum area of the vestibule. Coronal images should be adjusted for any obliquity of the scan plane. To adjust for any variable degree of perilymphatic enhancement.
All the endolymphatic structures sequentially identified on the axial sections.	Grading for vestibular hydrops is ideally performed at the widest part of the vestibule as per Barath et al. Specifically, identify the saccule within the inferior vestibule. The grade for cochlear hydrops by scrolling axially through the cochlea and recording the maximum grade. Record asymmetric or excessive cochlear (perilymphatic) enhancement. Assess any asymmetry of endolymphatic structures.

Table 12 - A summary of image analysis instructions using semiquantitative grading criteria. Taken from Connor et Pai 2020.

RESULTS

There were 8 participants included in the study in total, 4 healthy participants (3 female, 1 male), 2 clinically 'definite' MD patients (1 female, 1 male) and 2 clinically 'probable' MD patients (1 female, 1 male). There were no adverse events during the study and both contrast administration and MR scans were well tolerated.

As mentioned in the methods section, the varying scanning sequences resulted in 30 scans of 16 ears (Table 8). Due to the limitations of the scanner machine's settings, not all images with the same TR could have been combined with the same slice thickness resulting in some heterogeneity of data collected.

AFFECTED EARS OF MD PATIENTS

All MD patients (4 out of 4, 100%) had either vestibular or cochlear hydrops, or both, in the affected ears. Three out of four MD patients (75%) had vestibular hydrops and two out of four (50%) had cochlear hydrops in affected ears. Also, two out of four (50%) had both vestibular and cochlear hydrops in the affected ears.

All cases of affected ears in MD patients exhibiting vestibular hydrops (75%) were detected as defined per Nakashima criteria, but none (0%) were recorded as per Barath criteria. Vestibular hydrops was deemed to be of grade 1 in all three (100%) cases. The one MD patient who did not exhibit vestibular hydrops belonged to the clinically 'probable' group of participants.

All three MD patients with cochlear hydrops in affected ears had grade 2 cochlear hydrops as per both Nakashima and Barath criteria.

UNAFFECTED EARS OF MD PATIENTS

None of the unaffected ears of MD patients (0%) exhibited vestibular hydrops, defined by either Nakashima or Barath criteria. Three out of four MD patients (75%) exhibited cochlear hydrops in the unaffected ear. In two out of the three (66.7%) unaffected MD ears with cochlear hydrops, it was deemed to be of grade 2 as per both Nakashima and Barath criteria and one out of the three MD patients had grade 1 cochlear hydrops (33.3%) in the unaffected ear. The grade of cochlear hydrops was always the same as per both Nakashima and Barath criteria.

EARS OF HEALTHY PARTICIPANTS

Vestibular hydrops was not identified in any of the healthy participants. Cochlear hydrops was found in all healthy participants in at least one ear in four out of four cases (100%) and in both ears in two out of four cases (50%). Only one healthy participant out of four (25%) exhibited grade 2 cochlear hydrops, whereas the rest exhibited grade 1 cochlear hydrops. The grade of cochlear hydrops was always the same as per both Nakashima and Barath criteria.

A tabular description of the cochlear hydrops pickup rate broken down per each scanning parameter (contrast-e vs. non-contrast-enhanced), TR 6300 ms vs 12000 ms and slice thickness 0.7 mm vs 0.8 mm) is presented in tables 13A, 13 B and 13 C.

Table 13 A – Cochlear hydrops pickup rate as per different TR values

COCHLEAR HYDROPS PICKUP RATE	MD affected ear (N=9)	MD unaffected ear (N=9)	Healthy participants' ears (both left and right, N=18)
TR 6300 ms	7 (77.8%)	3 (33.3%)	7 (38.9%)
	MD affected ear (N=9)	MD unaffected ear (N=9)	Healthy participants' ears (both left and right, N=4)
TR 12000 ms	4 (44.4%)	1 (11.1%)	0 (0%)
	MD affected ear (N=1)	MD unaffected ear (N=1)	Healthy participants' ears (both left and right, N=0)
TR 10000 ms (Real IR)	1 (100%)	1 (100%)	0 (0%)

Table 13 A – Pickup rate of cochlear hydrops on MR images of affected MD ears, unaffected MD ears and ears of healthy participants broken down by different TR values. The total number (N) of unaffected or affected MD ears and healthy ears was calculated as the total number of ears scanned using these parameters (TR of 6300 ms, 10000 ms or 12000 ms). There were 18 scans with a TR of 6300 ms (36 ears, 9 MD affected vs. 9 MD unaffected ears and 18 healthy participants' ears), 11 scans with a TR of 12000 ms (22 ears, 9 MD affected vs. 9 MD unaffected ears and 4 healthy participants' ears) and 1 scan (2 ears, 1 MD affected vs. 1 MD unaffected) with a TR of 10000 ms. The total number of all scanned ears in the table amounts to 60 (see table 8). The TR of 10000 ms was automatically calibrated for the Real IR sequence on the Philips scanner.

Table 13 B - Cochlear hydrops pickup rate as per different slice thickness values

COCHLEAR HYDROPS PICKUP RATE	MD affected ear (N=10)	MD unaffected ear (N=10)	Healthy participants' ears (both left and right, N=6)
Slice thickness 0.7 mm	5 (50%)	2 (20%)	1 (16.6%)
	MD affected ear (N=9)	MD unaffected ear (N=9)	Healthy participants' ears (both left and right, N=16)
Slice thickness 0.8 mm	7 (77.8%)	3 (33.3%)	5 (3.1%)

Table 13 B– Pickup rate of cochlear hydrops of affected MD ears, unaffected MD ears and ears of healthy participants broken down by slice thickness. The total number (N) of unaffected or affected MD ears and healthy ears was calculated as the total number of ears scanned with these scanning parameters (slice thickness 0.7 mm and slice thickness 0.8 mm). There were 13 scans with a slice thickness of 0.7 mm (26 ears, 10 MD affected vs. 10 MD unaffected ears and 6 healthy participants; ears) and 17 scans (34 ears, 9 MD affected vs. 9 MD unaffected and 16 healthy participants' ears) with a slice thickness of 0.8 mm. The total number of scans amounts to 60 (see Table 8).

Table 13 C – Cochlear hydrops pickup rate as per contrast enhancement

COCHLEAR HYDROPS PICKUP RATE	MD affected ear (N=8)	MD unaffected ear (N=8)	Healthy participants' ears (both left and right, N=10)
Non-contrast-enhanced scans	4 (50%)	3 (37.5%)	4 (40%)
	MD affected ear (N=11)	MD unaffected ear (N=11)	Healthy participants' ears (both left and right, N=12)
Contrast-enhanced scans	8 (72.7%)	2 (18.2%)	2 (16.7%)

Table 13 C – Pickup rate of cochlear hydrops of affected MD ears, unaffected MD ears and ears of healthy participants in contrast-enhanced and non-contrast-enhanced MR scans. There were 13 non-contrast-enhanced scans (26 ears, 8 MD affected vs 8 MD unaffected ears and 10 healthy participants' ears) and 17 contrast-enhanced scans (34 ears, 11 MD affected vs 11 MD unaffected ears and 12 healthy participants' ears). The total number of scans amounts to 60 (see Table 8).

Below is a tabular representation of grades of detected cochlear hydrops broken down as per affected, unaffected and healthy participants' ears across all scans performed.

Table 14– Cochlear hydrops pickup rate by grade

COCHLEAR HYDROPS – **Distribution of grades across all scans (n=60)**	MD affected ear (N=19)	MD unaffected ear (N=19)	Healthy participants' ears (both left and right, N=22)
Total number of ears with cochlear hydrops	12 (63.2%)	5 (26.3%)	6 (27.3%)
Grade 1	5 (26.3%)	3 (15.7%)	4 (18.2%)
Grade 2	7 (36.8%)	2 (10.5%)	2 (9.1%)

Table 14 – Breakdown of cochlear hydrops pickup rate by grade (1 or 2) across all scans performed (MD affected and MD unaffected ears and healthy ears). This amounted to 60 ears scanned in total, 19 scans of MD patients (19 affected vs. 19 unaffected ears) and 11 scans of healthy participants (22 healthy ears in total).

It is visible from Table 13 A that the proposed suboptimal imaging technique (the TR of 6300 ms) detected cochlear hydrops in healthy ears rendering them likely false positives and the TR 12000 ms technique did not detect cochlear hydrops in any of the healthy participants' ears. The pickup rate of cochlear hydrops in unaffected MD ears (likely false positives) was also higher in scans using a TR of 6300 ms than a TR of 12000 ms.

Similarly, in Table 13 B, a slice thickness of 0.8 mm (the proposed suboptimal imaging parameter), resulted in higher detection of cochlear hydrops in unaffected MD ears and healthy participants' ears (likely false positives) than a slice thickness of 0.7 mm.

Also, in Table 13 C, the proposed suboptimal imaging technique (non-contrast-enhanced MR imaging) yielded a higher pickup rate of cochlear EH in healthy participants and unaffected MD ears (likely false positives) than the proposed optimal technique (contrast-enhanced). Also, contrast-enhanced images demonstrated

cochlear hydrops in a higher number of affected MD ears which are presumed to have hydrops (true positives).

As per the tables displayed above, there is a large rate of cochlear hydrops being detected where it is not expected (healthy participants, unaffected ears of MD patients) in this study. This is quite confounding, but most of these cases are seen on images presumed to be of suboptimal quality for EH detection (non-contrast-enhanced images, shorter TR images). The high rate of cochlear hydrops on these images could potentially reaffirm these sequences as being less reliable and indicate poorer quality. The presence or absence of contrast enhancement seems to have a greater impact on image quality than TR value. Hence, in some cases, it is possible that even with other parameters maximally optimised, it is the presence or absence of contrast enhancement that has the greatest bearing on image quality and reliability of assessment.

The figures below aim to depict the difficulty in ascertaining if there is cochlear hydrops on non-contrast-enhanced images or not and the subsequent corroboration of the readout on contrast-enhanced images which are more reliable, higher-quality images. A comparison between these two different sequences is illustrated below.

The quality of images was evaluated by the CNR. This was used to assess the best scanning protocol via box-whiskers plots along with the qualitative analysis of the following images. No analytical statistics were used in the study due to the small sample size, inconsistency, and significant heterogeneity of data.

COMPARISON OF NON-CONTRAST AND CONTRAST IMAGES

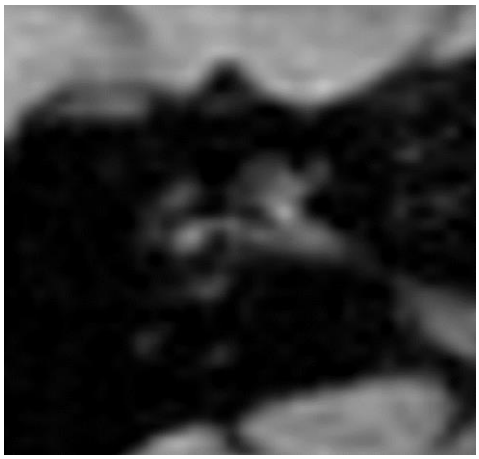

Figure 19 A

Figure 19 B

Figures 19 A and 19 B - A side-by-side comparison of the right cochlea in the same healthy participant on contrast-enhanced (19 A) and non-contrast-enhanced (19 B) images. The non-contrast-enhanced image (19 A) is on the left side and the contrast-enhanced (19 B) is on the right side. On the non-contrast image on the left-hand side the division between the saccule and the utricle is much harder to appreciate and there appears to be a degree of cochlear hydrops. However, on the contrast-enhanced image, it is easier to appreciate the normal outline of the cochlear turns and division between saccule and utricle suggesting this is a normal inner ear with no evidence of hydrops.

The same limitations of the non-contrast-enhanced scans in healthy participants also apply to MD patients. Coarser outlines and delineations of the shape and size of inner structures could potentially result in unreliable measurements and misdiagnosis as can be seen in figures 20 A, 20 B, 21 A and 21 B on the next page.

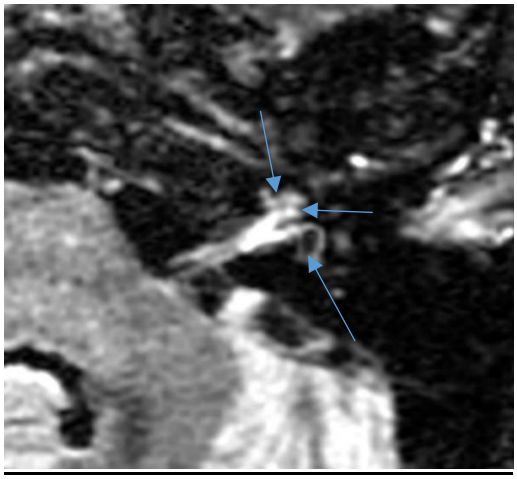

Figure 20 A

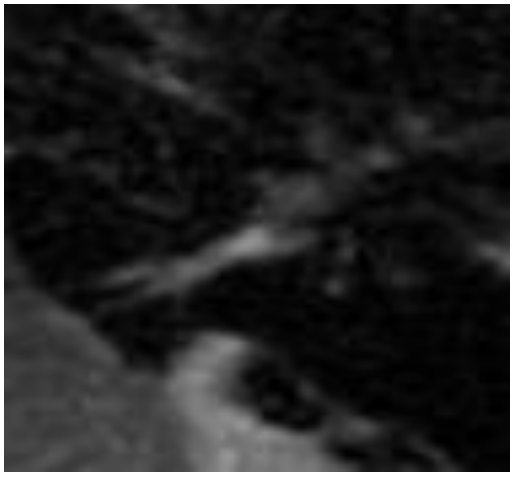

Figure 20 B

Figures 20 A and 20 B. A side-by-side comparison of the affected left ear in the same MD patient with left ear affected both contrast-enhanced (20 A, left side) and non-contrast-enhanced (20 B, right side). On the contrast-enhanced image, it is much easier to appreciate the hydropic changes (blue arrows) in both the vestibule and the cochlea whereas the enhancement on the non-contrast image is too faint to confidently decide whether there is hydrops.

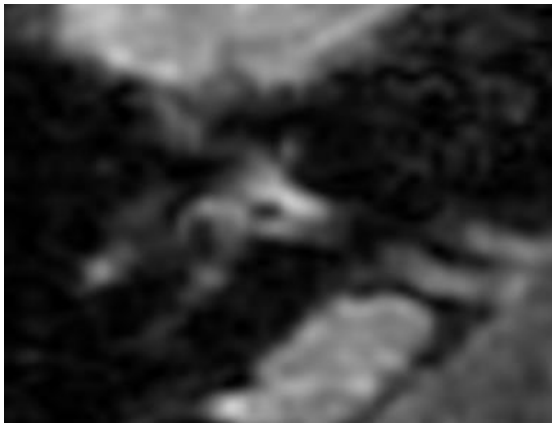

Figure 21 A

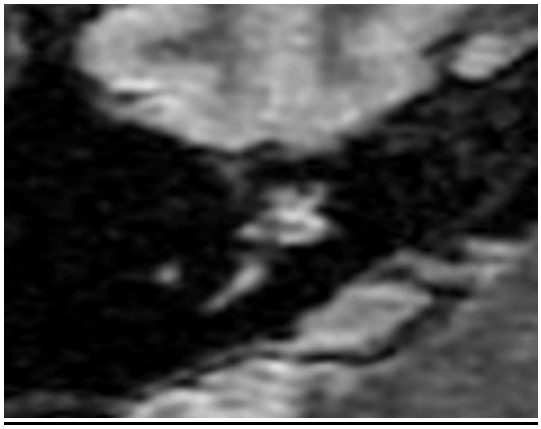

Figure 21 B

Figures 21 A and 21 B - A comparison of a non-contrast-enhanced (21 A) and the contrast-enhanced image (21 B) of the same MD patient with the affected right ear with a focus on the cochlea. There is right-sided cochlear hydrops in this patient, which could also be suspected visually on the non-contrast scan but could only be confidently corroborated on the contrast-enhanced image.

Below is a graphic representation of how CNR values compare in relation to the presence or absence of contrast (Figure 22)

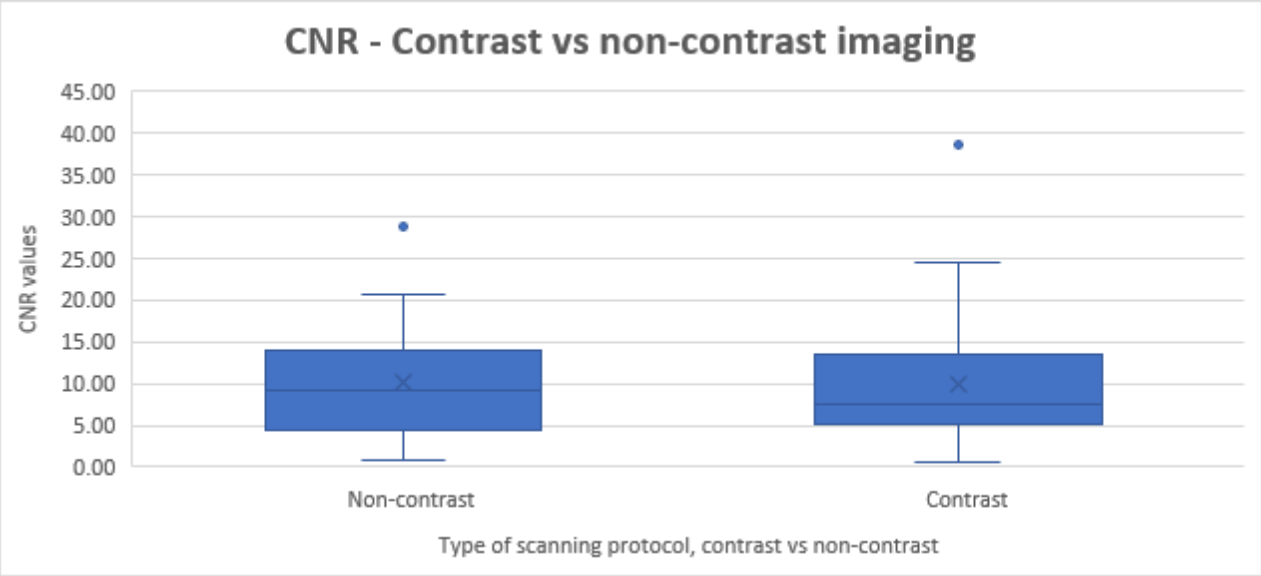

Figure 22 - CNR values comparison between non-contrast-enhanced and contrast-enhanced images. The average value of CNR being higher in the non-contrast cohort is discrepant with the expectation that contrast-enhanced images will have greater CNR values on average demonstrating superior quality. This could potentially be due to a single dose of gadolinium-based contrast agent used which resulted in less of an overall enhancement increase due to a lower concentration of contrast in the perilymphatic compartment, but the concentration was still sufficient to highlight delineation and contrast between endolymphatic and perilymphatic compartments. Statistical significance was not calculated. No analytical statistics were used in the study due to the small sample size, inconsistency, and significant heterogeneity of data.

COMPARISON BETWEEN IMAGES WITH DIFFERENT TR VALUES

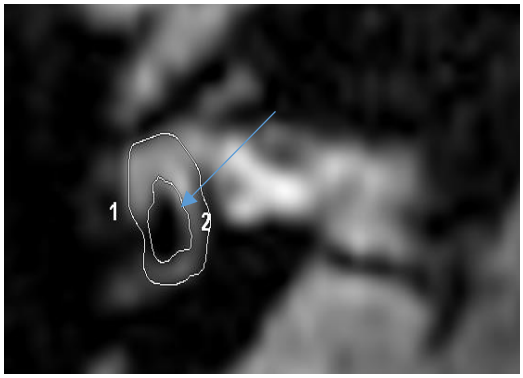

Figure 23 A

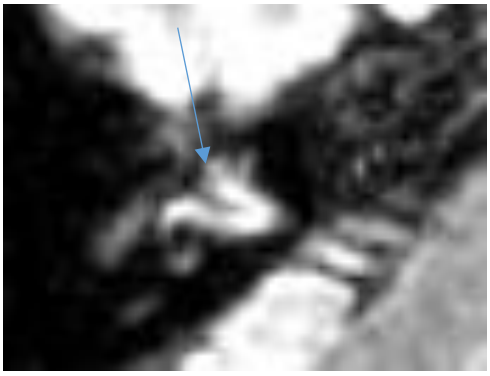

Figure 23 B

Figures 23 A and 23 B - images of the same MD patient (right ear affected) with a TR of 12000 ms (23 A, left side) and 6300 ms (23 B, right side). This is an example of a comparison between the two sequences with different TRs in the same participant. The longer TR time appears to produce higher-quality images that are more reliable, but changes can still be appreciated with a shorter TR. N.B The cochlea is not well captured on the TR 12000 ms image (23 A) as the slice is too low, however, on the TR 6300 ms image (23 B), both the vestibule and the cochlea (arrow) are captured on the same slice. The outer edge of the vestibule and the vestibular endolymphatic area are outlined on the image with a TR of 12000 ms as this was required to calculate the endolymph to total fluid area ratio. In this particular image, although saccule and utricle were confluent (hand-drawn ROI number 2, arrow), neither the Nakashima nor Barath criteria for vestibular hydrops were fulfilled.

Below is a graphical depiction of the comparison of CNR values between scans with different TR values (Figure 24).

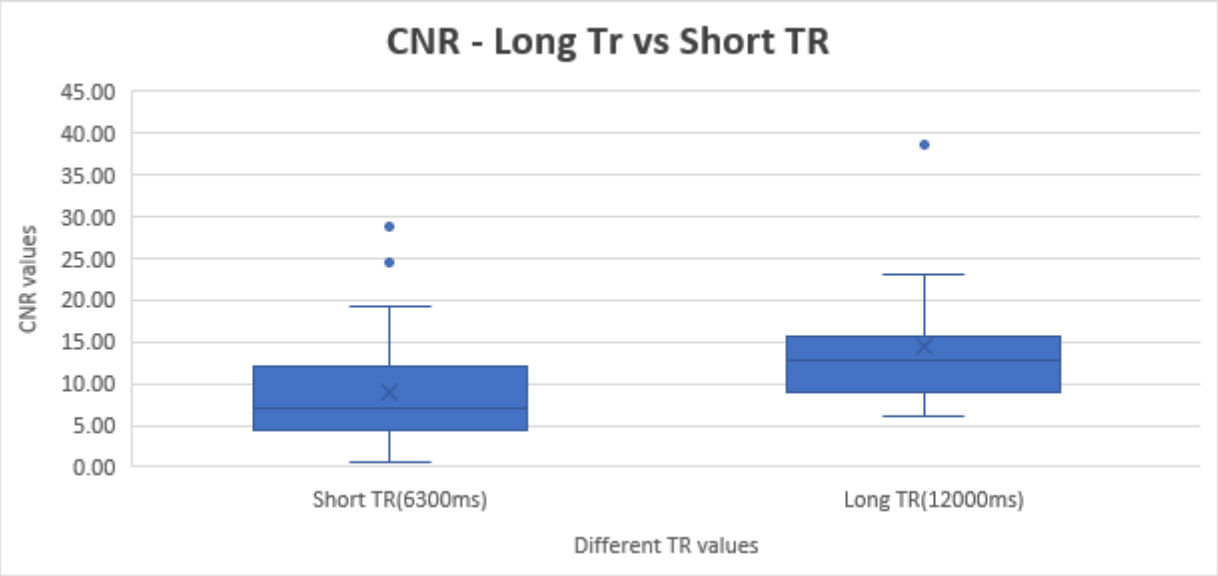

Figure 24 - CNR values comparison between different TR values. Higher average values and more condensed data in the TR 12000 ms group can be observed, potentially suggesting greater reliability and image quality (higher average CNR). N.B TR of 12000 ms also includes TI of 2500 ms and TR of 6300 ms includes TI of 1760 ms, hence the same result applies for these two TI values. No analytical statistics were used in the study due to the small sample size, inconsistency, and significant heterogeneity of data, hence statistical significance was not calculated.

COMPARISON BETWEEN IMAGES WITH DIFFERENT SLICE THICKNESSES

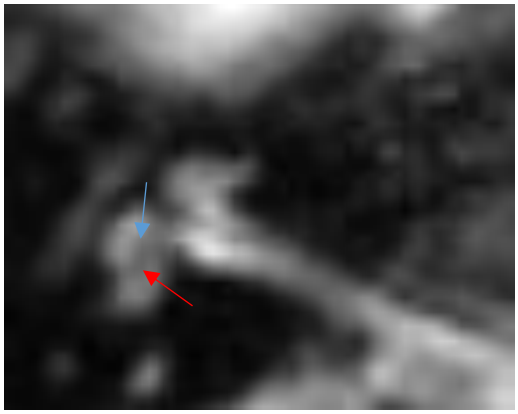

Figure 25 A

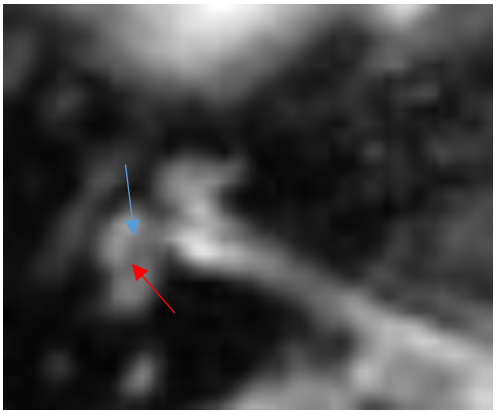

Figure 25 B

Figures 25 A and 25 B - These illustrate two contrast-enhanced images of a healthy participant's right ear with different slice thicknesses (figure 25 A 0.8 mm; figure 25 B, 0.7 mm) and the same TR values (6300 ms) rendering them comparable. Both saccule (blue arrow) and utricle (red arrow) are visible on both images and qualitatively there doesn't appear to be any significant difference between the two.

Below is a graphical depiction of CNR values in images with different slice thicknesses (Figure 26).

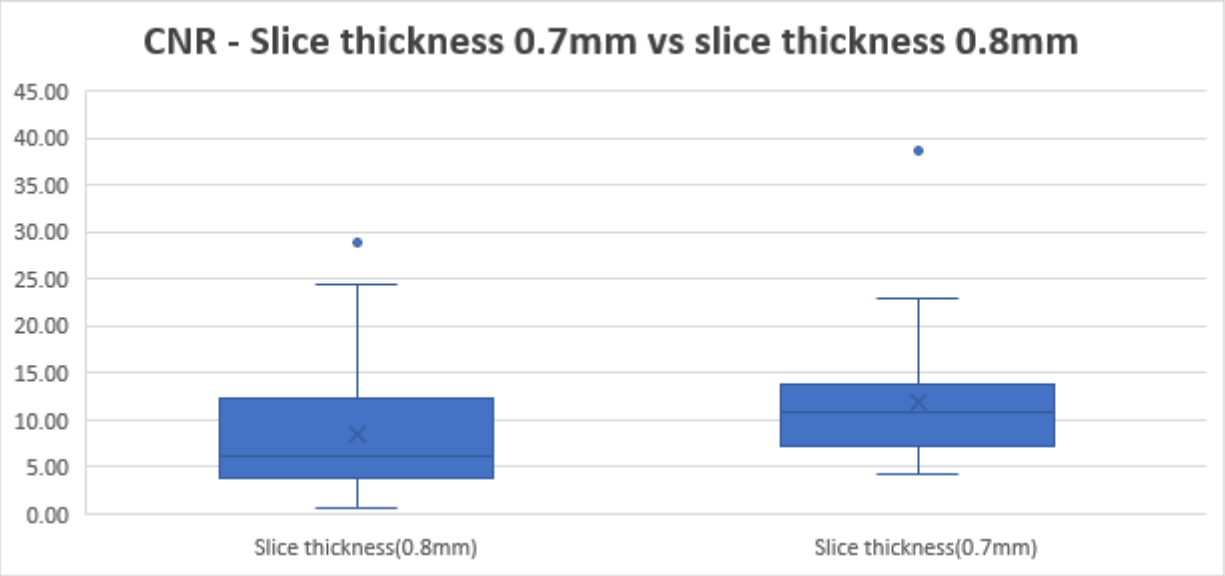

Figure 26 - Box-whiskers plot demonstrating higher average values and more condensed data in the 0.7 mm slice thickness group than 0.8 mm, potentially suggesting greater reliability and image quality from the quantitative analysis, but this is however not reflected in the qualitative analysis. No analytical statistics were used in the study due to the small sample size, inconsistency, and significant heterogeneity of data, hence statistical significance was not calculated.

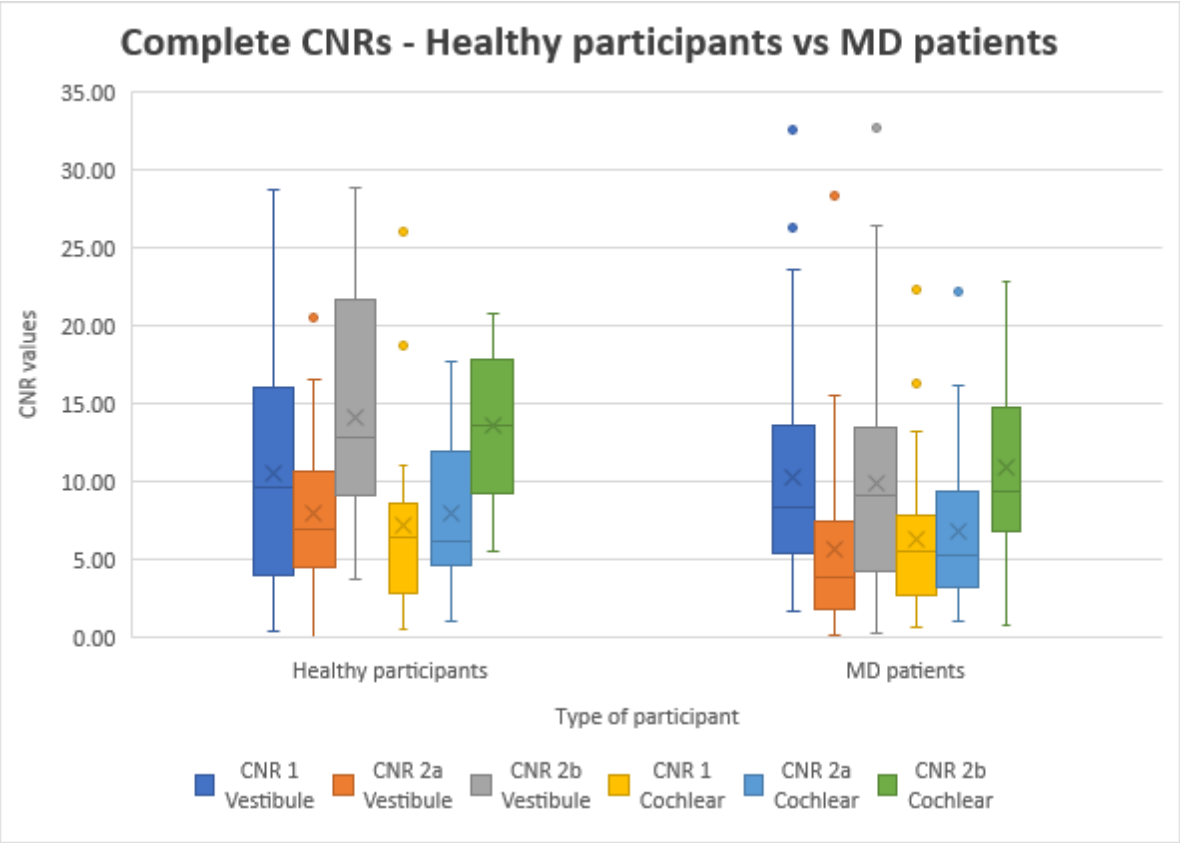

Figure 27- A box-whiskers plot of values of different types of CNR as calculated in the study, between healthy participants and MD patients. No analytical statistics were used in the study due to the small sample size, inconsistency, and significant heterogeneity of data, hence statistical significance was not calculated.

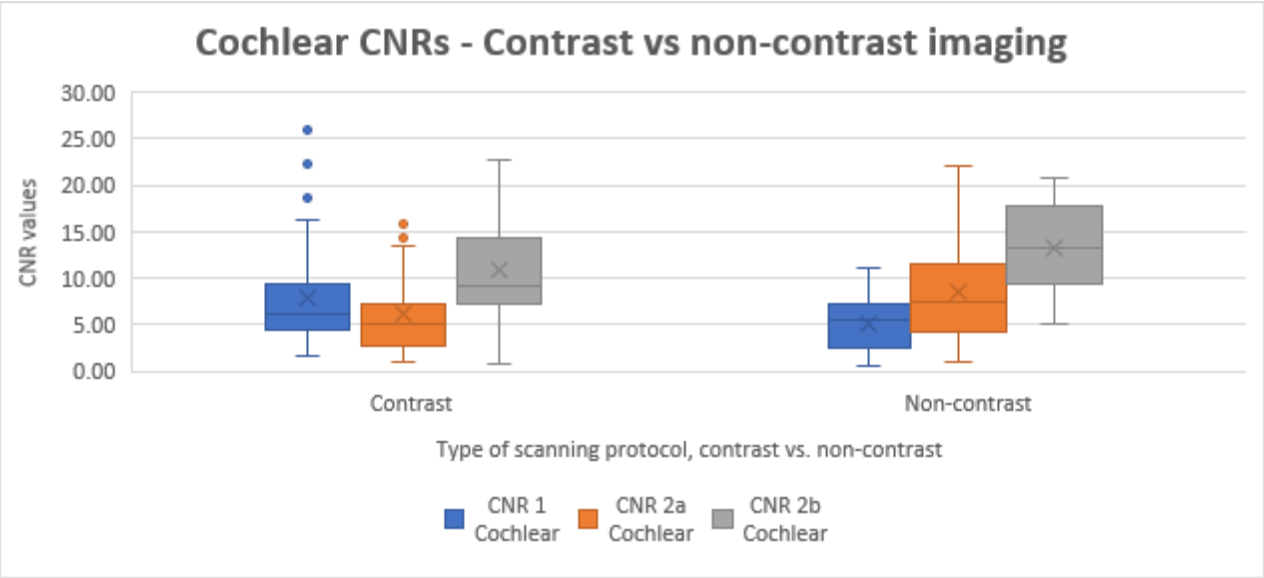

Figure 28 (on the previous page) - On this chart, a small difference in the consistency of data (narrower box) in the assessment of cochlear structures in the contrast group as opposed to the non-contrast group can be appreciated. However, due to the small sample size, all these minor variations can be random and hence conclusions drawn limited. No comparable difference was observed in the group of vestibular CNRs. No analytical statistics were used in the study due to the small sample size, inconsistency, and significant heterogeneity of data, hence statistical significance was not calculated.

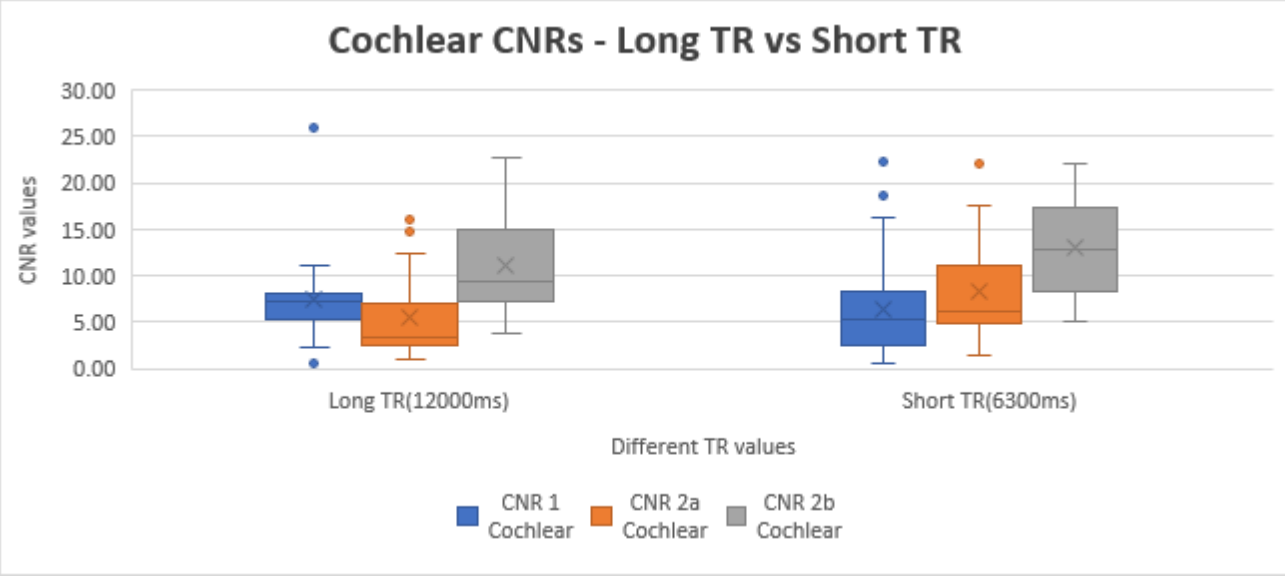

Figure 29 - A box-whiskers plot showing data on cochlear CNRs in both the long TR group and the short TR group, with more consistent data in the long TR group. No comparable difference was observed in the group of vestibular CNRs. No analytical statistics were used in the study due to the small sample size, inconsistency, and significant heterogeneity of data, hence statistical significance was not calculated.

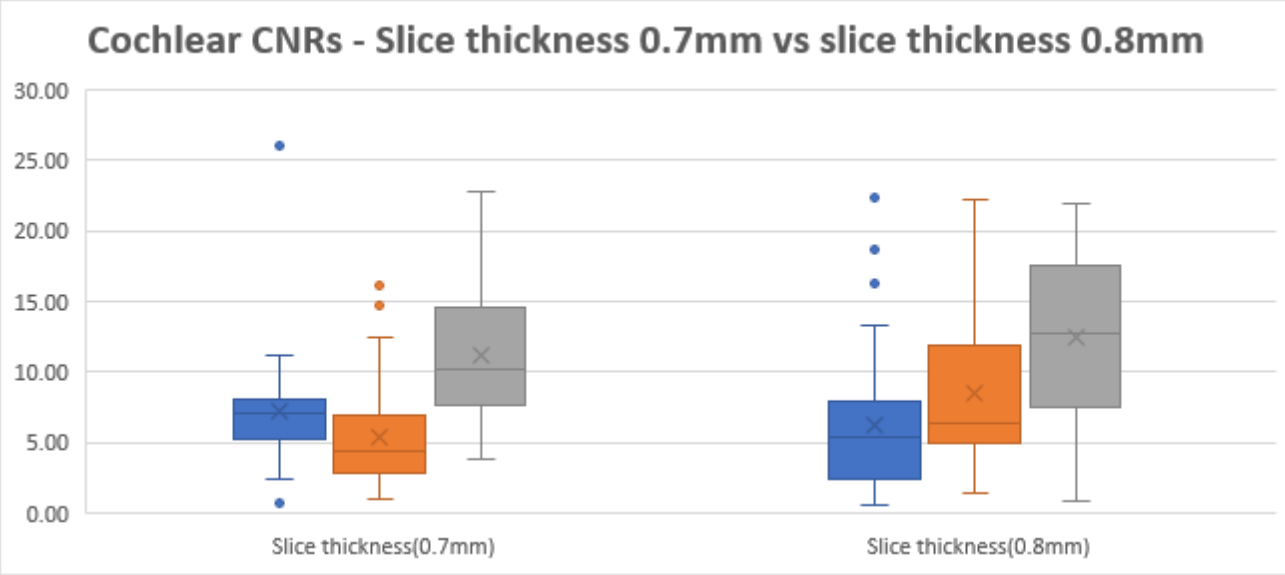

Figure 30 - A box-whiskers plot of different cochlear CNR values between the two types of slice thickness groups (scans with a slice thickness of 0.7 mm and slice thickness of 0.8 mm). No comparable difference was observed in the group vestibular CNRs. No analytical statistics were used in the study due to the small sample size, inconsistency, and significant heterogeneity of data, hence statistical significance was not calculated.

From the above graphs, it can be deduced that the additional samples of CNRs (CNR 1, CNR 2a, CNR 2b) rendered little in the way of conclusions drawn on image quality and reliability when assessing EH on MRI.

Furthermore, the single-observer review would be aptly supplemented by an additional blinded observer and calculation of the inter-reader agreement.

Below is a pictorial representation of all the image acquisition protocols employed for each participant. The images selected have been chosen at the most representative slice to depict the inner ear structures or pathology. N.B, in some cases, the cochlea and the vestibule could not be optimally visualised on the same slice, hence, for some participants, there are more images of the same ear imaged with the same scanning technique depicting the cochlea and the vestibule separately. These images serve the purpose of visually and qualitatively reporting on different scanning protocols.

1ST HEALTHY PARTICIPANT

LEFT EAR

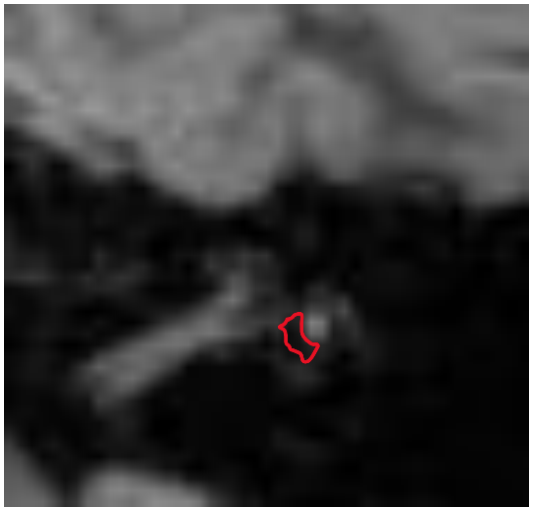

Figure 31 A

RIGHT EAR

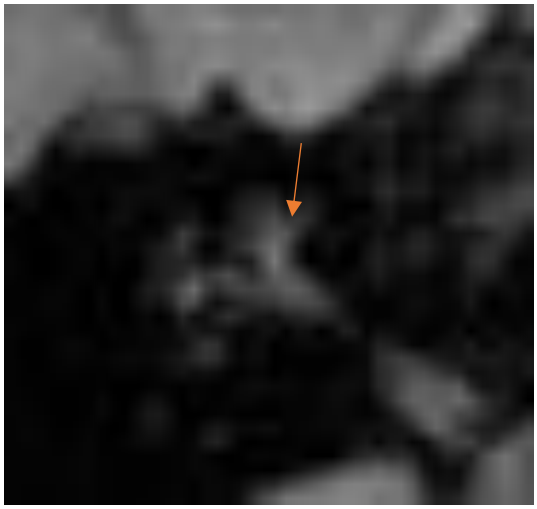

Figure 31 B

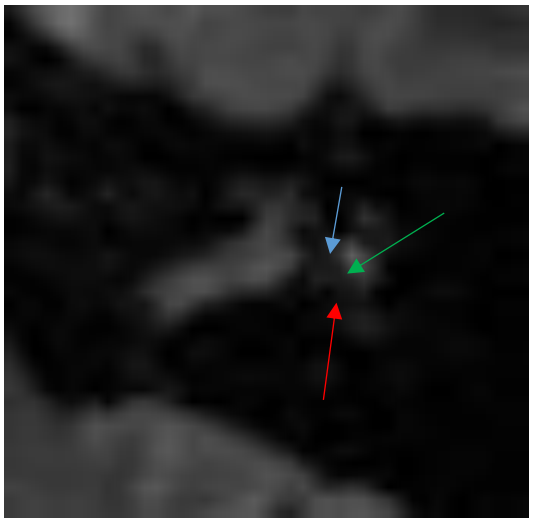

Figure 31 C

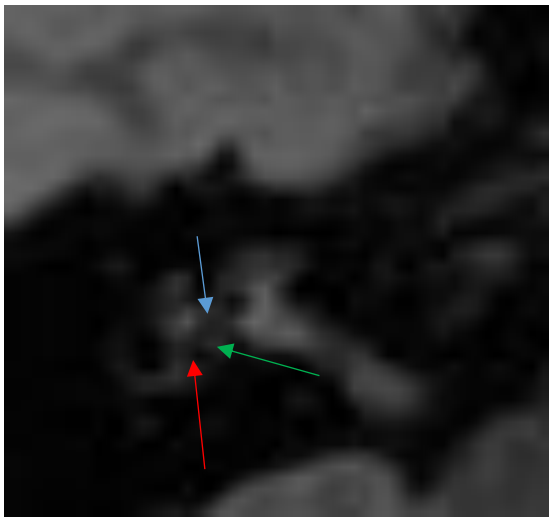

Figure 31 D

Figures 31 A, 31 B, 31 C and 31 D - Extended legend and image interpretation are available on the next page;

31 A - Non-contrast, 0.8 mm slice thickness, TR 6300 ms

31 B - Non-contrast, 0.8 mm slice thickness, TR 6300 ms

31 C - Contrast, 0.8 mm slice thickness, TR 6300 ms

31 D - Contrast, 0.8 mm slice thickness, TR 6300 ms

Figures 31 A, 31 B, 31 C and 31 D (on the previous page) - The blue arrow indicates saccule, the red arrow indicates utricle, the red outline indicates confluent saccule and utricle, and the green arrow indicates the thin strip of perilymph in the vestibule separating the saccule and the utricle. Although the inner ear structures can be appreciated on both the non-contrast and contrast images (on the previous page), the saccule and utricle (blue and red arrow) are only clearly delineated from each other on the contrast-enhanced scans and separated by a thin ribbon of vestibular perilymph (green area), whereas, on the non-contrast scan, they appear confluent (red outline). Although on the non-contrast image of the right ear, it seems like there is an encroachment of the scala media on the scala vestibuli (hydrops, amber arrow), this is refuted on the contrast image (which is the superior modality of scanning as per the contemporary literature) where a smooth outline of the cochlear turns with no endolymphatic encroachment can be observed. The contrast-enhanced image of the left ear at the first glance appears to demonstrate hydrops but on closer look or zoom, a faint perilymphatic enhancement is visible in scala vestibuli, suggesting normal cochlea.

2nd HEALTHY PARTICIPANT

LEFT EAR

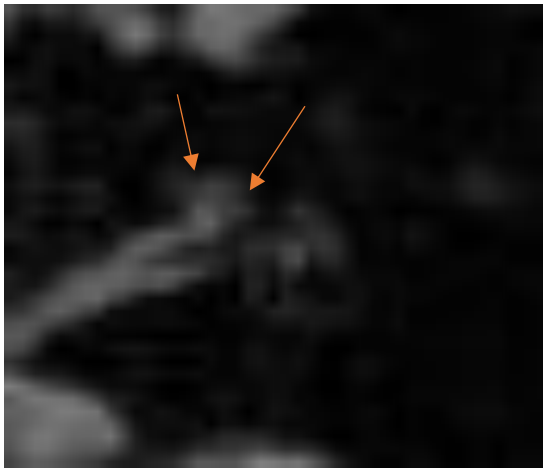

Figure 32 A

RIGHT EAR

Figure 32 B

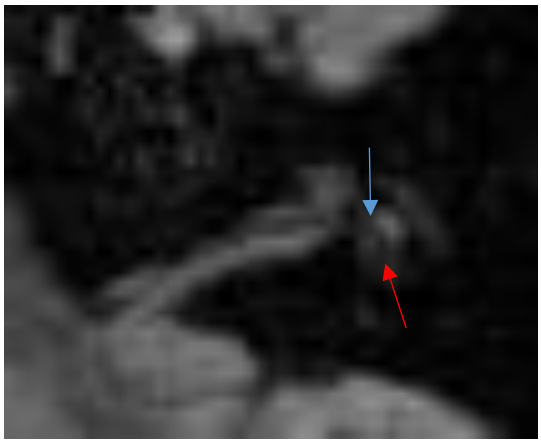

Figure 32 C

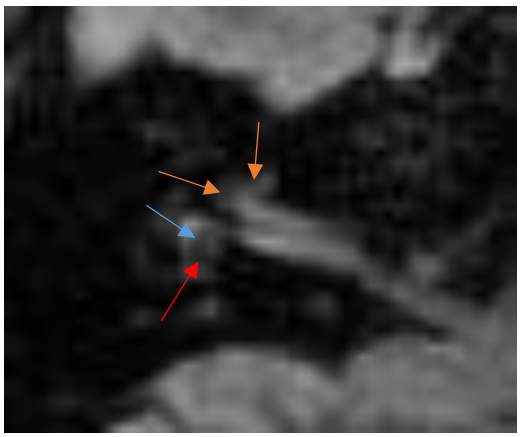

Figure 32 D

Figures 32 A, 32 B, 32 C and 32 D - Extended legend and image interpretation are available on the next page.

32 A - Non-contrast, 0.8 mm slice thickness, TR 6300 ms

32 B - Non-contrast, 0.8 mm slice thickness, TR 6300 ms

32 C - Contrast, 0.8 mm slice thickness, TR 6300 ms

32 D - Contrast, 0.8 mm slice thickness, TR 6300 ms

The blue arrow represents saccule, the red arrow represents utricle and the amber arrows indicate hydrops.

Figures 32 A, 32 B, 32 C and 32 D (on the previous page) - The encroachment of scala media (cochlear duct) on the scala vestibuli, endolymphatic hydrops (amber arrows), can be appreciated on the non-contrast scan of the left ear, but the contrast scan, by all accounts the superior imaging method, does not demonstrate this. On the right side, however, there appears to be an element of encroachment of the scala media on the scala vestibuli (hydrops, amber arrows) on the contrast images, but there is no such morphology on the non-contrast image which renders a smooth outline of the cochlear turns. This appearance of cochlear hydrops would be graded as grade 2 by both Nakashima and Barath criteria on the contrast scan as the scala vestibuli appears to be obliterated almost completely by the unenhanced hydropic scala media.

3rd HEALTHY PARTICIPANT

RIGHT EAR

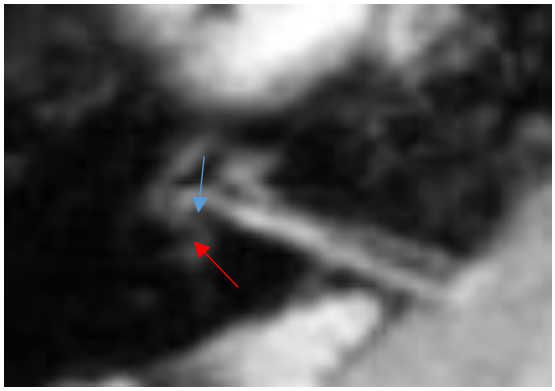

Figure 33 A

LEFT EAR

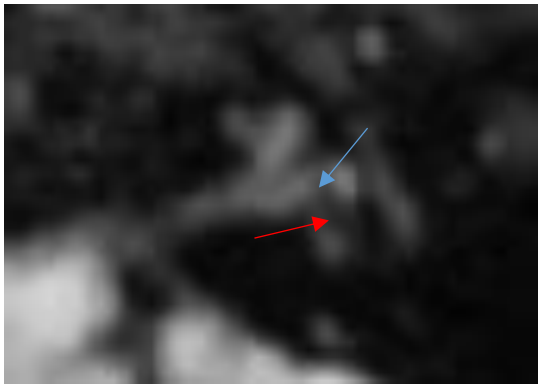

Figure 33 B

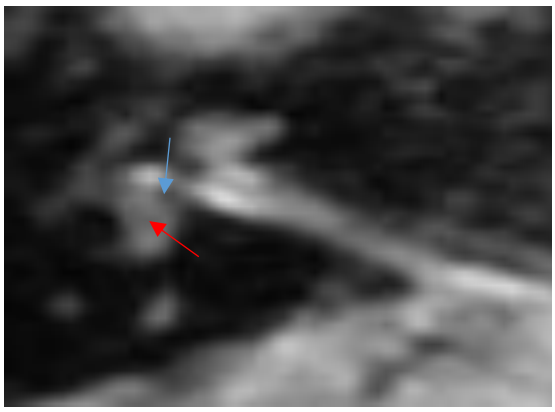

Figure 33 C

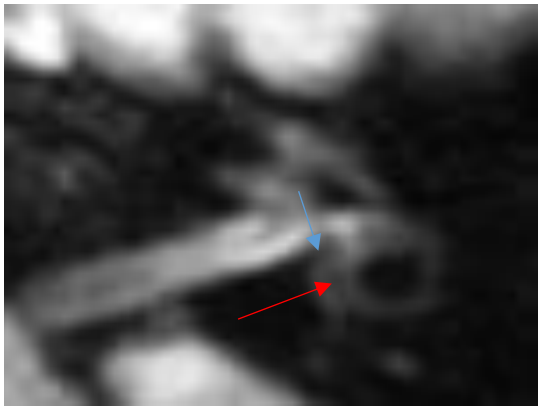

Figure 33 D

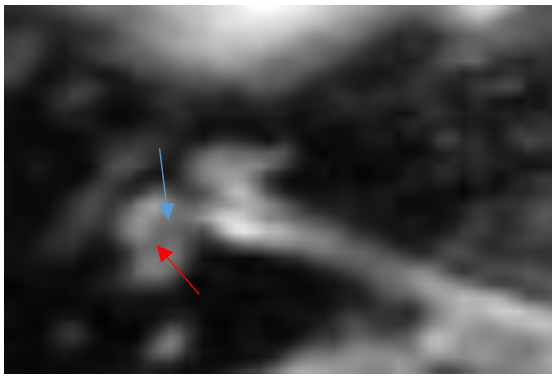

Figure 33 E

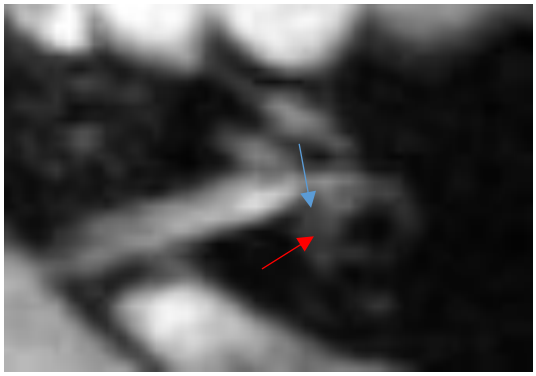

Figure 33 F

Figures 33 A, 33 B, 33 C, 33 D, 33 E and 33 F- Extended legend and image interpretation are available on the next page.

The blue arrow indicates saccule, and the red arrow indicates utricle.

Figure 33 A - Non-contrast, slice 0.8 mm, TR 6300 ms

Figure 33 B - Non-contrast, slice 0.8 mm, TR 6300 ms

Figure 33 C - Contrast, slice 0.8 mm, TR 6300 ms

Figure 33 D - Contrast, slice 0.8 mm, TR 6300 ms

Figure 33 E - Contrast, slice 0.7 mm, TR 6300 ms

Figure 33 F - Contrast, slice 0.7 mm, TR 6300 ms

Figures 33 A, 33 B, 33 C, 33 D, 33 E and 33 F (on the previous page) - The image quality on these images is suboptimal, and there are motion artefacts, but on most images, saccule and utricle (blue and red arrows) could be delineated with a significant degree of confidence and hence vestibular hydrops excluded. It is more challenging to assess the cochlea, particularly on the left side, where, on the non-contrast image, it seems there might be an element of cochlear hydrops. This appears less likely on contrast images, but the image quality still precludes a definitive assessment.

4th HEALTHY PARTICIPANT

LEFT EAR

Figure 34 A

RIGHT EAR

Figure 34 B

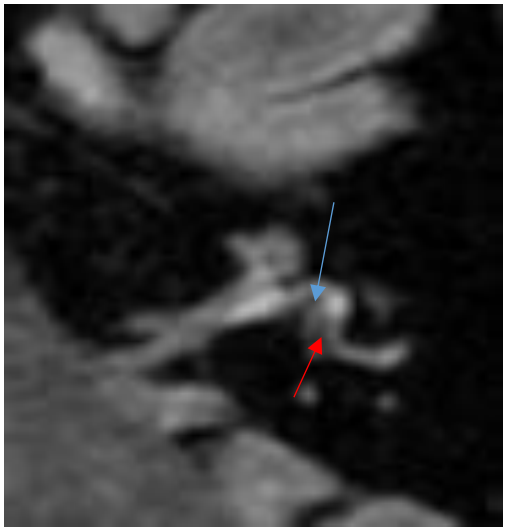

Figure 34 C

Figure 34 D

Figures 34 A, 34 B, 34 C and 34 D. Extended legend and image interpretation are available on page 118.

Figure 34 A - Non-contrast, 0.8 mm slice thickness, TR 6300 ms

Figure 34 B - Non-contrast, 0.8 mm slice thickness, TR 6300 ms

Figure 34 C - Non-contrast, 0.7 mm slice thickness, TR 12000 ms

Figure 34 D - Non-contrast, 0.7 mm slice thickness, TR 12000 ms

The blue arrow represents saccule and the red arrow represents utricle.

LEFT EAR

Figure 34 E

RIGHT EAR

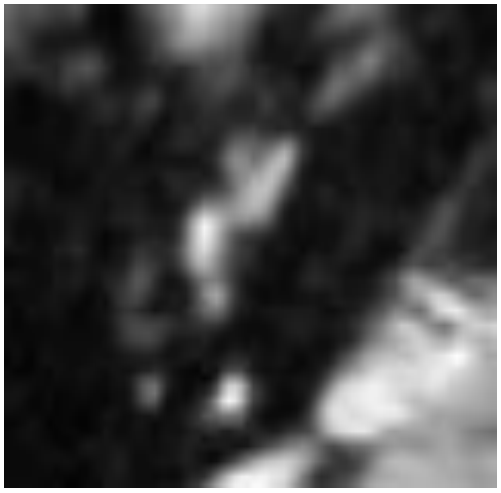

Figure34 F

Figure 34 G

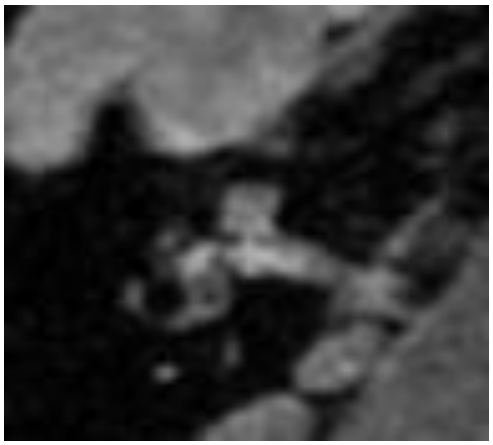

Figure 34 H

Figures 34 E, 34 F, 34 G and 34 H -Extended legend and image interpretation available on page 118.

Figure 34 E – *Contrast, TR 6300 ms, 0.8 mm slice*

Figure 34 F – *Contrast, TR 6300 ms, 0.8 mm slice*

Figure 34 G – *Contrast, TR 12000 ms, slice 0.7 mm*

Figure 34 H – *Contrast, TR 12000 ms, slice 0.7 mm*

The blue arrow represents saccule and the red arrow represents utricle.

Figures 34 A, 34 B, 34 C, 34 D, 34 E, 34 F, 34 G and 34 H (on pages 116 and 117) - On the non-contrast images with thicker slices (0.8 mm) and shorter TR (6300 ms) (figures 34 A, 34 B, 34 E, 34 F) there appears to be a thin strip of dark, unenhanced endolymph in the basal turn of cochleae, which could potentially represent hydropic cochlear duct, although the enhancement is fainter and outlines are not very stark. These 2 images are challenging to read. On the thinner slice (0.7 mm) and longer TR (12000 ms) scans (figures 34 C, 34 D, 34 G and 34 H), however, the enhancement is less faint and vestibular structures (saccule blue arrow, utricle red arrow) and cochlear turns are more clearly defined not demonstrating hydrops. The enhancement of pertinent structures and overall visibility and readability of images is markedly better on longer TR, thinner slice images.

1st MD PATIENT (Left ear symptomatic)

LEFT EAR

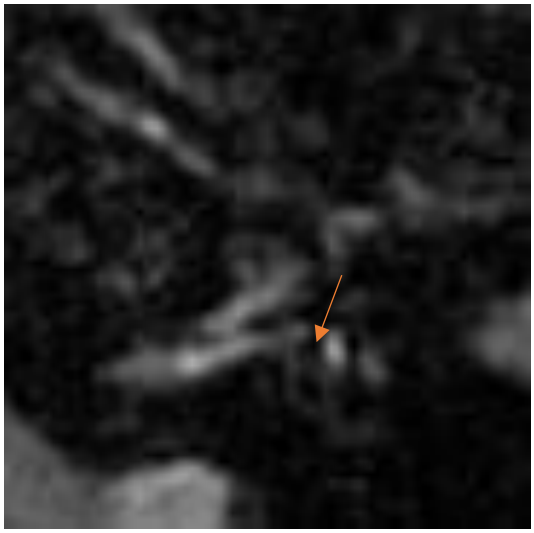

Figure 35 A

RIGHT EAR

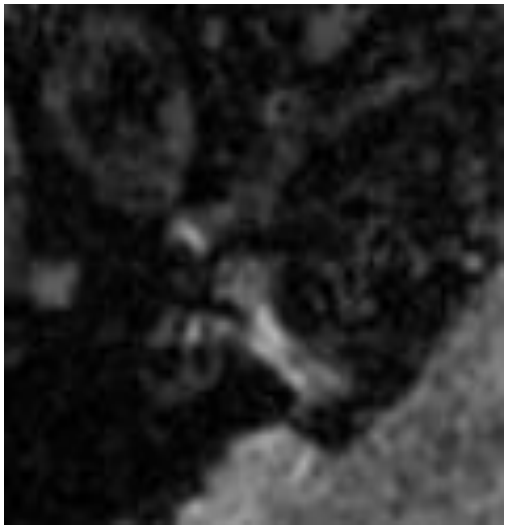

Figure 35 B

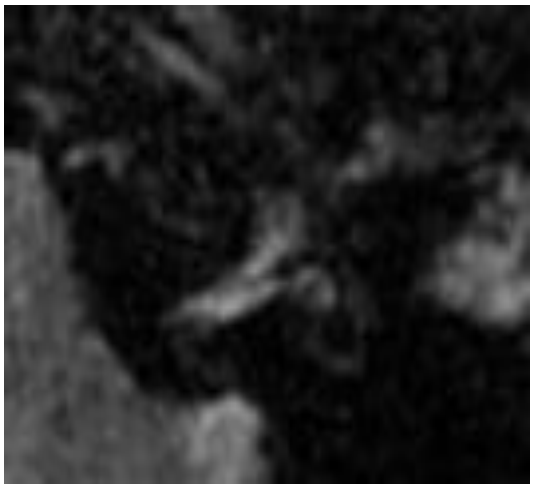

Figure 35 C

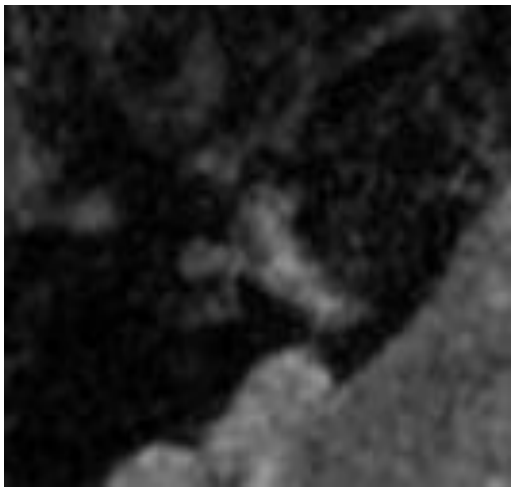

Figure 35 D

Figures 35 A, 35 B, 35 C and 35 D. Extended legend and image interpretation are available on page 120.

Figure 35 A - Non-contrast, 0.7 mm slice, TR 6300 ms

Figure 35 B -Non-contrast, 0.7 mm slice, TR 6300 ms

Figure 35 C - Non-contrast, 0.7 mm slice TR 12000 ms

Figure 35 D - Non-contrast, 0.7 mm slice, TR 12000 ms

Figures 35 A, 35 B, 35 C and 35 D (on the previous page) - What appears to be an enlarged saccule in figure 35 A (amber arrow) is likely the ampulla of LSCC. Arguably, the enhancement is fainter in the images with the longer TR and thinner slice thickness which are supposed to render higher image quality and greater reliability. This could potentially be due to the absence of contrast which seems to be the main factor in producing images with a sufficient degree of quality to reliably detect EH.
The figures displayed on the next page (figures 36 A, 36 B, 36 C and 36 D) corroborate this statement.

RIGHT EAR

Figure 36 A

LEFT EAR

Figure 36 B

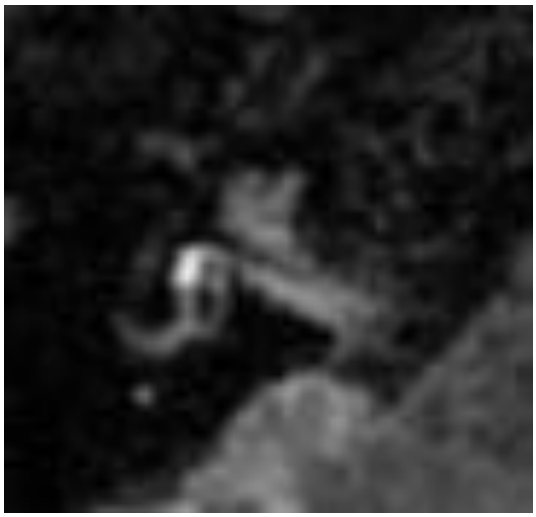

Figure 36 C

Figure 36 D

Figures 36 A, 36 B, 36 C and 36 D. Extended legend and image interpretation are available on the next page.

Figure 36 A - Contrast, slice 0.8 mm, TR 6300 ms

Figure 36 B - Contrast, slice 0.8 mm, TR 6300 ms

Figure 36 C - Contrast, slice 0.7 mm, TR 12000 ms

Figure 36 D - Contrast, slice 0.7 mm, TR 12000 ms

Figures 36 A, 36 B, 36 C and 36 D (on the previous page) - It is clear from the above images that images with longer TR and thinner slices offer better delineation between endolymph and perilymph optimising the sequence for EH imaging. Of note, on the left, symptomatic, side, there is clear cochlear hydrops in the form of nodular encroachment on the perilymph in the basal turn of the cochlea (blue arrows) and the confluence of saccule and utricle (red outline) occupying the majority of vestibule (its outer rim in green outline).

2nd MD PATIENT (Right ear symptomatic)

RIGHT EAR

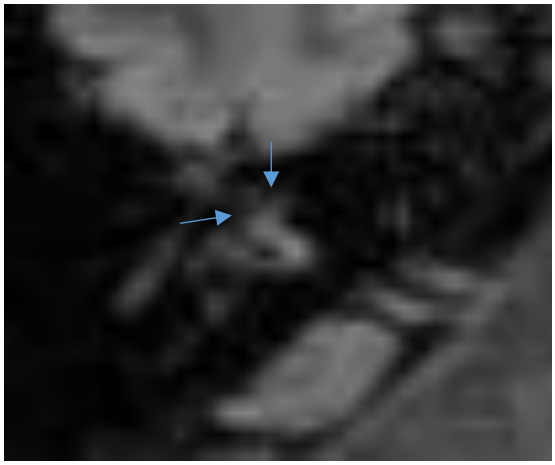

Figure 37 A

LEFT EAR

Figure 37 B

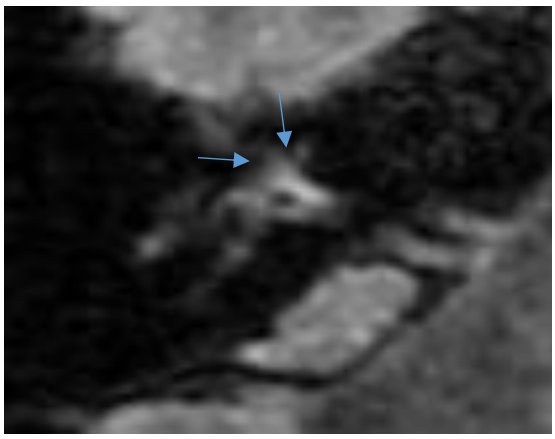

Figure 37 C

Figure 37 D

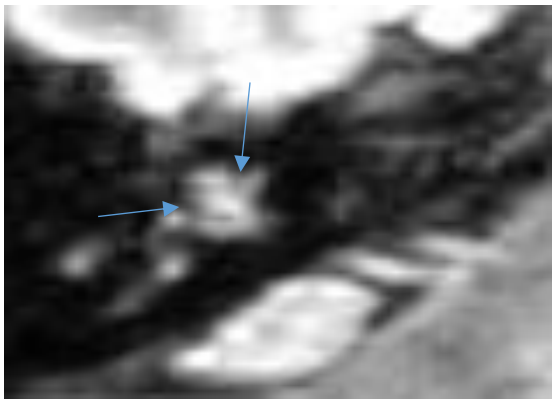

Figure 37 E

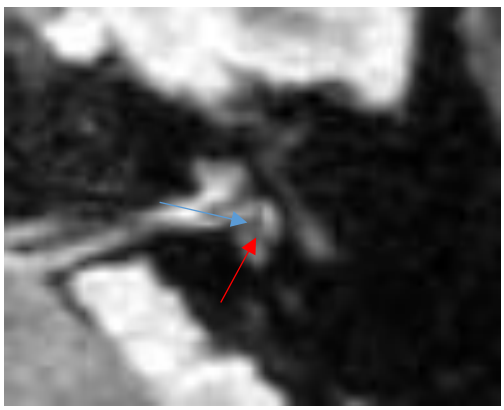

Figure 37 F

RIGHT EAR

Figure 37 G

LEFT EAR

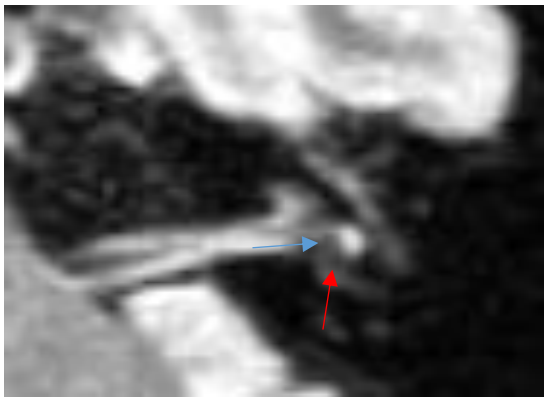

Figure 37 H

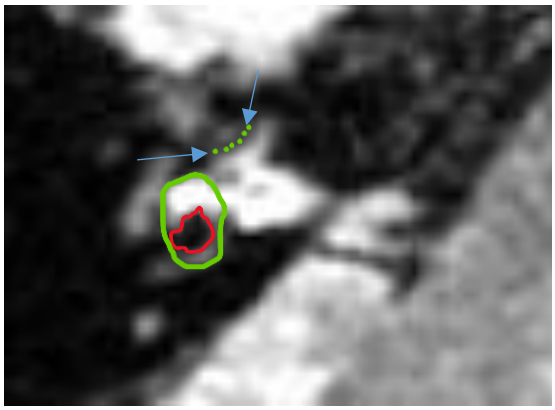

Figure 37 I

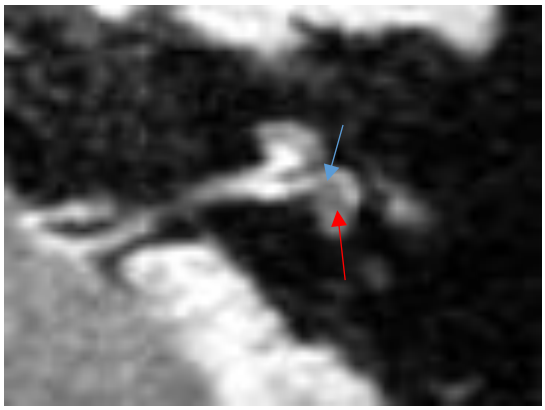

Figure 37 J

Figures 37 A, 37 B, 37 C, 37 D, 37 E, 37 F, 37 G, 37 H, 37 I and 27 J. Extended legend and image interpretation are available on the next page.

Figure 37 A - Non-contrast, slice 0.8 mm, TR 6300 ms

Figure 37 B - Non-contrast, slice 0,8 mm, TR 6300 ms

Figure 37 C - Non-contrast, slice 0.7 mm, TR 12000 ms

Figure 37 D - Non-contrast, slice 0.7 mm, TR 12000 ms

Figure 37 E - Contrast, slice 0.8 mm, TR 6300 ms, right cochlea

Figure 37 F - Contrast, slice 0.8 mm, TR 6300 ms, left cochlea

Figure 37 G- Contrast, slice 0.8 mm, TR 6300 ms, right vestibule

Figure 37 H - Contrast, slice 0.8 mm, TR 6300 ms, left vestibule

Figure 37 I - Contrast, slice 0.7 mm, TR 12000 ms

Figure 37 J - Contrast, slice 0.7 mm, TR 12000 ms

Figures 37 A, 37 B, 37 C, 37 D, 37 E, 37 F, 37 G, 37 H, 37 I and 27 J (on pages 123 and 124) -Although the presence of the cochlear hydrops (blue arrows)on the right side can be suspected even on non-contrast-enhanced images, the enhancement is much better on contrast-enhanced images and the cochlear hydrops is best depicted on the image with a slice thickness of 0.7 mm and TR 12000 ms (37 I) where it would be graded as grade 2 because the entire scala vestibuli is replaced with unenhanced endolymph (green dots), as opposed to the other images where it would be graded as grade 1 because it appears that the scala vestibuli is not replaced in its entirety. Also on the right side, the saccule and utricle are confluent but the overall ratio between the endolymph area (red outline) and the total fluid area (green outline) does not meet the Nakashima or Barath criteria for hydrops (figure 37 I). Normal anatomy can be appreciated on the left side with saccule (blue arrow) and utricle (red arrow) visible on contrast-enhanced images, but the enhancement is too faint for a confident assessment on the non-contrast-enhanced images.

3rd MD PATIENT (Right ear symptomatic)

RIGHT EAR

Figure 38 A

LEFT EAR

Figure 38 B

Figure 38 C

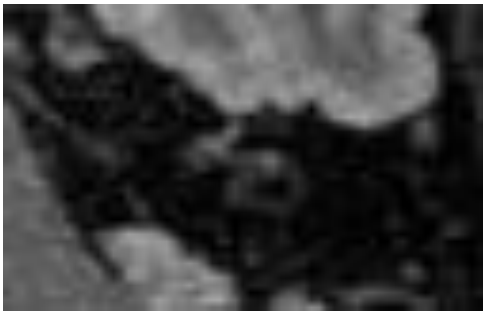

Figure 38 D

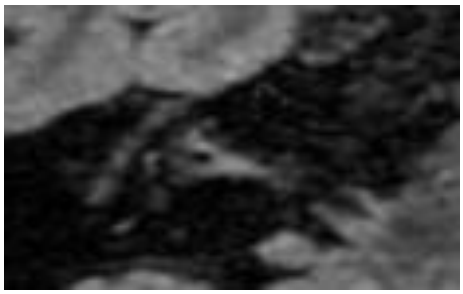

Figure 38 E

Figure 38 F

RIGHT EAR

Figure 38 G

LEFT EAR

Figure 38 H

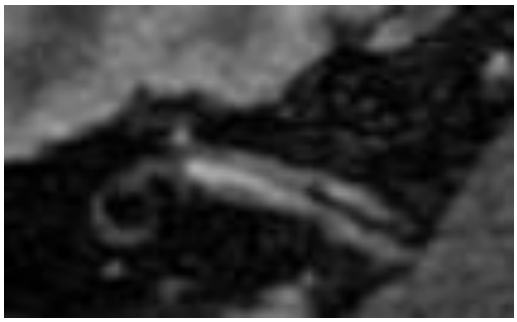

Figure 38 I

Figure 38 J

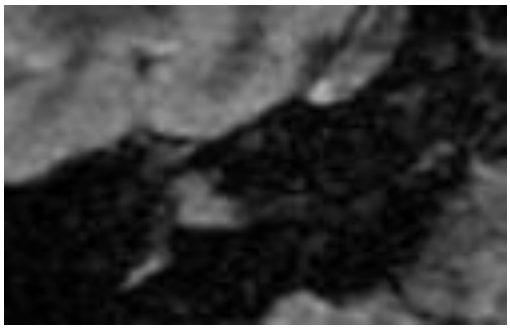

Figure 38 K

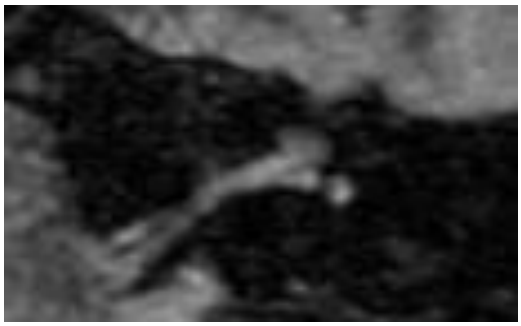

Figure 38 L

Figure 38 M

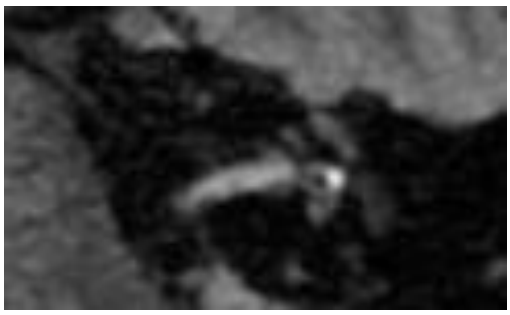

Figure 38 N

Figures 38 A, 38 B, 38 C, 38 D, 38 E, 38 F, 38 G, 38 H, 38 I, 38 J, 38 K, 38 L, 38 M and 38 N (on pages 126 and 127).

Figure 38 A - Non-contrast, slice 0.8 mm, TR 6300 ms, right cochlea

Figure 38 B - Non-contrast, slice 0.8 mm, TR 6300 ms, left cochlea

Figure 38 C - Non-contrast, slice 0.8 mm, TR 6300 ms, right vestibule

Figure 38 D - Non-contrast, slice 0.8 mm, TR 6300 ms, left vestibule

Figure 38 E - Non-contrast, slice 0.7 mm, TR 12000 ms

Figure 38 F - Non-contrast, slice 0.7 mm, TR 12000 ms

Figure 38 G - Contrast, slice 0.8 mm, TR 6300 ms, right cochlea

Figure 38 H - Contrast, slice 0.8 mm, TR 6300 ms, left cochlea

Figure 38 I - Contrast, slice 0.8 mm, TR 6300 ms, right vestibule

Figure 38 J - Contrast, slice 0.8 mm, TR 6300 ms, left vestibule

Figure 38 K - Contrast, slice 0.7 mm, TR 12000 ms, right cochlea

Figure 38 L - Contrast, slice 0.7 mm, TR 12000 ms, left cochlea

Figure 38 M - Contrast, slice 0.7 mm, TR 12000 ms, right vestibule

Figure 38 N -Contrast, slice 0.7 mm, TR 12000 ms, left vestibule

Extended legend and image interpretation are available below. All contrast-enhanced images were taken 4 hours post-contrast administration.

In the above images, regardless of the imaging technique, the level of enhancement is very faint and the presence of hydrops cannot be confidently confirmed in the symptomatic ear in either of the images. The cochlea in the affected ear appears to have more of a 'hydropic' appearance and the vestibule has more of the unenhanced endolymph occupying it than on the unaffected side. However, it is still very challenging to appraise the presence or absence of hydrops. For example, it is unclear how much of the unenhanced endolymph is made of the ampulla of the LSCC and how much of the confluent utricle and saccule. The faint enhancement renders the images almost uninterpretable and EH has not been detected in either of the images of this patient.

4th MD PATIENT (Right ear symptomatic)

RIGHT EAR

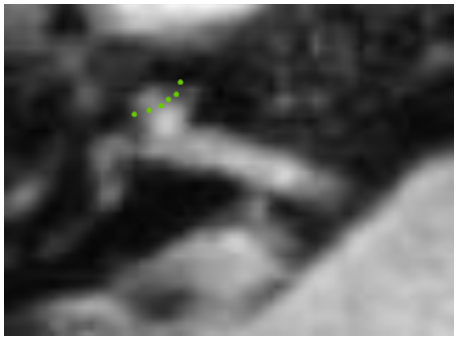

Figure 39 A

LEFT EAR

Figure 39 B

Figure 39 C

Figure 39 D

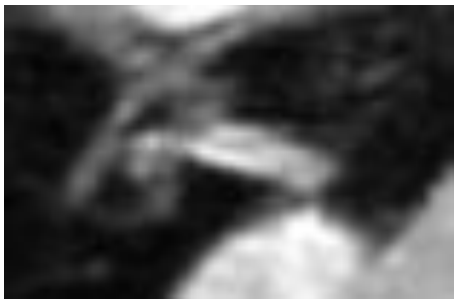

Figure 39 E

Figure 39 F

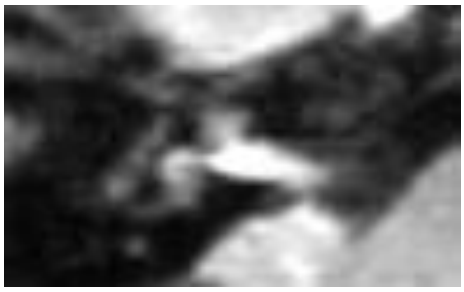

Figure 39 G

Figure 39 H

RIGHT EAR

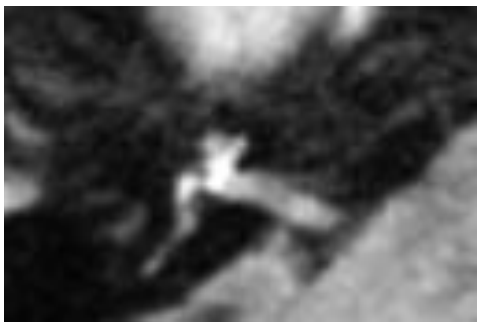

Figure 39 I

LEFT EAR

Figure 39 J

Figure 39 K

Figure 39 L

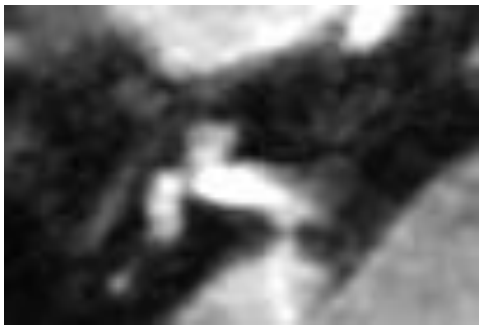

Figure 39 M

Figure 39 N

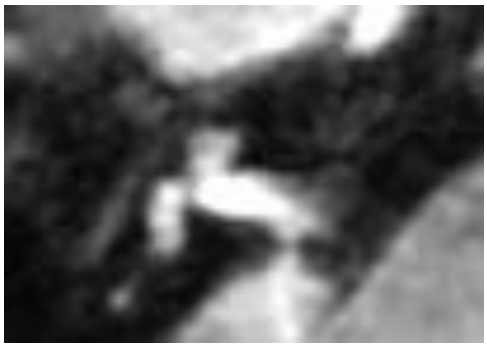

Figure 39 O

Figure 39 P

RIGHT EAR

Figure 39 Q

LEFT EAR

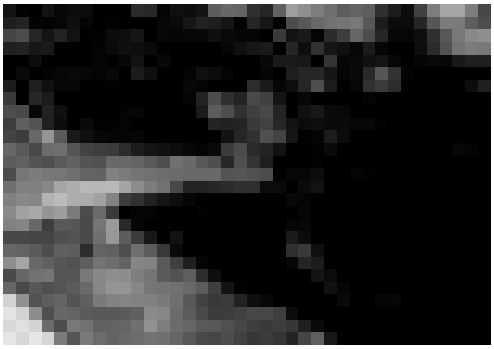

Figure 39 R (N.B. lower in-plane spatial resolution due to zoom effect)

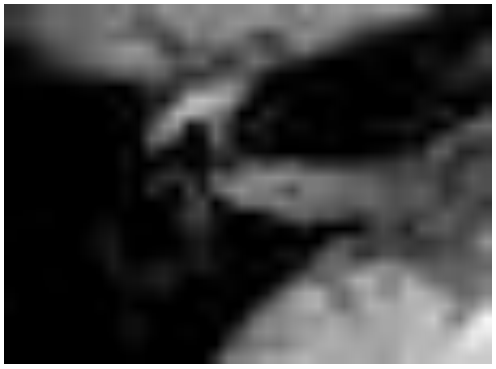

Figure 39 S

Figure 39 T

Figures 39 A, 39 B, 39 C, 39 D, 39 E, 39 F, 39 G, 39 H, 39 I, 39 J, 39 K, 39 L, 39 M, 39 N, 39 O and 39 (on pages 129, 130 and 131). Extended legend and image interpretation are available on the next page.

Figure 39 A - Non-contrast, slice 0.8 mm, TR 6300 ms

Figure 39 B - Non-contrast, slice 0.8 mm, TR 6300 ms

Figure 39 C - Non-contrast, slice 0.7 mm, TR 12000 ms, cochlea

Figure 39 D - Non-contrast, slice 0.7 mm, TR 12000 ms, cochlea

Figure 39 E - Non-contrast, slice 0.7 mm, TR 12000 ms, vestibule

Figure 39 F - Non-contrast, slice 0.7 mm, TR 12000 ms, vestibule

Figure 39 G - 2 hours post-contrast, slice 0.8 mm, TR 6300 ms

Figure 39 H - 2 hours post-contrast, slice 0.8 mm, TR 6300 ms

Figure 39 I - 2 hours post-contrast, slice 0.7 mm, TR 12000 ms, cochlea

Figure 39 J - 2 hours post-contrast, slice 0.7 mm, TR 12000 ms, cochlea

Figure 39 K - 2 hours post-contrast, slice 0.7 mm, TR 12000 ms, vestibule

Figure 39 L – 2 hours post-contrast, slice 0.7 mm, TR 12000 ms, vestibule

Figure 39 M -4 hours post-contrast, slice 0.8 mm, TR 6300 ms

Figure 39 N -4 hours post-contrast, slice 0.8 mm, TR 6300 ms

Figure 39 O - 4 hours post-contrast, slice 0.7 mm, TR 12000 ms

Figure 39 P - 4 hours post-contrast, slice 0.7 mm, TR 12000 ms

Figure 39 Q - 3D REAL IR sequence, slice 0.8 mm, cochlea

Figure 39 R - 3D REAL IR sequence, slice 0.8 mm, cochlea. N.B. lower in-plane spatial resolution due to the zoom effect.

Figure 39 S - 3D REAL IR sequence, slice 0.8 mm, vestibule

Figure 39 T - 3D REAL IR sequence, slice 0.8 mm, vestibule

In this series of images, it is visible how the cochlea and vestibule become clearer as the more optimal technique is being used, i.e. the faintest enhancement of the cochlea on the non-contrast images where EH can still be suspected (green dots) to the 3D Real IR sequence where grade 2 cochlear EH is visible (green arrows). However, cochlear EH could not be confidently appreciated in all of the images. Conversely, although the vestibule is poorly enhanced, no typical morphology would demonstrate vestibular hydrops on any of the images. Also, the quality of images in this patient appears to be degraded by motion artefacts further aggravating the difficulty of EH detection. Additionally, some resolution is lost in image 39 R due to the zooming in. Qualitatively, there doesn't appear to be a significant degree of difference in our example images of 2 and 4-hour post-contrast scans.

DISCUSSION

One of the unique aspects of the study's methodology was the direct comparison between the contrast-enhanced and non-contrast-enhanced scans of the same participants (both MD patients and healthy participants) obtained on the same day. This has not been reported in the literature at the time of writing and represents a novelty compared to the studies mentioned in the literature review. This enabled a real-time comparison between the results of qualitative and semiquantitative analyses of non-contrast-enhanced and contrast-enhanced images. Consequently, it provided an additional way of determining the reliability of non-contrast-enhanced images in diagnosing EH as contrast-enhanced scans (already established in the literature) served as a valid reference point.

Furthermore, the study's methods also included the use of variations in different scanning parameters as previously described (TR, TI and slice thickness). The adjustment of these parameters to provide the optimal scanning protocol has already been reported in previously published studies and that served as a starting point for this study (Naganawa et al., 2008; Zou et al., 2022; Kato et al., 2022). Nonetheless, this still represents one of the novelties of this study as a combined variation of several different parameters in the same participant provided a more detailed analysis of the participants' inner ears.

However, partly due to the small sample size, this also translated into a large heterogeneity and inconsistency of data which limits the conclusions that can be drawn from the study as reiterated later in the text. Nonetheless, this pilot study could and was envisioned to, serve as a reference point for a larger study which could eliminate the above limitations and infer more reliable conclusions on the optimal scanning protocol for EH.

EH was detected across all image acquisition protocols and in all participants, both healthy and MD patients, depending on the scanning protocol. However, EH was more

prevalent in affected ears of MD patients (100%) and was more often detected in healthy participants and unaffected ears of MD patients on scans with shorter TR and TI and thicker slices which infer lower quality (lower CNR) and reliability, both theoretically and as per the literature. Vice versa, 4-hour post-contrast sequences with longer TR (12000 ms) and TI (2500 ms) and thinner slice thickness (0. 7 mm) then carry higher quality and reliability in EH detection. As stated in the methods section, the TI values have automatically changed parallel to TR values, so the same observation can be inferred for the TI of 2500 ms, which is the value automatically chosen by the scanner when the TR of 12000 ms is employed. In the results section, the terms 'likely false positive' or 'likely true positive' were used instead of 'true positive' or 'false positive' to reflect the fact that although EH is less expected in unaffected MD ears and healthy participants' ears, it is still possible for them to exhibit EH and radiological detection simply picked up clinical silent pathology. This is particularly pertinent in unaffected MD ears as one of the premises of the study was to detect clinically silent EH. This underpins the study's exploratory nature as the author acknowledges that the image analysis (due to reader inexperience and small sample size) also might not be robust enough yet to infer definitive conclusions. However, the expectation was that if both ears (affected and unaffected) were assessed on the same MR scan, the existence of EH in one ear should, by comparison, aid in the assessment of a possible EH in the other ear.

Interestingly, none of the studies examined in the scoping literature review on non-contrast-enhanced EH imaging (as well as the vast preponderance of the studies on contrast-enhanced EH imaging) elaborated on the in-plane spatial resolution but rather reported the slice thickness. Consequently, in this study, the in-plane spatial resolution, or its effect, was not evaluated and the role of spatial resolution was confined to the theoretical explanation of the impact that chosen scanning parameters would have on it (page 85).

Additionally, the 3D Real IR and 2-hour post-contrast sequences yielded the same grade of cochlear hydrops in both the affected and the unaffected ear of a single MD patient.

EH (cochlear or vestibular) was more often detected in affected ears of MD patients (100%) than unaffected ears(75%) and it was of lower grade (grade 1 by both Nakashima and Barath) in 75% of cases of unaffected ears. This is to be expected as affected ears are more likely to have hydrops and be of higher grade, but the false positive rate (75%) is still considerable. However, in some images, interpretation was limited due to very poor enhancement of the inner ear structures in general potentially leading to misinterpretation. Moreover, EH was not demonstrated in the unaffected ear on either of the 4-hour post-contrast-enhanced FLAIR sequences. It was only detected in the unaffected ears on the 2-hour post-contrast (with a shorter TR) and 3D Real IR scans in a single case and on non-contrast scans with shorter TR and TI in other cases. This could mean that clinically silent ears demonstrated true EH which could herald symptoms or it could mean miss-interpretation as EH was detected in unaffected ears on sequences expected to be suboptimal(shorter TI and TR, 2 hours post-contrast) and wasn't detected on sequences expected to be optimal(longer TR and TI, 4-hours post-contrast). Notably, on the 3D Real IR sequence, both the affected and the unaffected ear demonstrated cochlear hydrops of the same grade (grade 2 by both Barath and Nakashima criteria). Given a single-case comparison, a definite conclusion regarding 2-hour post-contrast and 3D Real IR in comparison to FLAIR cannot be drawn, and more experience and more images with both techniques would provide appropriate conditions to infer significant results. Although the superior sequence in terms of quality and reliability, theoretically and as per literature (4-hour post-contrast FLAIR with longer TR and TI and thinner slice thickness) detected EH in just 75% of cases, it did not yield a single false positive case which further supports it as the optimal scanning protocol for EH detection on the GE Premier MRI machine.

Conversely, cochlear hydrops was detected in all of the healthy individuals as compared to the 75% of unaffected ears of MD patients, which is unusual as healthy participants are not expected to have EH. The high pickup rate of cochlear hydrops in healthy individuals could potentially mean that these individuals have early stages of MD, but it can also, more likely, be an erroneous reading of a scan due to poor image quality or

non-robust identification criteria. This is because all healthy ears that demonstrated EH were the ones imaged with a shorter TR and TI and thicker slices. It is logic-defying to conclude that the inferior-quality images had a higher yield of a more challenging pathology to detect. What this most likely represents is the inconsistency and inaccuracy of the interpretation of lower-quality images which only underpins the proof of concept that higher-quality images (longer TR and TI and thinner slices) are required for EH detection and false positives are present due to poor image quality. The quality of the non-contrast enhanced scans realistically does not support an attempt at hydrops identification and grading. More experience and intra- and inter-observer agreement would likely have improved the distinction of true EH from healthy ears. This, unfortunately, was not possible and it indicates a limitation within the study.

Based on visual qualitative assessment, the thinner slice sequence with longer TR and TI were preferred for accurate EH detection and this is reflected in the various CNR metrics employed in the study and presented in the results.

In this study, the optimal combination of scanning parameters (4 hours post-contrast FLAIR with thinner slice and longer TR and TI) as mentioned above successfully demonstrated EH in 3 out of 4 affected ears of MD patients with suggested a higher grade of EH. It did not detect EH in any of the unaffected ears of MD patients. In the one healthy participant scanned with this sequence, no pathology was demonstrated. It is worth noting that on other sequences in the same healthy participants, EH was detected. This is against clinical expectations as this healthy individual with no audiovestibular symptoms is not expected to have EH. This appears to underline the value of this combination of imaging parameters as potentially the optimal and most accurate image acquisition sequence for EH imaging on our MRI equipment.

Although the results of the study largely reaffirm the existing literature on the optimal scanning parameters for EH, particularly that contrast enhancement is essential for reliable EH detection, they add little in the way of informing on the optimal diagnostic (grading) criteria. This is partly due to the study's exploratory nature, extensive data

heterogeneity and small sample size but also due to reader inexperience and the learning curve involved in reading such scans. Even though no new diagnostic (grading) criteria were developed, the likeliest optimal scanning protocol was suggested in this study. However, as explained later in the text, a more robust study with a larger sample size and improved data consistency with multi-observer agreement decreasing the learning curve would corroborate the optimal scanning parameters more strongly and could potentially introduce new diagnostic (grading) criteria.

Recruitment of MD patients was challenging and the planned sample size was not achieved despite several amendments as explained in the methods. Additionally, the clinically 'probable' MD patients were also included, when it's known that EH severity and hence, chances of detection, are lower in this group. A larger, demographically more consistent sample size would be optimal for the inference of more significant results.

The heterogeneity of data (30 different sequences of 8 participants) also provides a limitation to the study. However, given its exploratory nature, this was expected and could not be circumvented.

Additionally, only a single-case comparison was provided for 2 hours post-contrast and the 3D Real IR sequence as this was not readily available and required further study amendments. A larger-group comparison with all MD patients scanned with both techniques would be required to better inform which is better on the GE Premier scanner.

The single unblinded observer's above description of data is likely not sufficient to inform the decision on particular image acquisition parameters and was aggravated by lack of experience. Furthermore, the lack of statistical tests also hampers results and conclusions, although, given the small sample size and extensive heterogeneity, these would likely not yield statistically significant results.

Lastly, MRI acceleration techniques were not used in this study, but they could be very helpful in imaging of small structures such as the inner ear as they shorten the scanning

time and by doing so, could potentially improve image quality by reducing motion artefacts and their impact on image quality.

All the above limitations apply in concluding, but taking them all into account and carefully interpreting the results of the pilot study, 4-hour post-contrast-enhanced FLAIR with TR of 12000ms (and subsequent TI of 2500ms) and with a slice thickness of 0.7mm appears to be most promising and reliable in accurately detecting and grading EH on MRI, at least on the 3T GE Premier MRI scanner, with the likely false positives attributable to poor image quality on various other sequences. However, a larger-sample homogenous study with robust statistical analysis and a calculation of an interobserver agreement would be required to corroborate this.

CONCLUSIONS

From the data gathered in this study, I have demonstrated that the SPMIC MRI equipment can be harnessed to successfully image inner ear structures and detect EH in MD patients. Moreover, the data collected informs on the potentially optimal MRI technique to achieve this, which is following the available literature. Acknowledging the aforementioned limitations it appears that the contrast-enhanced 3D FLAIR with the sequence parameter of TR 12000 ms, TI of 2500 ms and slice thickness of 0.7 mm is the most promising option for EH imaging on the 3T GE Premier MRI scanner. I was not able to infer any significant conclusions regarding EH imaging on non-contrast scans in this study and these images were deemed unreliable. Contrast-enhanced images appear to be the mainstay of MR imaging in MD, although conclusions on contrast-images from the pilot study are still limited. The findings were in line with the scoping review which suggested that a 4-hour post-contrast scan with longer TR and TI provided more reliable and higher-quality images for EH detection in MD. It also concorded well in terms of grading criteria used as Nakashima and Barath iterations, commonly used and reported in the literature proved effective and simple to use. The degraded image quality did, however, limit interpretation in some instances.

The next steps of implementation based on the pilot study and the vast literature would be to offer the protocol clinically and do a service evaluation by comparing inter-reader agreement on the presence and grade of EH.

Local implementation might require further sequence optimisation as I successfully did as I developed a protocol that is ready to be used clinically and needs further clinical evaluation in terms of interpreter agreement, tolerability and cost-effectiveness to advance EH-supported MD diagnosis.

In general, this pilot study informs the MRI equipment at SPMIC could be used to detect and grade endolymphatic hydrops confidently and opens the possibility of implementing this scanning protocol in routine clinical practice in the unit. This could, hopefully,

expedite the diagnosis of MD patients and allow patients to initiate treatment and prevention strategies earlier. This study provides a valid starting reference point for the local experts to begin scanning MD patients and accrue more experience in EH detection on MRI.

This opportunity to initiate MRI protocol for MD in the local unit in daily clinical practice is likely the greatest contribution of this study, which was also its aim rendering it successful. Furthermore, the results on the GE scanner will potentially help other units who are using the same equipment to replicate accurate inner ear images.

Another potentially important step would be to create a Delphi study (an online survey) involving experts in the field (ENT Surgeons and Radiologists) to help identify the barriers to implementing MRI in routine clinical practice of diagnosing MD in UK centres and under NICE guidelines.

These efforts would ideally produce a network of clinicians and researchers interested in implementing MRI in the diagnosis of MD in their practice. This network can be used to share raw data and exchange experiences to further optimise the use of MRI in MD, highlighting the opportunity to implement MRI as a tool for the diagnosis of MD in the UK.

These are the likely crucial steps in implementing MRI in the diagnosis of MD in routine clinical practice in the UK.

ACKNOWLEDGEMENTS

I would like to thank the British Society of Otology for supporting the project via their Small Grants Pathway and the Ménière's Society and BRC Hearing database for assisting with recruitment.

My supervisors Prof Dorothee Auer, Dr Ian Wiggins and Mr Anand Kasbekar, as well as the late Prof David Baguley, have been crucial in helping me to overcome the hurdles of a long and challenging research project. Their guidance and constant support have motivated me to continue striving and complete my work.

I would also like to thank Prof Paul Morgan and Dr Jagrit Shah, without their input the project wouldn't have been conceivable or feasible. Furthermore, my thanks go to Andrew Cooper and Jan Alappadan, the radiographers at SPMIC who were consistently there for me whenever I needed them.

Lastly, I'd like to thank my family, my mother Vesna and my sister Marija whose love and support were never in short supply and my partner Soo who understood and was my solace in trying times.

References

Adrion, C., Fischer, C.S., Wagner, J., Gürkov, R., Mansmann, U. and Strupp, M., 2016. Efficacy and safety of betahistine treatment in patients with Meniere's disease: primary results of a long term, multicentre, double blind, randomised, placebo controlled, dose defining trial (BEMED trial). *bmj*, *352*.

Ahmadzai, N., Cheng, W., Kilty, S., Esmaeilisaraji, L., Wolfe, D., Bonaparte, J., Schramm, D., Fitzpatrick, E., Lin, V., Skidmore, B. and Hutton, B., 2020. Pharmacologic and surgical therapies for patients with Meniere's disease: A systematic review and network meta-analysis. PLoS One, 15(9), p.e0237523.

Attyé, A., Eliezer, M., Boudiaf, N., Tropres, I., Chechin, D., Schmerber, S., Dumas, G. and Krainik, A., 2017. MRI of endolymphatic hydrops in patients with Meniere's disease: a case-controlled study with a simplified classification based on saccular morphology. *European radiology*, *27*, pp.3138-3146.

Attyé, A., Eliezer, M., Medici, M., Tropres, I., Dumas, G., Krainik, A. and Schmerber, S., 2018. In vivo imaging of saccular hydrops in humans reflects sensorineural hearing loss rather than Meniere's disease symptoms. *European radiology*, *28*, pp.2916-2922.

Baráth, K., Schuknecht, B., Naldi, A.M., Schrepfer, T., Bockisch, C.J. and Hegemann, S.C.A., 2014. Detection and grading of endolymphatic hydrops in Menière disease using MR imaging. *American Journal of Neuroradiology*, *35*(7), pp.1387-1392.

Basura, G.J., Adams, M.E., Monfared, A., Schwartz, S.R., Antonelli, P.J., Burkard, R., Bush, M.L., Bykowski, J., Colandrea, M., Derebery, J. and Kelly, E.A., 2020. Clinical practice guideline: Ménière's disease executive summary. *Otolaryngology–Head and Neck Surgery*, *162*(4), pp.415-434.

Belal, A. and Antunez, J.C., 1980. Pathology of endolymphatic hydrops. *The Journal of Laryngology & Otology*, *94*(11), pp.1231-1240.

Benson, J.C., Carlson, M.L. and Lane, J.I., 2020. MRI of the internal auditory canal, labyrinth, and middle ear: how we do it. *Radiology*, *297*(2), pp.252-265.

Bernaerts, A. and De Foer, B., 2019. Imaging of Ménière Disease. *Neuroimaging Clinics of North America*, *29*(1), pp.19-28.

Bernaerts, A., Janssen, N., Wuyts, F.L., Blaivie, C., Vanspauwen, R., Van Dinther, J., Zarowski, A., Offeciers, E., Deckers, F., Casselman, J.W. and De Foer, B., 2022. Comparison between 3D SPACE FLAIR and 3D TSE FLAIR in Menière's disease. *Neuroradiology*, *64*(5), pp.1011-1020.

Bernaerts, A., Vanspauwen, R., Blaivie, C., van Dinther, J., Zarowski, A., Wuyts, F.L., Vanden Bossche, S., Offeciers, E., Casselman, J.W. and De Foer, B., 2019. The value of four stage vestibular hydrops grading and asymmetric perilymphatic enhancement in the diagnosis of Menière's disease on MRI. *Neuroradiology*, *61*, pp.421-429.

Carfrae, M.J., Holtzman, A., Eames, F., Parnes, S.M. and Lupinetti, A., 2008. 3 Tesla delayed contrast magnetic resonance imaging evaluation of Meniere's disease. *The Laryngoscope*, *118*(3), pp.501-505.

Chen, W., Geng, Y., Niu, Y., Lin, M., Lin, N. and Sha, Y., 2022. Endolymphatic Hydrops Magnetic Resonance Imaging in Menire's Disease Patients on a Vertigo Attack. *Otology & Neurotology*, *43*(4), pp.489-493.

Colletti, V., Mandalà, M., Carner, M., Barillari, M., Cerini, R., Pozzi Mucelli, R. and Colletti, L., 2010. Evidence of gadolinium distribution from the endolymphatic sac to the endolymphatic compartments of the human inner ear. *Audiology and Neurotology*, *15*(6), pp.353-363.

Connor, S.E.J. and Pai, I., 2021. Endolymphatic hydrops magnetic resonance imaging in Ménière's disease. *Clinical Radiology*, *76*(1), pp.76-e1.

Connor, S., Grzeda, M.T., Jamshidi, B., Ourselin, S., Hajnal, J.V. and Pai, I., 2023. Delayed post gadolinium MRI descriptors for Meniere's disease: a systematic review and meta-analysis. *European Radiology*, *33*(10), pp.7113-7135.

Conte, G., Russo, F.L., Calloni, S.F., Sina, C., Barozzi, S., Di Berardino, F., Scola, E., Palumbo, G., Zanetti, D. and Triulzi, F.M., 2018. MR imaging of endolymphatic hydrops in

Ménière's disease: not all that glitters is gold. *Acta Otorhinolaryngologica Italica*, *38*(4), p.369.

Cureoglu, S., da Costa Monsanto, R. and Paparella, M.M., 2016. Histopathology of Meniere's disease. *Operative Techniques in Otolaryngology-Head and Neck Surgery*, *27*(4), pp.194-204.

de Pont, L.M., van Steekelenburg, J.M., Verhagen, T.O., Houben, M., Goeman, J.J., Verbist, B.M., van Buchem, M.A., Bommeljé, C.C., Blom, H.M. and Hammer, S., 2021. Hydropic ear disease: correlation between audiovestibular symptoms, endolymphatic hydrops and blood-labyrinth barrier impairment. *Frontiers in Surgery*, *8*, p.758947.

Devantier, L., Schmidt, J.H., Djurhuus, B.D., Hougaard, D.D., Händel, M.N., Liviu-Adelin Guldfred, F. and Edemann-Callesen, H., 2019. Current state of evidence for endolymphatic sac surgery in Menière's disease: a systematic review. *Acta Oto-Laryngologica*, *139*(11), pp.953-958.

Dougherty, J.M., Carney, M., Hohman, M.H. and Emmady, P.D. (2023). *[Figure, Inner Ear Anatomy. This illustration...]*. [online] www.ncbi.nlm.nih.gov. Available at: https://www.ncbi.nlm.nih.gov/books/NBK558926/figure/article-31138.image.f2/?report=objectonly [Accessed 31 Jul. 2024].

Eliezer, M., Gillibert, A., Tropres, I., Krainik, A. and Attyé, A., 2017. Influence of inversion time on endolymphatic hydrops evaluation in 3D-FLAIR imaging. *Journal of Neuroradiology*, *44*(5), pp.339-343.

Fang, Z.M., Chen, X., Gu, X., Liu, Y., Zhang, R., Cao, D.R. and He, H.G., 2012. A new magnetic resonance imaging scoring system for perilymphatic space appearance after intratympanic gadolinium injection, and its clinical application. *The Journal of Laryngology & Otology*, *126*(5), pp.454-459.

Fernández-Méndez, R., Wan, Y., Axon, P. and Joannides, A., 2023. Incidence and presentation of vestibular schwannoma: a 3-year cohort registry study. *Acta Neurochirurgica*, *165*(10), pp.2903-2911.

Fiorino, F., Mattellini, B., Vento, M., Mazzocchin, L., Bianconi, L. and Pizzini, F.B., 2016. Does the intravenous administration of frusemide reduce endolymphatic hydrops?. *The Journal of Laryngology & Otology*, *130*(3), pp.242-247.

Fiorino, F., Pizzini, F.B., Barbieri, F. and Beltramello, A., 2012. Magnetic resonance imaging fails to show evidence of reduced endolymphatic hydrops in gentamicin treatment of Meniere's disease. *Otology & Neurotology*, *33*(4), pp.629-633.

Fiorino, F., Pizzini, F.B., Barbieri, F. and Beltramello, A., 2012. Variability in the perilymphatic diffusion of gadolinium does not predict the outcome of intratympanic gentamicin in patients with meniere's disease. *The Laryngoscope*, *122*(4), pp.907-911.

Fiorino, F., Pizzini, F.B., Beltramello, A., Mattellini, B. and Barbieri, F., 2011. Reliability of magnetic resonance imaging performed after intratympanic administration of gadolinium in the identification of endolymphatic hydrops in patients with Ménière's disease. *Otology & Neurotology*, *32*(3), pp.472-477.

Foster, C.A. and Breeze, R.E., 2013. Endolymphatic hydrops in Ménière's disease: cause, consequence, or epiphenomenon?. *Otology & Neurotology*, *34*(7), pp.1210-1214.

Fraysse, B.G., Alonso, A. and House, W.F., 1980. Ménière's disease and Endolymphatic Hydrops Clinical-histopathological correlations. *Annals of Otology, Rhinology & Laryngology*, *89*(6_suppl2), pp.2-22.

Frejo, L., Soto-Varela, A., Santos-Perez, S., Aran, I., Batuecas-Caletrio, A., Perez-Guillen, V., Perez-Garrigues, H., Fraile, J., Martin-Sanz, E., Tapia, M.C. and Trinidad, G., 2016. Clinical subgroups in bilateral Meniere disease. *Frontiers in neurology*, *7*, p.182.

Fukuoka, H., Takumi, Y., Tsukada, K., Miyagawa, M., Oguchi, T., Ueda, H., Kadoya, M. and Usami, S.I., 2012. Comparison of the diagnostic value of 3 T MRI after intratympanic injection of GBCA, electrocochleography, and the glycerol test in patients with Meniere's disease. *Acta oto-laryngologica*, *132*(2), pp.141-145.

Fukushima, M., Kitahara, T., Oya, R., Akahani, S., Inohara, H., Naganawa, S. and Takeda, N., 2017. Longitudinal up-regulation of endolymphatic hydrops in patients with Meniere's disease during medical treatment. *Laryngoscope Investigative Otolaryngology*, *2*(6), pp.344-350.

Fukutomi, H., Hamitouche, L., Yamamoto, T., Denat, L., Zhang, L., Zhang, B., Prevost, V., Triaire, B., Dousset, V., Barreau, X. and Tourdias, T., 2022. Visualization of the saccule and utricle with non-contrast-enhanced FLAIR sequences. *European Radiology*, *32*(5), pp.3532-3540.

Global Market Insights Inc. (n.d.). *MRI Systems Market Share, Size & Trends Report, 2023-2032*. [online] Available at: https://www.gminsights.com/industry-analysis/magnetic-resonance-imaging-mri-systems-market?gclid=Cj0KCQjwwae1BhC_ARIsAK4Jfry0sKidFXGpEOogHFeTH2dl-pYHtzJ-J08WOyh1u9COBr8stwTrgbAaArJTEALw_wcB

Gluth, M.B., 2020. On the relationship between Menière's disease and endolymphatic hydrops. *Otology & Neurotology*, *41*(2), pp.242-249.

Grieve, S.M., Obholzer, R., Malitz, N., Gibson, W.P. and Parker, G.D., 2012. Imaging of endolymphatic hydrops in Meniere's disease at 1.5 T using phase-sensitive inversion recovery:(1) demonstration of feasibility and (2) overcoming the limitations of variable gadolinium absorption. *European Journal of Radiology*, *81*(2), pp.331-338.

Gu, X., Fang, Z.M., Liu, Y., Huang, Z.W., Zhang, R. and Chen, X., 2015. Diagnostic advantages of intratympanically gadolinium contrast-enhanced magnetic resonance imaging in patients with bilateral Meniere's disease. *American Journal of Otolaryngology*, *36*(1), pp.67-73.

Guo, P., Sun, W., Shi, S., Zhang, F., Wang, J. and Wang, W., 2019. Quantitative evaluation of endolymphatic hydrops with MRI through intravenous gadolinium administration and VEMP in unilateral definite Meniere's disease. *European Archives of Oto-Rhino-Laryngology*, *276*, pp.993-1000.

Gürkov, R., 2017. Menière and friends: imaging and classification of hydropic ear disease. *Otology & Neurotology*, *38*(10), pp.e539-e544.

Gürkov, R., Berman, A., Dietrich, O., Flatz, W., Jerin, C., Krause, E., Keeser, D. and Ertl-Wagner, B., 2015. MR volumetric assessment of endolymphatic hydrops. *European radiology*, *25*, pp.585-595.

Gürkov, R., Flatz, W., Ertl-Wagner, B. and Krause, E., 2013. Endolymphatic hydrops in the horizontal semicircular canal: a morphologic correlate for canal paresis in Ménière's disease. *Laryngoscope*, *123*(2).

Gürkov, R., Flatz, W., Keeser, D., Strupp, M., Ertl-Wagner, B. and Krause, E., 2013. Effect of standard-dose Betahistine on endolymphatic hydrops: an MRI pilot study. *European Archives of Oto-Rhino-Laryngology*, *270*, pp.1231-1235.

Gürkov, R., Flatz, W., Louza, J., Strupp, M. and Krause, E., 2011. In vivo visualization of endolyphatic hydrops in patients with Meniere's disease: correlation with audiovestibular function. *European archives of oto-rhino-laryngology*, *268*, pp.1743-1748.

Gürkov, R., Flatz, W., Louza, J., Strupp, M., Ertl-Wagner, B. and Krause, E., 2012. In vivo visualized endolymphatic hydrops and inner ear functions in patients with electrocochleographically confirmed Ménière's disease. *Otology & Neurotology*, *33*(6), pp.1040-1045.

Gürkov, R., Flatz, W., Louza, J., Strupp, M., Ertl-Wagner, B. and Krause, E., 2012. Herniation of the membranous labyrinth into the horizontal semicircular canal is correlated with impaired caloric response in Ménière's disease. *Otology & Neurotology*, *33*(8), pp.1375-1379.

Gürkov, R., Kantner, C., Strupp, M., Flatz, W., Krause, E. and Ertl-Wagner, B., 2014. Endolymphatic hydrops in patients with vestibular migraine and auditory symptoms. *European Archives of Oto-Rhino-Laryngology*, *271*, pp.2661-2667.

Gürkov, R., Lutsenko, V., Babkina, T., Valchyshyn, S. and Situkho, M., 2021. Clinical high-resolution imaging and grading of endolymphatic hydrops in hydropic ear disease

at 1.5 T using the two-slice grading for vestibular endolymphatic hydrops in less than 10 min. *European Archives of Oto-Rhino-Laryngology*, pp.1-7.

Gürkov, R., Pyykö, I., Zou, J. and Kentala, E., 2016. What is Menière's disease? A contemporary re-evaluation of endolymphatic hydrops. *Journal of neurology*, *263*, pp.71-81.

Hallpike, C.S. and Cairns, H., 1938. Observations on the pathology of Meniere's syndrome. *The Journal of Laryngology & Otology*, *53*(10), pp.625-655.

Homann, G., Vieth, V., Weiss, D., Nikolaou, K., Heindel, W., Notohamiprodjo, M. and Böckenfeld, Y., 2015. Semi-quantitative vs. volumetric determination of endolymphatic space in Menière's disease using endolymphatic hydrops 3T-HR-MRI after intravenous gadolinium injection. *PLoS One*, *10*(3), p.e0120357.

Horii, A., Osaki, Y., Kitahara, T., Imai, T., Uno, A., Nishiike, S., Fujita, N. and Inohara, H., 2011. Endolymphatic hydrops in Meniere's disease detected by MRI after intratympanic administration of gadolinium: comparison with sudden deafness. *Acta oto-laryngologica*, *131*(6), pp.602-609.

Hoskin, J.L., 2022. Ménière's disease: new guidelines, subtypes, imaging, and more. *Current opinion in neurology*, *35*(1), pp.90-97.

Inui, H., Sakamoto, T., Ito, T. and Kitahara, T., 2016. Volumetric measurements of the inner ear in patients with Meniere's disease using three-dimensional magnetic resonance imaging. *Acta oto-laryngologica*, *136*(9), pp.888-893.

Ito, T., Kitahara, T., Inui, H., Miyasaka, T., Kichikawa, K., Ota, I., Nario, K., Matsumura, Y. and Yamanaka, T., 2016. Endolymphatic space size in patients with Meniere's disease and healthy controls. *Acta oto-laryngologica*, *136*(9), pp.879-882.

Jerin, C., Floerke, S., Maxwell, R. and Gürkov, R., 2018. Relationship between the extent of endolymphatic hydrops and the severity and fluctuation of audiovestibular symptoms in patients with Menière's disease and MRI evidence of hydrops. *Otology & Neurotology*, *39*(2), pp.e123-e130.Katayama, N., Yamamoto, M., Teranishi, M., Naganawa, S., Nakata, S., Sone, M. and Nakashima, T., 2010.

Relationship between endolymphatic hydrops and vestibular-evoked myogenic potential. *Acta oto-laryngologica*, *130*(8), pp.917-923.

Kanegaonkar, R.G., Najuko-Mafemera, A., Hone, R. and Tikka, T., 2019. Menière's disease treated by grommet insertion. *The Annals of The Royal College of Surgeons of England*, *101*(8), pp.602-605.

Kato, Y., Bokura, K., Taoka, T. and Naganawa, S., 2019. Increased signal intensity of low-concentration gadolinium contrast agent by longer repetition time in heavily T 2-weighted-3D-FLAIR. *Japanese Journal of Radiology*, *37*, pp.431-435.

Keller, J.H., Hirsch, B.E., Marovich, R.S. and Branstetter IV, B.F., 2017. Detection of endolymphatic hydrops using traditional MR imaging sequences. *American journal of otolaryngology*, *38*(4), pp.442-446.

Kenis, C., Crins, T., Bernaerts, A., Casselman, J. and Foer, B.D., 2022. Diagnosis of Menière's disease on MRI: feasibility at 1.5 Tesla. *Acta Radiologica*, *63*(6), pp.810-813.

Kontorinis, G. and Han, A.Y., 2023. A systematic review on delayed acquisition of post-gadolinium MRI in meniere's disease: imaging of the endolymphatic spaces. *Journal of Laryngology and Otology*, *137*(3), pp.239-245.

Lee, S.Y., Kim, Y.S., Jeong, B., Carandang, M., Koo, J.W., Oh, S.H. and Lee, J.H., 2021. Intratympanic steroid versus gentamicin for treatment of refractory Meniere's disease: A meta-analysis. *American Journal of Otolaryngology*, *42*(6), p.103086.

Leng, Y., Fan, W., Liu, Y., Xia, K., Zhou, R., Liu, J., Wang, H., Ma, H. and Liu, B., 2023. Comparison between audio-vestibular findings and contrast-enhanced MRI of inner ear in patients with unilateral Ménière's disease. *Frontiers in Neuroscience*, *17*, p.1128942.

leonte.eu. (n.d.). *Ear*. [online] Available at: https://leonte.eu/A2R/214p-ear.php [Accessed 31 Jul. 2024].

Li, X., Wu, Q., Sha, Y., Dai, C. and Zhang, R., 2020. Gadolinium-enhanced MRI reveals dynamic development of endolymphatic hydrops in Ménière's disease. *Brazilian journal of otorhinolaryngology*, *86*, pp.165-173.

Li, Y., Sha, Y., Wang, F., Lu, P., Liu, X., Sheng, Y., Zhang, Z. and Liu, M., 2019. Comprehensive comparison of MR image quality between intratympanic and intravenous gadolinium injection using 3D real IR sequences. *Acta Oto-Laryngologica*, *139*(8), pp.659-664.

Liu, F., Huang, W., Chen, Q. and Gao, Z., 2015. Comparison of noninvasive evaluation of endolymphatic space in healthy volunteers in different age groups using magnetic resonance imaging. *Acta Oto-Laryngologica*, *135*(5), pp.416-421.

Liu, F., Huang, W., Chen, Q., Meng, X., Wang, Z. and He, Y., 2014. Noninvasive evaluation of the effect of endolymphatic sac decompression in Ménière's disease using magnetic resonance imaging. *Acta oto-laryngologica*, *134*(7), pp.666-671.

Liu, F., Huang, W., Meng, X., Wang, Z., Liu, X. and Chen, Q., 2012. Comparison of noninvasive evaluation of endolymphatic hydrops in Meniere's disease and endolymphatic space in healthy volunteers using magnetic resonance imaging. *Acta oto-laryngologica*, *132*(3), pp.234-240.

Liu, F., Huang, W., Wang, Z., Chen, Q., Liu, X., Li, S. and Wang, S., 2011. Noninvasive evaluation of endolymphatic space in healthy volunteers using magnetic resonance imaging. *Acta oto-laryngologica*, *131*(3), pp.247-257.

Liu, Y., Jia, H., Shi, J., Zheng, H., Li, Y., Yang, J. and Wu, H., 2015. Endolymphatic hydrops detected by 3-dimensional fluid-attenuated inversion recovery MRI following intratympanic injection of gadolinium in the asymptomatic contralateral ears of patients with unilateral Ménière's disease. *Medical science monitor: international medical journal of experimental and clinical research*, *21*, p.701.

Louza, J.P.R., Flatz, W., Krause, E. and Gürkov, R., 2012. Short-term audiologic effect of intratympanic gadolinium contrast agent application in patients with Ménière's disease. *American journal of otolaryngology*, *33*(5), pp.533-537.

Mavrommatis, M.A., Kaul, V.F., Chow, K., Fan, C.J., Bellaire, C.P., Cosetti, M.K., Wanna, G.B. and Perez, E., 2023. Temporal changes in endolymphatic hydrops on MRI with or without intervention: A systematic review. *American Journal of Otolaryngology*, *44*(2), p.103764.

Merchant, S.N., Adams, J.C. and Nadol Jr, J.B., 2005. Pathophysiology of Meniere's syndrome: are symptoms caused by endolymphatic hydrops?. *Otology & Neurotology*, *26*(1), pp.74-81.

Merchant, S.N., Adams, J.C. and Nadol Jr, J.B., 2005. Pathophysiology of Meniere's syndrome: are symptoms caused by endolymphatic hydrops?. Otology & Neurotology, 26(1), pp.74-81.

Miyagawa, M., Fukuoka, H., Tsukada, K., Oguchi, T., Takumi, Y., Sugiura, M., Ueda, H., Kadoya, M. and Usami, S.I., 2009. Endolymphatic hydrops and therapeutic effects are visualized in 'atypical'Meniere's disease. *Acta oto-laryngologica*, *129*(11), pp.1326-1329.

Monsanto, R.D.C., Pauna, H.F., Kwon, G., Schachern, P.A., Tsuprun, V., Paparella, M.M. and Cureoglu, S., 2017. A three-dimensional analysis of the endolymph drainage system in Ménière disease. *The Laryngoscope*, *127*(5), pp.E170-E175.

Morales-Luckie, E., Cornejo-Suarez, A., Zaragoza-Contreras, M.A. and Gonzalez-Perez, O., 2005. Oral administration of prednisone to control refractory vertigo in Ménière's disease: a pilot study. *Otology & Neurotology*, *26*(5), pp.1022-1026.

Naganawa, S. and Nakashima, T., 2014. Visualization of endolymphatic hydrops with MR imaging in patients with Ménière's disease and related pathologies: current status of its methods and clinical significance. *Japanese Journal of Radiology*, *32*, pp.191-204.

Naganawa, S., Ishihara, S., Iwano, S., Kawai, H., Sone, M. and Nakashima, T., 2010. Estimation of gadolinium-induced T1-shortening with measurement of simple signal intensity ratio between the cochlea and brain parenchyma on 3D-FLAIR: correlation with T1 measurement by TI scout sequence. *Magnetic Resonance in Medical Sciences*, *9*(1), pp.17-22.

Naganawa, S., Ishihara, S., Iwano, S., Sone, M. and Nakashima, T., 2010. Three-dimensional (3D) visualization of endolymphatic hydrops after intratympanic injection of Gd-DTPA: Optimization of a 3D-real inversion-recovery turbo spin-

echo (TSE) sequence and application of a 32-channel head coil at 3T. *Journal of Magnetic Resonance Imaging*, *31*(1), pp.210-214.

Naganawa, S., Kanou, M., Ohashi, T., Kuno, K. and Sone, M., 2016. Simple estimation of the endolymphatic volume ratio after intravenous administration of a single-dose of gadolinium contrast. *Magnetic Resonance in Medical Sciences*, *15*(4), pp.379-385.

Naganawa, S., Kawai, H., Ikeda, M., Sone, M. and Nakashima, T., 2015. Imaging of endolymphatic hydrops in 10 minutes: a new strategy to reduce scan time to one third. *Magnetic Resonance in Medical Sciences*, *14*(1), pp.77-83.

Naganawa, S., Kawai, H., Sone, M. and Ikeda, M., 2015. Ratio of vestibular endolymph in patients with isolated lateral semicircular canal dysplasia. *Magnetic Resonance in Medical Sciences*, *14*(3), pp.203-210.

Naganawa, S., Kawai, H., Sone, M. and Nakashima, T., 2010. Increased sensitivity to low concentration gadolinium contrast by optimized heavily T2-weighted 3D-FLAIR to visualize endolymphatic space. *Magnetic Resonance in Medical Sciences*, *9*(2), pp.73-80.

Naganawa, S., Kawai, H., Taoka, T. and Sone, M., 2017. Improved HYDROPS: imaging of endolymphatic hydrops after intravenous administration of gadolinium. *Magnetic Resonance in Medical Sciences*, *16*(4), pp.357-361.

Naganawa, S., Kawai, H., Taoka, T. and Sone, M., 2019. Improved 3D-real inversion recovery: a robust imaging technique for endolymphatic hydrops after intravenous administration of gadolinium. *Magnetic Resonance in Medical Sciences*, *18*(1), pp.105-108.

Naganawa, S., Ohashi, T., Kanou, M., Kuno, K., Sone, M. and Ikeda, M., 2015. Volume quantification of endolymph after intravenous administration of a single dose of gadolinium contrast agent: comparison of 18-versus 8-minute imaging protocols. *Magnetic Resonance in Medical Sciences*, *14*(4), pp.257-262.

Naganawa, S., Satake, H., Iwano, S., Fukatsu, H., Sone, M. and Nakashima, T., 2008. Imaging endolymphatic hydrops at 3 tesla using 3D-FLAIR with intratympanic Gd-DTPA administration. *Magnetic Resonance in Medical Sciences*, *7*(2), pp.85-91.

Naganawa, S., Satake, H., Kawamura, M., Fukatsu, H., Sone, M. and Nakashima, T., 2008. Separate visualization of endolymphatic space, perilymphatic space and bone by a single pulse sequence; 3D-inversion recovery imaging utilizing real reconstruction after intratympanic Gd-DTPA administration at 3 Tesla. *European radiology*, *18*, pp.920-924.

Naganawa, S., Sone, M., Yamazaki, M., Kawai, H. and Nakashima, T., 2011. Visualization of endolymphatic hydrops after intratympanic injection of Gd-DTPA: comparison of 2D and 3D real inversion recovery imaging. *Magnetic Resonance in Medical Sciences*, *10*(2), pp.101-106.

Naganawa, S., Sugiura, M., Kawamura, M., Fukatsu, H., Sone, M. and Nakashima, T., 2008. Imaging of endolymphatic and perilymphatic fluid at 3T after intratympanic administration of gadolinium-diethylene-triamine pentaacetic acid. *American journal of neuroradiology*, *29*(4), pp.724-726.

Naganawa, S., Suzuki, K., Nakamichi, R., Bokura, K., Yoshida, T., Sone, M., Homann, G., Nakashima, T. and Ikeda, M., 2013. Semi-quantification of endolymphatic size on MR imaging after intravenous injection of single-dose gadodiamide: comparison between two types of processing strategies. *Magnetic Resonance in Medical Sciences*, *12*(4), pp.261-269.

Naganawa, S., Suzuki, K., Yamazaki, M., Sakurai, Y. and Ikeda, M., 2014. Time course for measuring endolymphatic size in healthy volunteers following intravenous administration of gadoteridol. *Magnetic Resonance in Medical Sciences*, *13*(2), pp.73-80.

Naganawa, S., Yamazaki, M., Kawai, H., Bokura, K., Iida, T., Sone, M. and Nakashima, T., 2014. MR imaging of Ménière's disease after combined intratympanic and intravenous injection of gadolinium using HYDROPS2. *Magnetic Resonance in Medical Sciences*, *13*(2), pp.133-137.

Naganawa, S., Yamazaki, M., Kawai, H., Bokura, K., Sone, M. and Nakashima, T., 2013. Visualization of endolymphatic hydrops in Ménière's disease after intravenous administration of single-dose gadodiamide at 1.5 T. *Magnetic Resonance in Medical Sciences*, *12*(2), pp.137-139.

Naganawa, S., Yamazaki, M., Kawai, H., Bokura, K., Sone, M. and Nakashima, T., 2012. Visualization of endolymphatic hydrops in Ménière's disease after single-dose intravenous gadolinium-based contrast medium: timing of optimal enhancement. *Magnetic Resonance in Medical Sciences*, *11*(1), pp.43-51.

Naganawa, S., Yamazaki, M., Kawai, H., Bokura, K., Sone, M. and Nakashima, T., 2010. Visualization of endolymphatic hydrops in Ménière's disease with single-dose intravenous gadolinium-based contrast media using heavily T2-weighted 3D-FLAIR. *Magnetic Resonance in Medical Sciences*, *9*(4), pp.237-242.

Naganawa, S., Yamazaki, M., Kawai, H., Bokura, K., Sone, M. and Nakashima, T., 2012. Visualization of endolymphatic hydrops in Ménière's disease after single-dose intravenous gadolinium-based contrast medium: timing of optimal enhancement. *Magnetic Resonance in Medical Sciences*, *11*(1), pp.43-51.

Nakada, T., Teranishi, M., Sugiura, S., Uchida, Y., Naganawa, S. and Sone, M., 2021. Imaging of endolymphatic hydrops on a vertigo attack of Meniere's disease. *Nagoya Journal of Medical Science*, *83*(1), p.209.

Nakada, T., Yoshida, T., Suga, K., Kato, M., Otake, H., Kato, K., Teranishi, M., Sone, M., Sugiura, S., Kuno, K. and Pyykkö, I., 2014. Endolymphatic space size in patients with vestibular migraine and Ménière's disease. *Journal of neurology*, *261*, pp.2079-2084.

Nakashima, T., Naganawa, S., Katayama, N., Teranishi, M., Nakata, S., Sugiura, M., Sone, M., Kasai, S., Yoshioka, M. and Yamamoto, M., 2009. Clinical significance of endolymphatic imaging after intratympanic gadolinium injection. *Acta Oto-Laryngologica*, *129*(sup560), pp.9-14.

Nakashima, T., Naganawa, S., Pyykkö, I., Gibson, W.P., Sone, M., Nakata, S. and Teranishi, M., 2009. Grading of endolymphatic hydrops using magnetic resonance imaging. *Acta Oto-Laryngologica*, *129*(sup560), pp.5-8.

Nakashima, T., Naganawa, S., Sugiura, M., Teranishi, M., Sone, M., Hayashi, H., Nakata, S., Katayama, N. and Ishida, I.M., 2007. Visualization of endolymphatic hydrops in patients with Meniere's disease. *The Laryngoscope*, *117*(3), pp.415-420.

Nakashima, T., Sone, M., Teranishi, M., Yoshida, T., Terasaki, H., Kondo, M., Yasuma, T., Wakabayashi, T., Nagatani, T. and Naganawa, S., 2012. A perspective from magnetic resonance imaging findings of the inner ear: relationships among cerebrospinal, ocular and inner ear fluids. *Auris Nasus Larynx*, *39*(4), pp.345-355.

NICE. (n.d.). *CKS is only available in the UK*. [online] Available at: https://cks.nice.org.uk/topics/menieres-disease/[Accessed 31 Jul. 2024].

Niyazov, D.M., Andrews, J.C., Strelioff, D., Sinha, S. and Lufkin, R., 2001. Diagnosis of endolymphatic hydrops in vivo with magnetic resonance imaging. *Otology & neurotology*, *22*(6), pp.813-817.

Louza, J., Krause, E. and Gürkov, R., 2015. Hearing function after intratympanic application of gadolinium-based contrast agent: a long-term evaluation. *The Laryngoscope*, *125*(10), pp.2366-2370.

Obeidat, F.S. and Lewis Bell, S., 2019. Comparing the sensitivity and specificity of cervical vestibular-evoked myogenic potentials and electrocochleography in the diagnosis of Ménière's disease. *International Journal of Audiology*, *58*(11), pp.738-746.

Pender, D.J., 2014. Endolymphatic hydrops and Ménière's disease: a lesion meta-analysis. *The Journal of Laryngology & Otology*, *128*(10), pp.859-865.

Pyykkö, I., Manchaiah, V., Färkkilä, M., Kentala, E. and Zou, J., 2019. Association between Ménière's disease and vestibular migraine. *Auris Nasus Larynx*, *46*(5), pp.724-733.

Pyykkö, I., Nakashima, T., Yoshida, T., Zou, J. and Naganawa, S., 2013. Meniere's disease: a reappraisal supported by a variable latency of symptoms and the MRI visualisation of endolymphatic hydrops. *BMJ open*, *3*(2), p.e001555.

Rauch, S.D., Merchant, S.N. and Thedinger, B.A., 1989. Meniere's syndrome and endolymphatic hydrops: double-blind temporal bone study. *Annals of Otology, Rhinology & Laryngology*, *98*(11), pp.873-883.

Rizk, H.G., Mehta, N.K., Qureshi, U., Yuen, E., Zhang, K., Nkrumah, Y., Lambert, P.R., Liu, Y.F., McRackan, T.R., Nguyen, S.A. and Meyer, T.A., 2022. Pathogenesis and etiology of Meniere disease: a scoping review of a century of evidence. *JAMA Otolaryngology–Head & Neck Surgery*, *148*(4), pp.360-368.

Sano, R., Teranishi, M., Yamazaki, M., Isoda, H., Naganawa, S., Sone, M., Hiramatsu, M., Yoshida, T., Suzuki, H. and Nakashima, T., 2012. Contrast enhancement of the inner ear in magnetic resonance images taken at 10 minutes or 4 hours after intravenous gadolinium injection. *Acta oto-laryngologica*, *132*(3), pp.241-246.

Schmalbrock, P., 2000. Comparison of three-dimensional fast spin echo and gradient echo sequences for high-resolution temporal bone imaging. *Journal of Magnetic Resonance Imaging*, *12*(6), pp.814-825.

Sepahdari, A.R., Ishiyama, G., Vorasubin, N., Peng, K.A., Linetsky, M. and Ishiyama, A., 2015. Delayed intravenous contrast-enhanced 3D FLAIR MRI in Meniere's disease: correlation of quantitative measures of endolymphatic hydrops with hearing. *Clinical imaging*, *39*(1), pp.26-31.

Sharon, J.D., Trevino, C., Schubert, M.C. and Carey, J.P., 2015. Treatment of Meniere's disease. *Current treatment options in neurology*, *17*, pp.1-16.

Shi, S., Guo, P., Li, W. and Wang, W., 2019. Clinical features and endolymphatic hydrops in patients with MRI evidence of hydrops. *Annals of Otology, Rhinology & Laryngology*, *128*(4), pp.286-292.

Shimono, M., Teranishi, M., Yoshida, T., Kato, M., Sano, R., Otake, H., Kato, K., Sone, M., Ohmiya, N., Naganawa, S. and Nakashima, T., 2013. Endolymphatic hydrops

revealed by magnetic resonance imaging in patients with acute low-tone sensorineural hearing loss. *Otology & Neurotology*, *34*(7), pp.1241-1246.

Simon, F., Guichard, J.P., Kania, R., Franc, J., Herman, P. and Hautefort, C., 2017. Saccular measurements in routine MRI can predict hydrops in Menière's disease. *European Archives of Oto-Rhino-Laryngology*, *274*, pp.4113-4120.

Sperling, N.M., Paparella, M.M., Yoon, T.H. and Zelterman, D., 1993. Symptomatic versus asymptomatic endolymphatic hydrops: a histopathologic comparison. *The Laryngoscope*, *103*(3), pp.277-285.

Suárez Vega, V.M., Domínguez, P., Caballeros Lam, F.M., Leal, J.I. and Perez-Fernandez, N., 2020. Comparison between high-resolution 3D-IR with real reconstruction and 3D-flair sequences in the assessment of endolymphatic hydrops in 3 tesla. *Acta Oto-Laryngologica*, *140*(11), pp.883-888.

Suga, K., Kato, M., Yoshida, T., Nishio, N., Nakada, T., Sugiura, S., Otake, H., Kato, K., Teranishi, M., Sone, M. and Naganawa, S., 2015. Changes in endolymphatic hydrops in patients with Ménière's disease treated conservatively for more than 1 year. *Acta Oto-Laryngologica*, *135*(9), pp.866-870.

Suzuki, H., Teranishi, M., Sone, M., Yamazaki, M., Naganawa, S. and Nakashima, T., 2011. Contrast enhancement of the inner ear after intravenous administration of a standard or double dose of gadolinium contrast agents. *Acta oto-laryngologica*, *131*(10), pp.1025-1031.

Tagaya, M., Teranishi, M., Naganawa, S., Iwata, T., Yoshida, T., Otake, H., Nakata, S., Sone, M. and Nakashima, T., 2010. 3 Tesla magnetic resonance imaging obtained 4 hours after intravenous gadolinium injection in patients with sudden deafness. *Acta oto-laryngologica*, *130*(6), pp.665-669.

Takeda, T., Takeda, S. and Kakigi, A., 2020. A possible mechanism of the formation of endolymphatic hydrops and its associated inner ear disorders. *Auris Nasus Larynx*, *47*(1), pp.25-41.

Teixido, M.T., Kirkilas, G., Seymour, P., Sem, K., Iaia, A., Sabra, O. and Isildak, H., 2015. Normative inner ear volumetric measurements. *Journal of Craniofacial Surgery*, *26*(1), pp.251-254.

Thomsen, J., Bretlau, P., Tos, M. and Johnsen, N.J., 1981. Ménière's disease: endolymphatic sac decompression compared with sham (placebo) decompression. *Annals of the New York Academy of Sciences*, *374*, pp.820-830.

Tyrrell, J., Whinney, D.J. and Taylor, T., 2016. The cost of Ménière's disease: a novel multisource approach. *Ear and hearing*, *37*(3), pp.e202-e209.

Tyrrell, J.S., Whinney, D.J., Ukoumunne, O.C., Fleming, L.E. and Osborne, N.J., 2014. Prevalence, associated factors, and comorbid conditions for Meniere's disease. *Ear and hearing*, *35*(4), pp.e162-e169.

Uno, A., Imai, T., Watanabe, Y., Tanaka, H., Kitahara, T., Horii, A., Kamakura, T., Takimoto, Y., Osaki, Y., Nishiike, S. and Inohara, H., 2013. Changes in endolymphatic hydrops after sac surgery examined by Gd-enhanced MRI. *Acta oto-laryngologica*, *133*(9), pp.924-929.

Van Esch, B.F., van der Scheer-Horst, E.S., van der Zaag-Loonen, H.J., Bruintjes, T.D. and van Benthem, P.P.G., 2017. The effect of vestibular rehabilitation in patients with Ménière's disease: a systematic review. Otolaryngology–Head and Neck Surgery, 156(3), pp.426-434.

Van Esch, B., van der Zaag-Loonen, H., Bruintjes, T. and van Benthem, P.P., 2022. Betahistine in Meniere's disease or syndrome: a systematic review. *Audiology and Neurotology*, *27*(1), pp.1-33.

Van Steekelenburg, J.M., Van Weijnen, A., De Pont, L.M.H., Vijlbrief, O.D., Bommeljé, C.C., Koopman, J.P., Verbist, B.M., Blom, H.M. and Hammer, S., 2020. Value of endolymphatic hydrops and perilymph signal intensity in suspected Ménière disease. *American Journal of Neuroradiology*, *41*(3), pp.529-534.

Venkatasamy, A., Veillon, F., Fleury, A., Eliezer, M., Abu Eid, M., Romain, B., Vuong, H., Rohmer, D., Charpiot, A., Sick, H. and Riehm, S., 2017. Imaging of the saccule for the diagnosis of endolymphatic hydrops in Meniere disease, using a three-

dimensional T2-weighted steady state free precession sequence: accurate, fast, and without contrast material intravenous injection. *European Radiology Experimental*, *1*, pp.1-8.

Wang, P., Yu, D., Wang, H., Ye, H., Qiao, R., Chen, Z., Wu, Y., Li, Y., Shi, H., Zou, J. and Yin, S., 2020. Contrast-Enhanced MRI Combined With the Glycerol Test Reveals the Heterogeneous Dynamics of Endolymphatic Hydrops in Patients With Menière's Disease. *Journal of Magnetic Resonance Imaging*, *52*(4), pp.1066-1073.

Webster, K.E., George, B., Lee, A., Galbraith, K., Harrington-Benton, N.A., Judd, O., Kaski, D., Maarsingh, O.R., MacKeith, S., Murdin, L. and Ray, J., 2023. Lifestyle and dietary interventions for Ménière's disease. Cochrane Database of Systematic Reviews, (2).

What is Ménière's disease? - diagnosis and treatment (2024) *National Institute of Deafness and Other Communication Disorders* (Accessed: 05 December 2024).

Wnuk, E., Lachowska, M., Jasińska-Nowacka, A., Maj, E. and Niemczyk, K., 2022. Reliability of endolymphatic hydrops qualitative assessment in magnetic resonance imaging. *Journal of Clinical Medicine*, *12*(1), p.202.

Wu, Q., Dai, C., Zhao, M. and Sha, Y., 2016. The correlation between symptoms of definite Meniere's disease and endolymphatic hydrops visualized by magnetic resonance imaging. *The Laryngoscope*, *126*(4), pp.974-979.

www.medicines.org.uk. (n.d.). *Gadovist 1.0mmol/ml solution for injection - Summary of Product Characteristics (SmPC) - (emc)*. [online] Available at: https://www.medicines.org.uk/emc/product/2876/smpc.

Xie, J., Zhang, W., Zhu, J., Hui, L., Li, S., Ren, L., Wang, F. and Zhang, B., 2021. Differential diagnosis of endolymphatic hydrops between "probable" and "definite" Meniere's disease via magnetic resonance imaging. *Otolaryngology–Head and Neck Surgery*, *165*(5), pp.696-700.

Yamazaki, M., Naganawa, S., Tagaya, M., Kawai, H., Ikeda, M., Sone, M., Teranishi, M., Suzuki, H. and Nakashima, T., 2012. Comparison of contrast effect on the cochlear

perilymph after intratympanic and intravenous gadolinium injection. *American journal of neuroradiology*, *33*(4), pp.773-778.

Zhang, S., Leng, Y., Liu, B., Shi, H., Lu, M. and Kong, W., 2015. Diagnostic value of vestibular evoked myogenic potentials in endolymphatic hydrops: a meta-analysis. *Scientific reports*, *5*(1), p.14951.

Zhang, W., Hui, L., Zhang, B., Ren, L., Zhu, J., Wang, F. and Li, S., 2021. The correlation between endolymphatic hydrops and clinical features of Meniere disease. *The Laryngoscope*, *131*(1), pp.E144-E150.

Zou, J., Chen, L., Li, H., Zhang, G., Pyykkö, I. and Lu, J., 2022. High-quality imaging of endolymphatic hydrops acquired in 7 minutes using sensitive hT2W–3D–FLAIR reconstructed with magnitude and zero-filled interpolation. *European Archives of Oto-Rhino-Laryngology*, *279*(5), pp.2279-2290.

APPENDIX 1 – Study protocol

FUNDING-

This study was funded by the NIHR (National Institute for Health and Care Research) Biomedical Research Centre. Additional funding was provided by the British Society of Otology Small Grant in the amount of £1000.

CONFLICT OF INTEREST

The authors have no conflict of interest to declare.

FRAMEWORK-

The study was conducted as part of a part-time MRes degree (Master of Research) at The University of Nottingham which lasted from February 1st, 2022 to July 1st, 2024.

STUDY DURATION-

The study was initiated by submitting an application via IRAS (Integrated Research Application System) on August 15th, 2022 and it concluded on August 1st, 2024.

ETHICS AND OTHER NECESSARY APPROVALS-

The study was sponsored by The University of Nottingham and ethical approval was obtained from the West of Scotland Ethics Committee with subsequent approval from the Health Research Authority. The Research and Innovation Department at the Nottingham University Hospitals NHS Trust officially approved the study on December 8th, 2022 which is when the recruitment for the study commenced.

OBJECTIVES –

Firstly, I aimed to locally establish high-quality MRI of inner ear structures using both dedicated contrast-enhanced MRI and non-contrast-enhanced MRI in healthy participants (phase 1).

Secondly, I tried to determine the feasibility of detecting and grading endolymphatic hydrops in patients with Meniere's disease (phase 2) by MR imaging both with and without contrast enhancement.

To explore the heterogeneity of endolymphatic hydrops ipsi- and contralateral to the most affected ear.

TRIAL CONFIGURATION –

I conducted a single-centre feasibility and pilot study in healthy controls and participants with Meniere's disease. Our primary endpoint was to obtain high-quality magnetic resonance images of the participants' inner ears with measurable inner ear compartments. Our secondary endpoint was to detect and grade endolymphatic hydrops on the MR images obtained, including both the 2-hour post-contrast scan and the 4-hour post-contrast scan.

Our safety endpoint was to successfully obtain images with no AEs (adverse events) reported during the study, no incidental findings on the scans and no discontinuations/withdrawals due to AEs or other reasons.

TRIAL SETTINGS –

The study was conducted in secondary care, in a tertiary centre University Teaching Hospital, Queens Medical Centre in Nottingham which is part of the Nottingham University Hospitals NHS Trust. The scanning facilities were on the Queens Medical Centre grounds, but in a separate section that belongs to The Sir Peter Mansfield Imaging Centre which is part of The University of Nottingham.

TRIAL/STUDY MANAGEMENT -

The Chief Investigator had overall responsibility for the study and oversaw all study management. The data custodian was also the Chief Investigator. There were no committees involved in the management of the study. Monthly meetings with the entire research team were held to monitor the progress of the study and any concerns

identified and relayed. The student, Dr Raul Simon, who was the Deputy Principal Investigator held weekly meetings with his supervisor(s) to make sure the project was running smoothly. The student took ownership of arranging both meetings. One of the supervisors, Mr Anand Kasbekar, was also the Principal Investigator and served as the point of contact and was responsible for the conducting of research in general. The student established first contact and had discussions with potential participants to help them decide if they wish to take part or not. The student was also responsible for obtaining informed consent from participants, and cannulation. The Principal Investigator, the Deputy Principal Investigator and one of the medical collaborators (Dr Jagrit Shah) were the ones prescribing and administering contrast with the Deputy PI performing this duty on most occasions.

DATA PROTECTION

All trial staff and investigators endeavoured to protect the rights of the trial's participants to privacy and informed consent, and adhere to the Data Protection Act, 2018. The CRF only collected the minimum required information for the purposes of the trial. CRFs will be held securely, in a locked room, or locked cupboard or cabinet. Access to the information was limited to the trial staff investigators and relevant regulatory authorities Computer-held data including the trial database was held securely and password protected. All data was stored on a secure dedicated local web server. Access was restricted by user identifiers and passwords (encrypted using a one-way encryption method). Information about the trial in the participant's medical records/hospital notes was treated confidentially in the same way as all other confidential medical information. Electronic data was backed up every 24 hours to both local and remote media in encrypted format. All data was anonymised and encrypted password-protected files (Mac OS supports 256 encryption as standard). Laptop computers are 256-bit-encrypted and password-controlled.

SAMPLE SIZE –

This feasibility study was conducted in 2 phases, to examine if our MRI equipment can be harnessed to obtain high-quality images of the inner ear and detect endolymphatic hydrops, hence a small sample size of up to 20 is required with no statistical analysis necessary. I required two groups of participants, one with no endolymphatic hydrops to see if adequate images could be obtained and to gauge the MRI machines appropriately (up to 10 healthy participants), and the other with clinically diagnosed Meniere's disease, to detect and grade endolymphatic hydrops (10 participants). The proposed sample size was based on our long-standing experience in MRI sequence optimisation, and to capture expected biological heterogeneity across different stages of the condition, and anatomical variation of the inner ear.

PARTICIPANTS –

Healthy individuals with no audio-vestibular symptoms and no previous ENT surgery were recruited as phase 1 of the study. Meniere's disease patients, clinically 'definite' and clinically 'probable' were recruited as part of phase 2.

The Meniere's disease cohort was recruited, naturally, as these patients were expected to have endolymphatic hydrops in the affected ear and potentially in the clinically non-affected ear.

ELIGIBILITY CRITERIA -

Phase 1 - a group of up to 10 healthy, English-speaking participants, both male and female, aged between 20 and 60 years, without audio-vestibular symptoms and any history of major ear surgery, who can give informed consent and with no contraindications to MRI or Gadolinium

Phase 2 - a group of up to 10 patients, English-speaking, both male and female, aged between 20 and 60, who have been diagnosed as having either 'clinically probable' or 'clinically definite' Meniere's disease as per AAOHNS 2020 criteria, who can give informed consent, with no contraindications to MRI or Gadolinium

INCLUSION CRITERIA

Phase 1 - a group of 10 healthy participants

• Both male and female

• aged between 20 and 60 years

• Without any audio-vestibular symptoms

• Without any history of major ear surgery

• Who speak English

• Who can give informed consent

Phase 2 - a group of 10 patients •

Both male and female aged between 20 and 60

• who have been diagnosed as having ‘clinically probable’ or 'clinically definite' Meniere's disease as per AAOHNS 2020 criteria

• Who speak English

• Who can give informed consent

EXCLUSION CRITERIA

Phase 1 participants –

• Individuals with any history of kidney disease

• Pregnant or breast-feeding individuals

• Diabetic patients and patients on metformin

• Patients in perioperative liver transplantation period

• Patients with renal transplant, patients on haemodialysis

• Elderly and neonates and infants

• Patients with poorly controlled asthma

• Patients with multiple allergies or documented severe allergies requiring therapy

• Patients with cardiac disease

• Patients with a cochlear implant, deep brain stimulator, any metallic foreign bodies such as aneurysm clips and any query/potential metallic foreign bodies. Note that there are some pacemaker/defibrillators & wires that are compatible with MRI

• Individuals who are allergic to Gadolinium contrast individuals who have taken part in a research study in the last 3 months involving invasive procedures or an inconvenience allowance

Phase 2 participants (in addition to the above criteria for Phase 1 participants) –

• Patients with undiagnosed audio-vestibular illness

• Patients with prior ENT surgery

RECRUITMENT –

The recruitment criteria were kept very rigid to minimise the risk of harm to the participants that could potentially arise due to the use of Gadolinium contrast. Hence, groups that were at higher risk of adverse reactions were excluded (i.e., asthmatic patients, and patients with renal insufficiency).

Additionally, the criteria were limited to only patients with clinically 'definite' Meniere's disease as I felt these should rule out diagnostic uncertainties and similar presenting conditions such as vestibular migraine, sudden sensorineural hearing loss etc., and hence provide appropriate pathological substrate on subsequent imaging (endolymphatic hydrops).

Initially, the route of recruitment was envisioned in two ways.

Phase 1 participants were recruited from the multiple established pathways including medical students, NUH staff and junior doctor body via word of mouth, invitational leaflets distributed at university sites and departmental newsletters and emails circulated on regional teaching days. I experienced no difficulties with recruiting the healthy participant cohort and although ten healthy participants agreed to take part, I adjusted this number to five as it correlated better with the number of recruited Meniere's disease patients (four), and helped to guide the image acquisition parameter adjustments.

Participants who fell into phase 2 were initially recruited from the ENT Department's clinics at the Queens Medical Centre in Nottingham. The initial approach was from a

member of the patient's usual care team (which may include the investigator) and invitation letters were then sent to potential participants via post.

Additionally, a pool of patients coded as having been diagnosed with Meniere's disease has been provided by the Clinical Governance Team at Nottingham University Hospitals NHS Trust(NUH Trust).

However, these routes of recruitment did not provide a sufficient number of participants despite several months of recruitment. Only three Meniere's disease patients were successfully recruited using these methods. Subsequently, an amendment was submitted and approved which allowed for broadening of the inclusion criteria and the ways participants were included. This meant that both patients with clinically 'definite' and clinically 'probable' Meniere's disease were now eligible. Additionally, participants who fell into phase 2 were recruited indirectly via two databases that included patients with Meniere's disease. The first one of these was the Nottingham Biomedical Research Centre Participant Database and the second one was Meniere's Society.

Participant information sheets with the list of inclusion and exclusion criteria were given to the custodians of these databases and subsequently distributed to the potential participants who then stepped forward and contacted the research team of their volition. This amendment yielded an extra one participant who was diagnosed with clinically 'probable' Meniere's disease. The Deputy Principal Investigator or their nominee, e.g., from the research team informed the participant of all aspects pertaining to participation in the study. It was explained to the potential participants that entry into the trial is entirely voluntary and that their treatment and care will not be affected by their decision. It was also explained that they can withdraw at any time (decline the offer to enrol, during scanning, between scans etc.) without any consequences or explanations. All participants were given £50 inconvenience allowance in the form of cheques.

INFORMED CONSENT –

All participants provided written informed consent. The Informed Consent Form was signed and dated by the participants before they entered the trial. The Investigator explained the details of the trial and provided a Participant Information Sheet, ensuring

that the participant had sufficient time to consider participating or not. The Investigator answered any questions that the participant had concerning study participation. The participant had to be able to speak English and have full capacity to give informed consent. Informed consent was collected from each participant before they underwent any interventions related to the study. One copy of this was kept by the participant, one was kept by the Investigator, and a third was retained in the patient's hospital records, where applicable.

TRIAL / STUDY TREATMENT AND REGIMEN

An initial interview occurred between the Deputy Principal Investigator and the potential participant at the initiation of the participant who contacted the Deputy PI once informed about, or invited to the study. This interview will either occur face-to-face, via telephone or Microsoft Teams. At this point, the Deputy PI explained the study in detail and the participants had sufficient time to ask questions. The participants could have decided immediately after this conversation whether or not they would participate but they were also given two weeks to make up their minds. Should they decide to participate, a slot for an MRI scan of the temporal bones (with and without contrast) was booked at either The Sir Peter Mansfield Imaging Centre at Queens Medical Centre or the clinical scanner at Queens Medical Centre, at a time convenient for the participant. Each participant will have to attend only once at the QMC. There they met the Deputy Principal Investigator or one of the Investigators and gave written explicit informed consent. The history of the disease in MD patients and their demographics was assessed at the first meeting with the Deputy PI only to the extent of identifying the inclusion and exclusion criteria. Only once inclusion and exclusion criteria have been checked and consent obtained, did they have the first non-contrast MRI scan and then an intravenous cannula placed and contrast agent injected. Two delayed MRI scans of their brain performed 2 and 4 hours post-injection were required for the best image enhancement and delineation of important structures. Both the contrast and the 4 hours between the injection and the last scan are considered standard NHS care when trying to visualise inner ear structures. There is some evidence that images of the same quality can be

obtained with only a 2-hour delay after contrast injection, hence I decided to include the third scan performed 2 hours post-injection to review and potentially add to the body of evidence supporting the shorter time interval between the contrast injection and the scan. The additional scan carried no additional threats to the participant's safety and was convenient to implement as the participant had to wait on site for 4 hours anyway. Only one participant had an MRI scan both 2 hours and 4 hours post-contrast administration. The feasibility of this practice (earlier scanning) would greatly improve patient care and make the diagnostic tool more accessible with better resource allocation. The same participant was also the only one scanned with two different MRI techniques 4 hours post contrast administration(3D FLAIR and 3D Real IR) which carried no risk to the participant as the contrast was already administered.

The participants had to remain on-site (on hospital grounds) for these four hours for the purpose of monitoring for any adverse reactions to the contrast. They were kept in the unit itself for the first 15 minutes just in case an acute reaction ensued as per Trust protocol. No preassessment was required prior to the scanning according to the hospital protocol with our exclusion criteria and low-risk contrast agent. There is no documented interaction between gadolinium contrast and other medications and more than 90% of the contrast is excreted from the subject’s body by the kidneys within the first 12 hours. Hence, participants could have taken any concomitant medications/treatment on the day of the scan. Since there are no adverse events within these four hours, the participants are well and haven’t withdrawn their consent they undergo two further MRI scans with each of them taking less than 20 minutes while lying down flat on the scanner table in the MR machine. During the scans, there was an open channel of communication between the radiographer and the participant and they had a ‘panic button’ they could press should they at any time feel overwhelmed or claustrophobic. Their right to withdraw applied even at this time while the scan was being performed. Once the scans are performed and images obtained, their participation in the study will end and no further visits or follow-ups are required. The participants were made aware that the MRI scans performed were not clinically diagnostic and that the investigator would not

provide clinical interpretation of these scans. If an abnormality that may require clinical investigation was found during the review of a scan, then the investigator would recommend that the participant arrange to see their nominated healthcare professional (e.g. their General Practitioner In this situation, the investigator provided relevant details of the abnormality to the nominated healthcare professional.

MRI SCANNER –

All images were obtained on the Premier GE 3 Tesla MRI scanner.

I used a Premier GE MRI scanner with a 3 Tesla coil strength. The bulk of the literature on the topic is published using Siemens scanners and there are multiple variables across different scanner machines that affect the image acquisition and therefore the result, a high-quality image. However, using a different scanner, potentially makes it easier for other units with different scanners to replicate the images of the inner ear and endolymphatic hydrops.

The details of the image acquisition protocol can be found in our exam cards in the appendices.

CONTRAST AGENT –

The main contrast agent that is used in inner ear imaging, and magnetic resonance imaging in general, is gadolinium-based and comes under brand names such as Gadovist, Magnevist or Omniscan. In this study, I used Gadovist, which contains Gadobutrol (gadolinium+dihydroxy-hydroxymethylpropyl tetraazacyclododecane-triacetic acid) as an active substance to provide contrast. The dose used was 0.1ml/kg of 1 M solution. In all participants, the contrast was administered intravenously through a peripheral vein via cannula. After injection, participants were closely observed for the next 15-20 minutes as this was the period when the risk of serious adverse events was at its highest. After this period elapsed, the cannula was taken out and the participants left the scanning facility only returning for the subsequent scan(s).

Gadolinium is a chemical compound, mostly present in the solution as a chelate which renders it inert and unreactive with surrounding tissues which suppresses its toxicity. The usual dosage as per the electronic medicines compendium is 1mL/kg of 1M (mmol)

solution, but several studies have reported using a double dose for the intravenous route of administration to achieve higher concentration in the inner ear and hence, potentially, better delineation of structures (Electronic Medicines Compendium; Connor et Pai, 2021).

The most frequently observed adverse drug reactions (over 0.5 %) in patients receiving Gadovist are headache, nausea and dizziness. Injecting Gadovist into veins with a small lumen there is the possibility of adverse effects such as reddening of the skin and some swelling around the injection site. Most of the undesirable effects are of mild to moderate intensity.

The most serious adverse drug reactions in patients receiving Gadovist are cardiac arrest and severe anaphylactoid reactions (including respiratory arrest and anaphylactic shock). This is at a rate less than 1:10000. Hypersensitivity reactions (1:1000, rare) As with other intravenous contrast agents, Gadovist can be associated with anaphylactoid/hypersensitivity or other idiosyncratic reactions, characterized by cardiovascular, respiratory or cutaneous manifestations, and ranging to severe reactions including shock. It is considered uncommon (1:1000) (Electronic medicines compendium).

While hypersensitivity reactions do occur with gadolinium-based contrast, they are very rare and usually amenable to standard treatment, with one study reporting an incidence of 0.079% in 141,623 total doses (Jung et al., 2012). The risk of hypersensitivity reactions may be higher in the case of:

4. previous reaction to contrast media
5. history of bronchial asthma
6. history of allergic disorders
7. history of previous cardiac disease
8. patients due to undergo thyroid surgery (as contrast can cause treatment delays if a patient needs radioactive iodine post-op)

Most of these reactions occur within half an hour of administration. Therefore, post-procedure observation of the patient is recommended. Delayed reactions (after hours up to several days) have been rarely observed.

The other most serious adverse reaction is Nephrogenic Systemic Fibrosis (NSF), a poorly understood, serious condition which can have severe health consequences and even result in a fatal outcome. Nephrogenic systemic fibrosis is a known risk in patients with renal failure; hence, patients who at are risk, i.e. people with diabetes on metformin and chronic kidney disease patients, should be carefully screened for their renal function prior to receiving the contrast. (www.rcr.ac.uk, 2020) Guidelines like these and other international guidelines resulted in a significant reduction of nephrogenic systemic fibrosis (Bauerle et al., 2021). The risk for acute kidney injury and nephrogenic systemic fibrosis (NSF) is greater in patients with the below conditions.

• Chronic kidney disease (CKD) – eGFR < 40 ml/min/1.73m2 and any known renal impairment

• Diabetes Mellitus & Metformin therapy - need to stop 48 hours pre-contrast scan if possible

• Pregnant and breastfeeding patients

• Perioperative liver transplantation period

• Renal transplant

• 75 years of age (renal function required in all over 65 years of age.)

• Haemodialysis

(Electronic Medicines Compendium)

Another adverse effect of Gadolinium-based contrast is the retention of deposits in the brain and reticuloendothelial system (RES) with unknown significance. Kanda et al. originally reported that signal intensity in the GP(globus pallidus) and DN(dentate nucleus) on unenhanced T1 weighted imaging (T1WI) might be a result of the previous gadolinium-based contrast agents (GBCAs) administration. (Kanda et al., 2014) Since then, several studies have examined the potential link between the gadolinium deposits in the brain and a clinical effect, but no clinical significance has been attached to the

retention of Gadolinium. (Clement et al., 2021; Dillman et al, 2020; Strickler et al., 2021)
Some studies have advocated the ALARA(as low as reasonably achievable) approach to using Gadolinium contrast mimicking the procedure for ionising radiation as it was shown that the deposits are retained even after a single dose. (Dillman et al., 2020)
The overarching effect of Gadolinium retention is a subject of much debate and more clinical trials are required to fully elucidate its significance.
The usual safety requirements for magnetic resonance imaging, especially the exclusion of ferromagnetic materials, also apply when using Gadolinium-based contrast agents.
USER AND PUBLIC INVOLVEMENT -
In April 2022, two productive Patient and Public Involvement (PPI) meetings held between the Principal Investigator, the members of the patient support groups and members of the public (patients) were held to clarify the planned design of the study and to receive input from the people representing potential research subjects or the potential research subjects themselves. The PPI representatives were satisfied with the way the study was envisioned and had suggestions that mostly pertained to keeping the participants comfortable during the scan and the 4-hour wait between the contrast injection and the scan. As a result, the PI and the research assistant visited the SPMIC and met with the head radiographer and clarified these points, most notably on keeping the communication channel constantly open between the participant and the radiographers, i.e., visor, panic button and keeping the participant comfortable, i.e., a pillow to elevate the head will be available to make it more comfortable for people with cervical spine issues. The PPI team also suggested an inconvenience allowance, stipulating that it is unreasonable to expect that people arrange transport to QMC, pay for parking, be injected with contrast and wait for 4 hours on-site without some form of reimbursement. Following two Patient and Public Involvement (PPI) meetings held between the Principal Investigator, the members of the patient support group and members of the public (patients), an inconvenience allowance of £50 was deemed appropriate to give to the participants for the travel costs, the trouble of having to stay on site for more than four hours , parking and refreshments during this period.